



5-2007

Century-Scale Trends in Climatic Variability for the Pacific Northwest from Western Juniper (*Juniperus occidentalis* Hook. ssp. *occidentalis*) Tree-Ring Data

Christopher Aaron Underwood
University of Tennessee, Knoxville

Follow this and additional works at: https://trace.tennessee.edu/utk_gradthes



Part of the [Geography Commons](#)

Recommended Citation

Underwood, Christopher Aaron, "Century-Scale Trends in Climatic Variability for the Pacific Northwest from Western Juniper (*Juniperus occidentalis* Hook. ssp. *occidentalis*) Tree-Ring Data. " Master's Thesis, University of Tennessee, 2007.
https://trace.tennessee.edu/utk_gradthes/4440

This Thesis is brought to you for free and open access by the Graduate School at TRACE: Tennessee Research and Creative Exchange. It has been accepted for inclusion in Masters Theses by an authorized administrator of TRACE: Tennessee Research and Creative Exchange. For more information, please contact trace@utk.edu.

To the Graduate Council:

I am submitting herewith a thesis written by Christopher Aaron Underwood entitled "Century-Scale Trends in Climatic Variability for the Pacific Northwest from Western Juniper (*Juniperus occidentalis* Hook. ssp. *occidentalis*) Tree-Ring Data." I have examined the final electronic copy of this thesis for form and content and recommend that it be accepted in partial fulfillment of the requirements for the degree of Master of Science, with a major in Geography.

Henri D. Grissino-Mayer, Major Professor

We have read this thesis and recommend its acceptance:

Carol P. Harden, Roger Tankersley, Jr.

Accepted for the Council:


Carolyn R. Hodges

Vice Provost and Dean of the Graduate School

(Original signatures are on file with official student records.)

To the Graduate Council:

I am submitting herewith a thesis written by Christopher Aaron Underwood entitled "Century-Scale Trends in Climatic Variability for the Pacific Northwest from Western Juniper (*Juniperus occidentalis* Hook. ssp. *occidentalis*) Tree-Ring Data." I have examined the final paper copy of this thesis for form and content and recommend that it be accepted in partial fulfillment of the requirements for the degree of Master of Science, with a major in Geography.

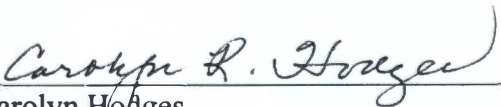

Henri D. Grissino-Mayer, Major Professor

We have read this thesis and
recommend its acceptance:


Carol P. Harden


Roger Tankersley, Jr.

Accepted for the Council:


Carolyn Hodges,
Vice Provost and Dean of the Graduate School

Thesis
2007
.463

**Century-Scale Trends in Climatic Variability for the Pacific
Northwest from Western Juniper (*Juniperus occidentalis* Hook.
ssp. occidentalis) Tree-Ring Data**

A Thesis Presented
for the Master of Science Degree
The University of Tennessee, Knoxville

Christopher Aaron Underwood
May 2007

Dedication

This work is dedicated to my family.

I lost my father during the course of this project. He was always my rock, my biggest supporter, and the one I sought for assistance when no one else could help. Losing him has created a void in my life that is still being bridged, yet only through God's grace and the love and support offered by my family. Even though you have not sanded a single sample, counted a lone ring, or written a solitary word of this thesis, you are the foundation on which this project rests. Thank you.

Acknowledgments

This project was conducted under the guidance of Dr. Henri D. Grissino-Mayer. I owe him a debt of gratitude for taking me in when I was searching for an academic home. Henri's expertise, teaching, assistance, friendship, and critiques have been invaluable throughout the duration of this research. I also thank my other committee members, Drs. Carol P. Harden and Roger Tankersley, Jr. for their support, knowledge, and reviews during this project. Dr. Kenneth H. Orvis provided additional expertise and comments during the review process.

I wish to thank Daniel Lewis, who, along with Dr. Grissino-Mayer, collected the samples for my project. Central Oregon in early August can be brutally hot with almost no shade, and temperatures were well above 30 °C during sample collection in the High Desert. Guys, I am still indebted to you for this. The Bureau of Land Management is also owed a great deal of thanks for allowing the collection of these samples. I am further indebted to Justin Hart, Jessica Brogdon, and Lisa LaForest for their thorough reviews of my manuscripts. Many thanks to the three of you for making my writing better. The personnel in the Laboratory of Tree-Ring Science have been instrumental in conveying to me their knowledge of dendrochronology. I thank you all for your assistance and friendship during the past two years. I am grateful to Will Fontanez and the staff at the University of Tennessee Cartographic Services for the two very nice maps they provided for this thesis. Randy Heise of the High Desert Museum, Bend, Oregon, provided some very helpful information that only an Oregonian would know. Thanks, Randy. I would also like to recognize the editorial staff in Graduate Student Services for their great job of technical editing.

I thank my parents for their unconditional love and support. I want to especially thank my mother, Mary, and my high school science teacher, John Jones, for instilling in me a love of nature, science, and the environment. Finally, my loving wife, Sherri, has been a grounding spirit throughout this experience. She gives me motivation to better myself and to push ahead in my academic career. I will be forever thankful to her.

Abstract

The history of the Earth's climate shows many fluctuations, and there is reason to believe that climatic fluctuations will continue to occur in the future. Climatic shifts related to processes such as the Pacific Decadal Oscillation (PDO) initiate many environmental anomalies, including interruptions in traditional storm tracks, average precipitation, fire regimes, streamflow, and animal behavior. Our historical climatic records are too short to fully illustrate climatic fluctuations over long time scales. Proxy records are often used to extend these historical climatic records. In this dendroclimatological study, I used western juniper (*Juniperus occidentalis* Hook. ssp. *occidentalis*) from central Oregon as a climatic proxy.

Western juniper is the tree species most suitable for this project because of its extensive range, longevity, high sensitivity to moisture, and low sensitivity to temperature. Twenty-five western juniper cross sections were prepared and measured using standard dendrochronological techniques. A master chronology that extends from A.D. 797–2000 was established using the 25 western juniper cross sections. Pearson's product-moment correlation analyses were conducted using regional precipitation data, the PDO index, and the Niño 3 index. The correlation between regional precipitation and radial tree growth was the strongest, suggesting that moisture is the most influential limiting factor of growth in central Oregon. Significant positive relationships, however, were also discovered between radial tree growth and the other climatic variables. Regression analyses were performed and climatic variables were reconstructed for the entire length of the tree-ring chronology.

Many climatic episodes are evident in the reconstructions. The most prominent features of the tree-ring chronology include sustained periods of suppressed radial tree growth during A.D. 1351–1390 and 1917–1947, as well as a long-term period of above-average growth during A.D. 1948–1999. These new data provide a better understanding of the strength and periodicity of past climatic change in the Pacific Northwest, and strengthens our predictive capabilities of potential future climatic shifts.

Table of Contents

1.	Introduction	1
1.1	Background	1
1.2	Climatic Reconstructions from Proxy Data	2
1.3	Major Climatic Oscillations that Affect the Pacific Northwest	7
1.3.1	El Niño-Southern Oscillation (ENSO).....	7
1.3.2	The Pacific Decadal Oscillation (PDO).....	11
1.4	Problem Statement.....	14
1.5	Objectives of the Study.....	18
2.	Literature Review.....	19
2.1	Dendroclimatology in the Pacific Northwest.....	19
2.1.1	Keen (1937)	19
2.1.2	Knapp <i>et al.</i> (2002)	21
2.1.3	Pohl <i>et al.</i> (2002).....	25
2.1.4	Knapp <i>et al.</i> (2004)	26
2.2	The Pacific Decadal Oscillation (PDO).....	28
2.2.1	Mantua <i>et al.</i> (1997).....	28
2.2.2	Minobe (1997)	29
2.2.3	Biondi <i>et al.</i> (2001).....	31
2.2.4	Gedalof and Smith (2001).....	32
2.3	Western Juniper Ecology and Recent Biogeography.....	34
2.3.1	Burkhardt and Tisdale (1976)	34
2.3.2	Miller and Rose (1995)	37
2.3.3	Miller and Rose (1999)	39
2.3.4	Soulé <i>et al.</i> (2003).....	42
3.	Site Description	45
3.1	Introduction.....	45
3.2	Geology.....	46
3.2.1	Physiography.....	46
3.2.2	Geomorphology	46
3.2.3	Soils.....	50
3.3	Oregon Climate.....	52
3.3.1	General Overview Along a West–East Transect	52
3.3.1.1	Oregon Climatic Zones	53
3.3.2	Climate of Frederick Butte.....	55
3.3.2.1	Temperature	55
3.3.2.2	Precipitation	56
3.3.3	Typical Factors That Affect Oregon Climate	57
3.3.3.1	Seasonal Climatic Regimes.....	57
3.3.3.2	Air Masses	59

3.4	Land Use and Fire History	61
3.4.1	Land Use	61
3.4.2	Fire	65
3.4.3	Climate/Fire Relationships.....	69
3.5	The Ecology and Biogeography of Western Juniper	71
3.5.1	Associated Flora.....	75
3.5.2	Associated Fauna	78
3.5.3	Life History of Western Juniper	79
3.5.4	Western Juniper Invasion.....	81
3.5.5	Special Uses and Economic Value	83
4.	Methods	85
4.1	Field Methods	85
4.1.1	Site Selection	85
4.1.2	Collection of Cross Sections	86
4.2	Laboratory Methods.....	88
4.2.1	Sample Preparation and Selection	88
4.2.2	Crossdating	89
4.2.3	Measurement.....	89
4.2.4	Quality Control with COFECHA.....	90
4.2.5	Standardization and Chronology Development.....	91
4.2.6	Analyzing the Climatic Response.....	92
5.	Results.....	95
5.1	Quality Control	95
5.2	Western Juniper Chronology	95
5.3	Climatic Analyses	101
5.3.1	Climatic Trends.....	108
6.	Discussion.....	127
6.1	Chronology	127
6.2	Dynamics of Oregon Climate	127
6.2.1	The PDO and ENSO	128
6.2.2	Air Mass Boundaries	129
6.3	Trends in Central Oregon Climate	133
6.3.1	A.D. 799–1000.....	134
6.3.2	A.D. 1001–1200.....	135
6.3.3	A.D. 1201–1400.....	135
6.3.4	A.D. 1401–1600.....	136
6.3.5	A.D. 1601–1800.....	138
6.3.6	A.D. 1801–2000.....	141
7.	Conclusions	147
7.1	Major Conclusions	147

7.2	Improvements and Limitations to This Study.....	153
7.3	Future Research	154
7.4	Concluding Remarks.....	158
References.....		159
Appendix		177
A-1. Frederick Butte COFECHA Output.....		179
A-2. Frederick Butte Standard ARSTAN Output.....		201
Vita		211

List of Tables

<u>Table</u>	<u>Page</u>
5.1 The longest western juniper tree-ring chronologies in the western United States	100
5.2 The statistical quality of the longest western juniper tree-ring chronologies in the western United States.....	102
5.3 Regression statistics and diagnostics	114
5.4 Marker years of extreme above-average anomalous radial tree growth	119
5.5 Marker years of extreme below-average anomalous radial tree growth.....	120

List of Figures

<u>Figure</u>	<u>Page</u>
1.1 Typical November to March weather anomalies and atmospheric circulation during El Niño or a warm phase of the PDO	9
3.1 The High Lava Plains and other physiographic provinces of Oregon	47
3.2 Oregon climatic zones.....	54
3.3 Early snow on a Newberry Crater lava flow.....	58
3.4 Air masses that affect Oregon.....	60
3.5 Native American petroglyph in the Oregon High Desert	62
3.6 Oregon High Desert cattle drive	62
3.7 Sheep in central Oregon.....	63
3.8 An abandoned homestead in the Oregon High Desert.....	64
3.9 Native range of western juniper	72
3.10 Western juniper stem with berries and seeds.....	74
3.11 <i>Juniperus occidentalis</i> Hook. ssp. <i>occidentalis</i> in its native habitat.....	75
4.1 Western juniper cross section	87
4.2 Sample collection from a fallen western juniper	87
4.3 Chain-sawed cross section of western juniper	88
4.4 Magnification of western juniper annual growth rings.....	90
5.1 Frederick Butte western juniper chronology.....	96
5.2 Frederick Butte western juniper chronology (A.D. 799–1000).....	97
5.3 Frederick Butte western juniper chronology (A.D. 1001–1200).....	97
5.4 Frederick Butte western juniper chronology (A.D. 1201–1400).....	98

5.5	Frederick Butte western juniper chronology (A.D. 1401–1600)	98
5.6	Frederick Butte western juniper chronology (A.D. 1601–1800)	99
5.7	Frederick Butte western juniper chronology (A.D. 1801–2000)	99
5.8	FBS 004, with an inner-ring date of A.D. 797, is the oldest series in the chronology	103
5.9	FBN 050, with 1,062 rings, is the longest series in the chronology	103
5.10	Pearson’s product-moment correlation coefficients (r) between western juniper radial growth and Oregon Zone 7 precipitation data (1920–2000)	104
5.11	Pearson’s product-moment correlation coefficients (r) between western juniper radial growth and the PDO index (1948–2000)	105
5.12	Pearson’s product-moment correlation coefficients (r) between western juniper radial growth and the Niño 3 index (1950–2000)	106
5.13	Pearson’s product-moment correlation coefficients (r) between western juniper radial growth and Niño 3 index anomaly (1950–2000)	107
5.14	Pearson’s product-moment correlation coefficients (r) between western juniper radial growth and selected seasonalized climatic variables	109
5.15	Observed and reconstructed Oregon Zone 7 precipitation (July _{t-1} to June _t)	110
5.16	Observed and reconstructed PDO index (March _t to April _t)	111
5.17	Observed and reconstructed Niño 3 index (May _t to June _t)	112
5.18	Observed and reconstructed Niño 3 anomaly (May _t to June _t)	113
5.19	10-year moving average of the Frederick Butte western juniper chronology	116
5.20	20-year moving average of the Frederick Butte western juniper chronology	117
5.21	50-year moving average of the Frederick Butte western juniper chronology	118
5.22	Marker year trends (A.D. 799–1000)	121
5.23	Marker year trends (A.D. 1001–1200)	121
5.24	Marker year trends (A.D. 1201–1400)	122

5.25	Marker year trends (A.D. 1401–1600).....	122
5.26	Marker year trends (A.D. 1601–1800).....	123
5.27	Marker year trends (A.D. 1801–2000).....	123
6.1	Western United States major equivalent air mass boundaries and climatic regions	131
6.2	Pacific Northwest climatic subregions.....	132
7.1	Global thermohaline circulation	156

Chapter 1

Introduction

1.1 Background

Changes in future climatic variability are expected and could be severe (Fedorov and Philander 2000, Urban *et al.* 2000, Cole 2001, Pohl *et al.* 2002). Atmosphere-ocean general circulation models (AOGCMs) predict that global surface temperatures may increase by 1.4 to 5.8 °C above 1990 levels by A.D. 2100 (Intergovernmental Panel on Climate Change 2007). Currently, our knowledge of trends in long-term climate is improving, but effects of long-term climate in some geographical areas are largely unknown, in part because historical climatic records are too short to illustrate such trends over longer time scales (Keen 1937, Pohl *et al.* 2002). The practice of using proxy information from natural records (e.g., fossil pollen, corals, ice cores, or tree rings) to extend historical climatic records allows us to better identify and understand past trends in climate (Evans *et al.* 2001). Climatic fluctuations that occurred in the past may reveal an oscillation pattern, and this pattern could repeat itself in the future. The ability of these proxy data sets to manifest these trends, however, may be influenced by unexpected or multiple climatic (e.g. drought, frost, storm), geomorphic (e.g. erosion, landslide, earthquake, volcanic eruption), biotic (e.g. insect outbreaks, competition), geographic (e.g. substrate, topography), and anthropogenic (e.g. pollution, agriculture) factors (Fritts 1976, Banks 1991).

1.2 Climatic Reconstructions from Proxy Data

Dendrochronology is the method of scientific dating based on the analysis of tree-ring growth patterns. Tree rings are excellent indicators of weather conditions that may affect tree growth (Jessup 1935, Keen 1937, Fritts 1976, Grissino-Mayer 1996, Nash 1999). Each tree ring is usually the result of growth during just one year, beginning in spring and ceasing in late summer or early autumn. Precise dating is possible from ring widths because tree growth is affected by the sequence of favorable and unfavorable weather from year to year that is recorded by the sequence of wide and narrow rings (Fritts 1976). By examining these patterns, tree-ring data provide information about past climate that enables us to more accurately assess future climate (Keen 1937, Fritts 1976). Extracting information from tree rings, however, is only one of many proxy approaches to reconstructing past climate.

Palynology is the study of the pollen grains and spores of plants (Erdtman 1969). Pollen grains are often used as an indicator of past climatic conditions (Vale 1982). Climate is a major factor that controls the spatial distribution of plants (Young *et al.* 2003); therefore, as climate changes through time, the species composition of plant communities in specific geographic areas may also change. For example, pollen produced by xerophytic plant types is likely to be more abundant during periods of drier climate, while pollen produced by mesophytic plant types is likely to be more abundant during periods of wetter climate. The same holds true for plant/temperature relationships. Where pollen accumulates and is preserved in marine and lake sediments, acid bogs, peatlands, ice cores, and sometimes soil, evidence of the plant taxa that once inhabited the immediate and surrounding areas may be preserved (Vale 1982, Young *et al.* 2003).

For example, Pisias *et al.* (2001) used pollen and radiolaria from marine sediment cores from the northeastern Pacific Ocean to reconstruct oceanographic and continental climatic change during the past glacial cycle (0–150,000 years B.P.). Radiolarian microfossils associated with coastal upwelling were often found in association with redwood (*Sequoia sempervirens* (D. Don) Endl.), western hemlock (*Tsuga heterophylla* (Raf.) Sarg.), and alder (*Alnus* spp.) pollen. This association is consistent with the relationship between coastal upwelling, coastal fog, and redwood forests (Pisias *et al.* 2001).

The skeletal growth of hermatypic (reef-building) corals is also a sensitive indicator of environmental conditions (Dodge and Helmle 2003). Because of this sensitivity, the annual growth bands in reef corals can be utilized as a good environmental proxy (Dodge and Vaisnys 1975, Linsley *et al.* 1994, 2000a, 2000b). Cross sections or cores can be taken from coral skeletons to analyze annual growth bands. Annual growth band measurements can relate, through regression techniques, growth band time series to some fluctuating environmental factor such as water pollution, turbidity, air temperature, sea level atmospheric pressure, or oceanic temperature. As with tree rings, coral growth bands tend to be wider during years of satisfactory growing conditions and narrower during years of less-than satisfactory growing conditions.

Coral skeletons consist mainly of calcium carbonate, but also contain trace metals (such as Sr and Mg). Analyses of the trace metals found within annual growth bands can also provide proxy evidence of past environmental conditions. For example, Silenzi *et al.* (2005) used non-tropical stone coral (*Cladocora caespitosa* Linn.) as a proxy for Mediterranean Sea surface temperatures (SST). As SST decreases, Sr replaces Ca in

coral skeletons at an increasingly higher rate. A significant negative correlation between the coral Sr/Ca ratio and November to January SST allowed them to reconstruct the November to January Mediterranean SST record back to 1906 (Silenzi *et al.* 2005). They discovered a cooling trend from 1916–1944 when SST decreased from 16.1 to 12.6 °C. The pattern changed to a warming trend (from 14.1 to 17.5 °C) from 1945–1970, followed by another cooling trend (from 14.8 to 12.9 °C) from 1971–1993. A new warming trend likely began after 1993 (Silenzi *et al.* 2005). Mediterranean cooling has been linked to atmospheric haze, and these trends are slightly different from global trends.

Linsley *et al.* (2000b) also used a coral Sr/Ca ratio to accurately record decadal changes in South Pacific Ocean SST. They created a coral Sr/Ca ratio record back to 1726 that shows repeated decadal and interdecadal South Pacific SST regime shifts > 0.75 °C. They compared the South Pacific Ocean oscillatory pattern illustrated by their Sr/Ca coral proxy record with decadal climatic oscillatory patterns for the North Pacific Ocean and found that several of the largest decadal-scale SST variations in the South Pacific Ocean occurred coherently with SST regime shifts in the North Pacific Ocean (Linsley *et al.* 2000b). This hemispheric symmetry led them to conclude that tropical forcing may be an important factor in decadal-scale climatic variability in the Pacific Ocean.

Finally, the ratios of carbon isotopes ($^{14}\text{C}/^{12}\text{C}$) and oxygen isotopes ($^{18}\text{O}/^{16}\text{O}$) that accumulate within coral growth bands can be used as climatic proxies. Atmospheric carbon and oxygen isotopes enter oceanic surface water through vertical mixing and are then available for uptake by coral. Increased levels of atmospheric ^{14}C occur during

periods of decreased solar activity. When solar activity decreases, the temperature of the earth may also decrease. Increased levels of ^{18}O also occur during extended periods of colder temperatures. Therefore, increased levels of ^{14}C and ^{18}O in annual coral growth bands may indicate periods of below normal temperatures. For example, evidence of the Maunder sunspot minimum, associated with the cooler temperatures of the Little Ice Age, was found in growth bands from corals growing in the early 1700s in the Florida Straits (Druffel 1982). As solar activity and global temperatures decreased during the Maunder sunspot minimum, $^{14}\text{C}/^{12}\text{C}$ ratios increased. Levels of ^{14}C increased in coral growth bands during this time (Druffel 1982). In addition, $^{18}\text{O}/^{16}\text{O}$ ratios increased, and higher levels of ^{18}O were discovered in the coral growth bands from the latter part of the Little Ice Age (1700–1725) (Druffel 1982).

Ice cores, another type of past-climatic proxy, are extracted from areas where millennia-old glaciers and ice caps are found (Liu *et al.* 1998, 2005). Chronological layers of ice in these cores contain pollen, dust, gases, isotopes, and chemical signatures that can be used to extract climatic proxy data. The information preserved in most ice cores is extremely valuable because most ice-core records are retrieved from locations rarely, if ever, disturbed by humans (Mayewski 1988).

The types of pollen trapped within an ice layer will reveal the types of plants (xeric or mesophytic) that were locally present during the period the ice layer formed. This information can be used to deduce the type of climatic regime that may have affected the area during the same period. For example, Liu *et al.* (1998) created an ice-core pollen record of climatic change in the central Andes during the last 400 years. Their pollen record corroborates the oxygen isotopic and ice accumulation records from

the Quelccaya Ice Cap, Peru (Thompson *et al.* 1985, 1986), and shows that the Little Ice Age consisted of two distinct phases: a wet period from 1500–1700, and a dry period from 1700–1880. During the dry period, xerophytic shrubs (Asteraceae) expanded to replace bunch grasses (Poaceae) on the Altiplano as suggested by a dramatic drop in Poaceae pollen and an increase in Asteraceae pollen (Liu *et al.* 1998).

Analyses of other ice-core constituents can reveal even more information about past climate. For example, atmospheric dust, typically of volcanic origin, can cool the earth by partially blocking solar radiation. Increased amounts of dust within layers of ice typically indicate periods of cooler than normal temperatures (Petit *et al.* 1999, Augustin *et al.* 2004). Atmospheric ^{18}O reflects changes in the hydrologic cycle and global ice volume, and an increased $^{18}\text{O}/^{16}\text{O}$ isotopic ratio typically indicates that glacial ice was formed during a period of cooler than normal temperatures. Deuterium is a proxy of local temperature change, and increased concentrations indicate that glacial ice was formed during a period of warmer temperatures. CO_2 and CH_4 are greenhouse gases that become trapped in air bubbles within glacial ice. Layers of ice that contain increased concentrations of these greenhouse gases typically correspond with periods of warmer temperatures (Petit *et al.* 1999, Augustin *et al.* 2004).

Two recent Antarctic ice core projects significantly extended our knowledge of glacial cycles. A 420,000-year climatic and atmospheric history, which included the last four glacial periods, was created from the Vostok ice core (Petit *et al.* 1999), and a 740,000-year climatic and atmospheric history, which included the last eight glacial periods, was created from the Dome C ice core (Augustin *et al.* 2004). Both studies analyzed five constituents of ice-core strata: dust, $\delta\text{D}_{\text{ice}}$ (deuterium), $\delta^{18}\text{O}$, CO_2 , and CH_4 .

Periods of glacial decline from both ice cores were marked by a decrease in dust and atmospheric ^{18}O , and an increase in deuterium, CO_2 , and CH_4 (Petit *et al.* 1999, Augustin *et al.* 2004). Records from the Dome C ice core also show that the last eight glacial-interglacial cycles occurred approximately every 100,000 years (Augustin *et al.* 2004).

1.3 Major Climatic Oscillations that Affect the Pacific Northwest

1.3.1 El Niño-Southern Oscillation (ENSO)

During an average winter in the eastern Pacific, the water off of the western coast of South America is relatively cool. The Humboldt Current brings water northward from Antarctic regions, and the easterly trade winds push warmer surface water away from the coast and allow colder water to upwell toward the surface. This colder water is pushed westward from the coast by the easterly trade winds and joins with Equatorially upwelled water to form a cool tongue that stretches along the Equator. Water in the western Pacific, near Indonesia and the Philippines, tends to be much warmer (Aguado and Burt 2007).

More than 75 years ago, Sir Gilbert Walker, a British meteorologist, first noticed a climatic phenomenon in the South Pacific Ocean as he studied Indian monsoonal failures (Taylor and Hannan 1999). He realized that above-average SSTs corresponded with warmer and more humid marine air, lower barometric pressure, and a higher occurrence of convective storms. He also realized that lower than average barometric pressure in the eastern Pacific coincided with higher than average barometric pressure in the western Pacific, and vice versa. He named this phenomenon the Southern Oscillation (Taylor and Hannan 1999). The term “El Niño” (in reference to the Christ Child) was

coined by South American fishermen as they described the unusually warm waters off the Ecuadorian and Peruvian coasts that periodically occurred around Christmas. This is especially important to South American fishermen because a lack of upwelling significantly reduces available food for fish and creates poor fishing conditions (Taylor and Hannan 1999). Today, because El Niño and the Southern Oscillation are recognized as parts of the same phenomenon, they are often referred to as El Niño-Southern Oscillation (ENSO).

El Niño (warm) events occur approximately every three to seven years as the Pacific Ocean off the South American coast suddenly warms, upwelling diminishes, the easterlies weaken, and water temperatures in the western Pacific decrease. During strong El Niño events, warmer than normal waters cover nearly all of the eastern and central tropical Pacific Ocean (National Oceanic and Atmospheric Administration 2002a, Aguado and Burt 2007). El Niño affects weather patterns in the Pacific Northwest as the Aleutian Low becomes stronger and splits the normal storm track (Figure 1.1) (Taylor and Hannan 1999, Pohl *et al.* 2002). This typically results in drier and warmer than average winters and drought conditions during the growing season for many areas (McCabe and Dettinger 1999). An El Niño event, therefore, reduces available moisture to many areas in the Pacific Northwest, which could be manifested as reduced radial tree growth. These changes in climate and tree growth provide the basis for a dendroclimatological reconstruction of ENSO. Elsewhere in the United States, El Niño events contribute to drier than normal Southwestern monsoons and increased winter

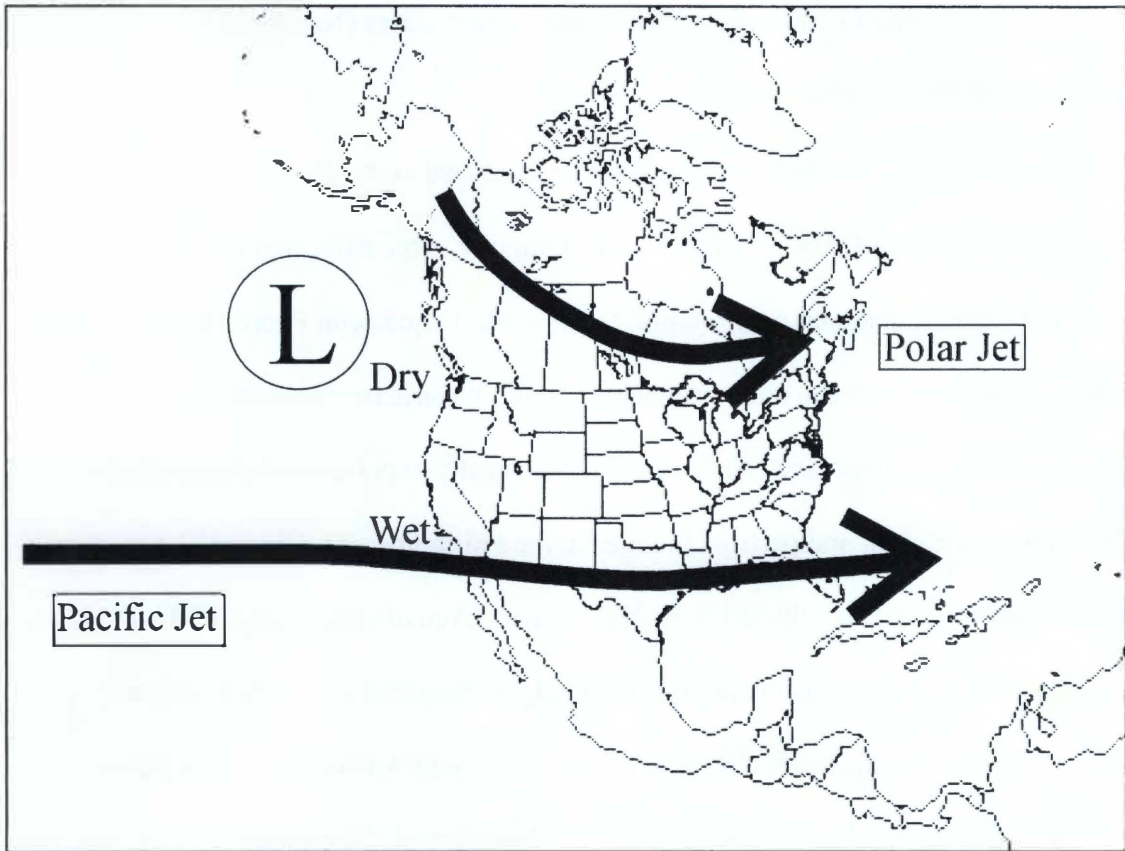


Figure 1.1 Typical November to March weather anomalies and atmospheric circulation during El Niño or a warm phase of the PDO. As the Aleutian Low strengthens, the storms that travel along the paths of the polar and Pacific jet streams are diverted away from the Pacific Northwest.

precipitation in much of California and the Gulf Coastal states (National Oceanic and Atmospheric Administration 2002a).

Globally, El Niño events typically bring increased December to February precipitation to coastal Ecuador, Peru, Brazil, Uruguay, Argentina, and eastern equatorial Africa, and increased annual precipitation to the central equatorial Pacific Ocean. Much of the western Pacific Ocean and northeastern South America experiences drier than normal December to February conditions, India typically experiences below-average June to August precipitation, and parts of Indonesia, the Philippines, and Australia experience an annual precipitation deficit during El Niño events (Aguado and Burt 2007).

La Niña (cold) events occur approximately as frequently as El Niño events. During a La Niña event, Pacific Ocean waters off of South America are cooler than normal and the western Pacific is much warmer than normal. The sequence of events that transpires to form a La Niña event is basically the reverse of the sequence that transpires to form an El Niño event. In many ways, the two climatic events are opposites of one another. During a La Niña event, heavy December to February precipitation is concentrated in the western Pacific, where the warmest SSTs occur, and in the Pacific Northwest. The Aleutian Low is weakened by La Niña conditions, and the storm track traces a path through the Pacific Northwest. The subtropical jet stream moves northeastward across the Pacific and focuses its warm, humid air on the region, and severe arctic outbreaks follow the polar jet stream as it dips southward over the Pacific Northwest. The La Niña-induced positioning of these air masses can bring either warm, intense tropical rain or heavy snow to the Pacific Northwest (Taylor and Hannan 1999).

La Niña events can also bring below-average precipitation to coastal California and the Gulf Coastal States (Aguado and Burt 2007).

Because ENSO oscillates on an interannual scale, numerous phase shifts have been discovered in both instrumental and proxy records. Dating back to the early 17th century, some of the strongest El Niño events occurred from 1680–1681, 1721–1722, 1792–1793, 1815–1816, 1831–1832, 1854–1856, 1876–1877, 1914–1915, 1940–1941, 1982–1983, and 1997–1998, while some of the strongest La Niña events occurred from 1622–1623, 1632–1633, 1675–1676, 1695–1696, 1715–1716, 1747–1748, 1789–1790, 1846–1847, 1920–1921, 1924–1925, 1955–1956, and 1988–1989 (Lough 1992, Green *et al.* 1997, Taylor and Hannan 1999).

1.3.2 The Pacific Decadal Oscillation (PDO)

Strong interdecadal climatic variability has also been demonstrated in the extratropical regions of the Pacific Ocean Basin. Climatic variability in the Pacific and the global tropics had long been considered to be related mainly to ENSO activity (Rasmussen and Wallace 1983, Mantua and Hare 2002, Nash 2002, Babkina 2003). During the latter part of the 20th century, however, the extratropical Pacific Ocean exhibited El Niño-type conditions despite the absence of tropical El Niño phases during much of the period (Mantua and Hare 2002). This pattern originated during the winter of 1976, and appeared as a shift to warmer ocean waters off the western coast of North America.

Since the discovery of the Pacific Decadal Oscillation (PDO) in the late 1990s, researchers have realized that climate in the Pacific Basin has gone through several phase

shifts. During positive (warm) phases of the PDO, SSTs tend to be anomalously cool in the central North Pacific Ocean, while anomalously warm SSTs prevail along the western coast of the Americas (Mantua and Hare 2002). During November to March, a positive PDO phase coincides with anomalously low sea level pressures over the North Pacific Ocean that lead to enhanced counterclockwise winds. Concurrent with this, anomalously high sea level pressures over the northern subtropical Pacific Ocean lead to enhanced clockwise winds (Mantua and Hare 2002).

PDO-driven changes in precipitation regimes also occur. As with El Niño events, positive-phase PDO patterns bring drier than average conditions to much of the Pacific Northwest as the Aleutian Low strengthens and jet streams are diverted northward and southward (Figure 1.1) (Enfield and Mestas-Núñez 2001, Pohl *et al.* 2002). A positive phase of the PDO, therefore, reduces available moisture to many areas in the Pacific Northwest, and this effect could be manifested in reduced radial tree growth. These changes in climate and tree growth provide the basis for a dendroclimatological reconstruction of the PDO. Climatic variations associated with negative (cool) phases of the PDO are opposites of climatic variations associated with positive (warm) phases of the PDO (Mantua and Hare 2002).

The PDO likely experienced a prolonged period of weakened oscillation that began in the early 1700s and lasted until the early 1900s (Evans *et al.* 2001, Knapp *et al.* 2002). Gedalof and Smith (2001), however, suggested this period of weakened oscillation occurred only from 1840–1923, while Biondi *et al.* (2001) suggested it occurred only from the late 1700s until the middle 1800s. Instrumental records suggest that negative (cool) PDO regimes prevailed from the early 1900s–1924, and again from

1947–1976 (Francis and Hare 1997, Mantua *et al.* 1997, Minobe 1997, Kadonaga *et al.* 1999, Linsley *et al.* 2000a, 2000b, Biondi *et al.* 2001, Evans *et al.* 2001, Gedalof and Smith 2001, Knapp *et al.* 2002, Mantua and Hare 2002, Pohl *et al.* 2002). The PDO may have experienced positive phases in the 1500s and early 1600s (Evans *et al.* 2001, Knapp *et al.* 2002). In the 20th century, the PDO was in a positive phase from 1925–1946, and from 1977 through (at least) the late 1990s (Francis and Hare 1997, Mantua *et al.* 1997, Minobe 1997, Kadonaga *et al.* 1999, Linsley *et al.* 2000a, 2000b, Biondi *et al.* 2001, Evans *et al.* 2001, Gedalof and Smith 2001, Knapp *et al.* 2002, Mantua and Hare 2002, Pohl *et al.* 2002).

Three basic characteristics differentiate the PDO from ENSO. First, PDO oscillatory modes persist for 20 to 30 years, while normal ENSO oscillatory modes persist for 6 to 18 months. Second, spatial climatic evidence of the PDO is most apparent in the extratropics, especially the North Pacific/North American sector, while secondary signatures are visible in the tropics. In contrast, ENSO has its strongest expression in the tropics. Third, the factors leading to the PDO are not well known, while causes for ENSO fluctuations are relatively well known (Mantua *et al.* 1997). The PDO, however, is related spatially and temporally to ENSO, and tropical forcing may dominate North Pacific climatic oscillations (Mantua *et al.* 1997, Linsley *et al.* 2000). ENSO and the PDO can occur simultaneously, and their effects may be synergistic (Gershunov *et al.* 1999, Pohl *et al.* 2002). If occurring out of phase with one another, their effects may be reduced.

1.4 Problem Statement

Evidence of ENSO and PDO trends has been found in historical climatic records (Kaplan *et al.* 2000), and many studies have already shown success in using tree-ring data to uncover past regional climatic variability in the Pacific Northwest (Jessup 1935, Keen 1937, Gedalof and Smith 2001, Knapp *et al.* 2001a, 2001b, 2002, Pohl *et al.* 2002). In the interior Pacific Northwest, however, few tree-ring chronologies extend back earlier than A.D. 1000. To thoroughly analyze past climatic trends, it is important that climatic proxy data extend as deeply into the past as possible. An extension of the interior Pacific Northwest tree-ring record would afford the potential to better analyze past climatic trends and make better predictions of future climatic shifts.

Little research, however, has directly examined the effects of ENSO, the PDO, and other possible interoceanic teleconnections in the interior Pacific Northwest. This has left a void in our understanding of how the climate of this region is linked to and affected by synoptic-scale climatic variability. These large-scale climatic oscillations have profound effects on the Pacific Northwest, and a more thorough knowledge of how they affect the Pacific Northwest on a regional scale may afford us a better overall understanding of how they influence climate on a global scale.

ENSO has a significant effect on the position of atmospheric ridges and troughs across North America that leads to vast differences in continental weather patterns. In the Pacific Northwest, ENSO phase shifts can affect temperature, precipitation, stream flow (Taylor and Hannan 1999), and fire regimes (Heyerdahl *et al.* 2002). In 1997–1998, during the most recent severe El Niño event, much of Oregon was not adversely affected. Winter temperatures were milder than normal, and precipitation and stream flow were

average or slightly below-average, depending on the exact location within the state (Taylor and Hannan 1999, Aguado and Burt 2007).

In comparison to El Niño, however, La Niña events have much more potential to bring severe winter weather to Oregon and other parts of the Pacific Northwest. Severe flooding occurred in many parts of Oregon during the La Niña-influenced winters of 1995–1996 and 1996–1997. Nearly every river in Oregon reached or exceeded flood stage, and some set all-time records. Several people were killed during this La Niña event, and mudslides, landslides, and property loss were widespread across the state (Taylor and Hannan 1999). Many of the previous harsh winters in the Pacific Northwest have also coincided with strong La Niña events (Taylor and Hannan 1999).

The damaging effects of ENSO, however, are not restricted to the Pacific Northwest or even North America. During the 1997–1998 El Niño, much of coastal California experienced severe flooding, mudslides, and extensive property damage, while rainfall totals in parts of Florida were more than twice the previous December record (Aguado and Burt 2007). The total U.S. economic impacts of the 1997–1998 El Niño were estimated to be \$25 billion (National Oceanic and Atmospheric Administration 2002a). Globally, El Niño events can lead to Indian monsoonal failure and widespread famine, and severe droughts, wildfires, and floods in other locations around the world (Taylor and Hannan 1999, Aguado and Burt 2007).

Variations in the PDO may also have significantly influenced climate-sensitive natural resources in the Pacific Northwest and over other parts of North America in the 20th century (D'Arrigo *et al.* 2001, Gedalof and Smith 2001, Peterson and Peterson 2001, Heyerdahl *et al.* 2002, Knapp *et al.* 2002, Benson *et al.* 2003, Norman and Taylor 2003,

Knapp *et al.* 2004). In the Pacific Northwest, phase shifts in the PDO can affect stream flow (Mantua *et al.* 1997, Pohl *et al.* 2002), hydroelectric-power generation (Pohl *et al.* 2002), agricultural production (Hamlet and Lettenmaier 1999, Graumlich *et al.* 2003), and fire regimes (Heyerdahl *et al.* 2002, Norman and Taylor 2003).

In the late 1970s, during a well-documented PDO phase shift (from negative to positive), biologists noted changes in much of the biota around the North Pacific (Mantua and Hare 2002). Mantua and Hare (2002) found that the 70-year catch history of Pacific salmon (*Oncorhynchus* spp.) provided a strong link between the interdecadal fluctuations of North Pacific climate and North Pacific fisheries. The catch history showed that Alaskan salmon population production responds abruptly to interdecadal climatic forcing, with more fish being caught during periods of positive-phase PDO (Francis and Hare 1997). So far, these connections between climatic variability and Alaskan salmon production have been found at the interdecadal (PDO) scale, but not at the interannual (ENSO) scale (Francis and Hare 1997). The far-reaching effects of broad-scale climatic fluctuations, however, do not end with Alaskan salmon. Other fish, zooplankton (Francis *et al.* 1998, Hollowed *et al.* 1998), birds (Vandenbosch 2000), and other organisms are also affected.

As with ENSO, the consequences of the PDO may reach beyond the regional ecology and economy of the Pacific Northwest, the Pacific Ocean, and even the Northern Hemisphere (Benson *et al.* 2003). The PDO may affect climate on a global scale, as well, and climatic anomalies that persist for decades at a time can drastically affect ecosystems and societies (Enfield and Mestas-Núñez 2001, Pohl *et al.* 2002). New studies suggest a symmetry in climatic variations in the Northern and Southern Hemispheres (Linsley *et al.*

2000b, Dettinger *et al.* 2001, Kitzberger *et al.* 2001), and signature PDO responses have been observed in North, South, and Central America, East Asia, and Australia (Enfield and Mestas-Núñez 2001, Mantua and Hare 2002). It is becoming increasingly obvious that climatic fluctuations that occur at one point on the globe may be teleconnected to climatic changes that occur in an opposite hemisphere or in a different ocean.

Understanding these synoptic-scale climatic oscillations, and the effects they have on regional, hemispheric, and global climate, is becoming increasingly important (Biondi *et al.* 2001, Pohl *et al.* 2002) because of the current warming of global temperatures (Burkhardt and Tisdale 1976). Because of these rising temperatures, climatic shifts in the northeastern Pacific Ocean are likely (Ingraham *et al.* 1998) and may become more frequent and more intense in the coming years (Biondi *et al.* 2001, Knapp *et al.* 2002, Pohl *et al.* 2002, Speth 2004). The PDO seems to be intensifying and reversing phases more frequently with the current climatic warming trend (Pohl *et al.* 2002), and the past quarter-century has seen two of the most devastating El Niño events (1982–1983 and 1997–1998) on record. A better understanding of the temporal and spatial extents of ENSO and the PDO, as well as their interactions with other climatic anomalies, will assist us in preparing for future shifts in regional and global climate. More research of this type is especially needed to directly examine the function of large-scale, interannual and interdecadal patterns of climatic variability in the interior portion of the Pacific Northwest. The effects of these climatic fluctuations on ecosystems of the more arid interior locations deserve more attention.

1.5 Objectives of the Study

The specific objectives of my study are:

- to extend the current regional (central Oregon) tree-ring record back in time using western juniper (*Juniperus occidentalis* Hook. ssp. *occidentalis*) samples,
- to statistically analyze the climate-tree growth response,
- to dendrochronologically reconstruct the variability of precipitation, the PDO, and ENSO for south central Oregon for the full length of the chronology, and
- to develop a better understanding of the periodicity, magnitude, and duration of past climate by evaluating trends in radial tree growth.

Chapter 2

Literature Review

2.1 Dendroclimatology in the Pacific Northwest

In Oregon, tree rings serve as meaningful, high-resolution climatic indicators because they are sensitive to certain climatic variables such as late-spring and summer droughts, winter precipitation, and summer temperatures (Brubaker 1980). The best mechanism for reconstructing past climatic conditions in the Pacific Northwest, therefore, may be a dendroclimatological analysis. Dendroclimatological studies in the Pacific Northwest have been previously used to illustrate climatic events. The first section of my literature review summarizes selected examples of these studies. Keen's (1937) seminal work has been a foundation for many Pacific Northwest climatic studies. The Pohl *et al.* (2002) paper is relevant to my work because of the methods they chose, and because of the close proximity of their study area to mine. The Knapp *et al.* (2002, 2004) papers look at some of the same climatic factors (e.g., drought) as this study, and their interpretation of air mass boundaries in central Oregon is important to my study.

2.1.1 Keen (1937)

In the early 20th century, ponderosa pine (*Pinus ponderosa* Douglas ex C. Lawson) forests in eastern Oregon and northeastern California were decimated because of drought and bark beetles. Desert-like climatic conditions invaded areas where pine stands once stood. Foresters questioned whether the drought and the consequential retreat of pine stands represented a long- or short-term trend. At the same time,

entomologists questioned whether pine mortality linked to bark beetle damage might be alleviated by a reversal in climatic change (i.e., an increase in precipitation). Weather records were too short, and lacustrine evidence was too recent or indefinite to shed light on these questions. Therefore, Keen turned to tree-ring data to help answer these questions. By reconstructing past climatic fluctuations from tree rings, he hoped to forecast future climatic behavior and predict the potential duration of the early-20th century drought (Keen 1937).

His study began in 1923 at Klamath Falls, Oregon, and was the first dendroclimatological study performed in eastern Oregon. Ponderosa pine was selected for the study primarily because it was the tree of concern. A radial section or increment core was taken from 1,240 ponderosa pines at 44 locations in eastern Oregon and northeastern California. He believed moisture was the limiting growth factor for the trees in his study, and he hoped to demonstrate the effect of drought on ponderosa pine radial growth rates. He found that trees growing in humid areas exhibited complacent ring patterns; therefore, the trees best suited for his study were the ones growing on the desert edge. The arid-area trees showed much more sensitivity to drought conditions than trees growing anywhere else in the study area, and their rings exhibited obvious fluctuations in growth from year to year (Keen 1937).

During cross identification of his samples, Keen found few false rings, but missing rings were not uncommon, especially following abrupt interruptions in growth. Keen noticed a similar dominant growth pattern that was distinguishable throughout the wide study area, leading him to believe the area consisted of a broad climatic zone, covering a large region east of the Cascade Range. The scope of this climatic zone was

not completely known at the time of his study. Keen believed, however, that major climatic phase shifts produced similar effects throughout the entire study area, and that these effects were only slightly modified by regional climatic conditions.

Keen determined that precipitation was in fact the dominant limiting factor that affected his trees. In his study, seasonal precipitation and tree-ring widths were highly correlated; however, there was sometimes a one-year lag in growth response to precipitation. After 1917, he noticed a definite reduction in radial growth related to a reduction in available moisture. Curiously, this moisture deficit was more noticeable in the tree-ring chronology and Columbia River discharge record than it was in the instrumental precipitation record.

His data suggested that the 15th, 17th, early 19th, and late 19th centuries were particularly wet. The 18th century was interspersed with floods and dry periods. Precipitation amounts for the early 20th century were relatively normal, and the 16th and middle 19th centuries were relatively dry. A severe drought began in 1917 but showed evidence of ending around the late 1930s. The cumulative radial growth suppression of 627% during the years 1917–1936 far exceeded the radial growth suppression of any other period. Keen suggested that this drought was likely related to a major climatic forcing event that affected the entire northern Great Basin (Keen 1937).

2.1.2 Knapp *et al.* (2002)

Knapp *et al.* (2002) developed a method using an index to determine single-year drought events for the interior Pacific Northwest during the period 1500–1998. They also defined climatic boundaries based on a precipitation variance index to (1) provide spatial

guides to years that reflected large-scale unfavorable growing conditions, (2) illustrate radial-growth patterns that were distinctly regional and therefore served as a proxy means to identify climatic boundaries, and (3) discuss the driving forces that accounted for both climatic boundaries and the frequency of single-year droughts.

Chronologies from 18 Pacific Northwest western juniper sites were either developed for the study or selected from ones previously-developed from nearby sites. Because too few chronologies extended prior to 1500, the period 1500–1998 was selected as a common period. To identify single-year drought events, a method was developed using a three-year window in which the annual radial growth index for a single year was divided by the average of the growth indices from the previous and following years. This index was called the climatic pointer year index (CPYI) (Knapp *et al.* 2002).

Although annual winter/spring precipitation was the climatic variable that most affected the growth of western junipers in their area, annual winter/spring precipitation amounts varied considerably from region to region within the Pacific Northwest. This was indicated in climatic records from local weather stations. To account for this variability, the CPYI variance for the 18 chronologies was calculated for the common interval 1734–1979 and then divided by the variance in mean monthly precipitation obtained from the climate station closest to the site from where the samples were collected. This calculation provided a value they called the precipitation variability index (PVI). This index was used for the identification of climatic boundaries.

PVI was mapped for each chronology, and distinct clusters of sites with similar values were identified. After conducting a principal components analysis (PCA), they retained three PCs. PC1 most closely aligned with their Northwest region, PC2 most

closely aligned with their East region, and PC3 most closely aligned with their Southwest region. These regions differed by variability in either the CPYI or monthly precipitation. Varimax orthogonal rotation was then used to search for spatial clusters of stations. The CPYI from all sites within a given region was averaged to obtain a regional value for each year. When the mean CPYI regional value from all sites fell within the lowest 10% CPYI values of all years, that year was labeled an extreme climatic pointer year (CPY). An extreme CPY was identified as “super-regional” if the extreme CPY occurred in all three regions, “regional” if it occurred in two, and “subregional” if it occurred in one.

Extreme CPY occurrence varied considerably across the regions. The Northwest region had high CPYI variance, but low monthly precipitation variance. The East and Southwest regions both had low CPYI variances, but differed in variance in monthly precipitation. The pattern of PC loadings for the 18 sites closely matched the regionalization identified by the PVI map. The Northwest region, with high CPYI variance, was the most distinct of the three regions. This is likely to be because of the location of the region on the marine/interior air mass boundary. Additionally, La Niña events typically promote above average amounts of precipitation in the Pacific Northwest, and El Niño events typically promote below average amounts of precipitation in the Pacific Northwest. ENSO variability may have contributed to high variance in the CPYI. The Northwest regional sites, however, all fall within a region that has a positive, but not significant, correlation with ENSO events. This makes the relationship a bit uncertain. In the East and Southwest regions, winter/spring precipitation events were not correlated with ENSO, and CPYI variances were very consistent. There were more

severe droughts in the Northwest region than in the East and Southwest regions (Knapp *et al.* 2002).

The CPYI identified 11 super-regional extreme CPYs that were common to all three regions. Of these extreme CPYs, seven occurred between 1502 and 1657, while only two occurred after 1717. Following a super-regional drought event in 1717, no CPYs were simultaneously extreme in all three regions until 1924. This suggests a synoptic-level climatic control was in effect during those years. These results are in close agreement with changes that occur along the winter air-mass boundary. The winter air-mass boundary has varied spatially during the past four centuries. A meridional orientation occurred during the 1600s, early 1700s, and 1900s, while a zonal orientation prevailed during the 1700s and 1800s. Changes in the degree of meridionality were likely promoted by a strong wintertime high over Vancouver Island that steered midlatitude storms north of their usual track. This blocking high is a possible cause of the high concentration of drought events during the 1600s (Knapp *et al.* 2002).

The extended period without a CPY may also have been related to the PDO. Cool phases of the PDO occurred from 1900–1924 and 1947–1976, while warm phases of the PDO occurred from 1925–1946 and 1977–1996 (Francis and Hare 1997, Mantua *et al.* 1997, Minobe 1997, Kadonaga *et al.* 1999, Linsley *et al.* 2000b, Biondi *et al.* 2001, Evans *et al.* 2001, Gedalof and Smith 2001, Knapp *et al.* 2002, Mantua and Hare 2002, Pohl *et al.* 2002). The oscillatory frequency of the PDO increased markedly after 1924, concurrent with an increase in frequency and variance of CPYs. In fact, severe and widespread short-term droughts were relatively nonexistent during the period 1717–1923, a period marked by little variation in the PDO (Evans *et al.* 2001, Knapp *et al.* 2002).

2.1.3 Pohl *et al.* (2002)

Ponderosa pine was used by Pohl *et al.* (2002) to develop a 545-year tree-ring chronology in order to study the drought history of central Oregon. They were interested in the relationship between radial growth, drought, ENSO, and the PDO. A secondary function of their study was to compare their ponderosa pine chronology to similar chronologies from western juniper to see if the proxy information from these different species is interchangeable.

The study area was located in Lava Cast Forest in central Oregon where the climate is semi-arid and largely influenced by the rainshadow effect of the Cascade Mountains. Isolated ponderosa pines growing within lava flows were chosen for the study because they were extremely moisture-limited and very sensitive to changes in moisture. Paired increment cores were taken at breast height from each of 50 isolated trees growing on lava flows. A chronology was constructed and calibrated with instrumental climatic data from 1930–1999. They used the four climatic variables from uninterrupted instrumental records that exhibited the strongest relationships with tree growth: two precipitation records, one temperature record, and the Palmer Drought Severity Index (PDSI). The remainder of the instrumental climatic data (1900–1929) was used for independent verification (Pohl *et al.* 2002).

PDSI had the strongest overall relationship with annual radial growth. Temperature and precipitation showed significant relationships with annual radial growth during some months. The ponderosa pine data explained 35% of the variance in historical PDSI values, and revealed four severe drought periods. The most pronounced drought periods in the reconstruction occurred during the 1480s, 1620s, 1700s, and

1930s. The modeled PDSI for A.D. 1489 exhibited the greatest departure from normal. The longest sustained drought during the study period was the Dust Bowl of the 1930s. A significant, but weak relationship was found between the chronology and ENSO (9%) and between the chronology and the PDO (12%), suggesting that the PDO had a slightly greater effect on tree growth than did ENSO. Annual radial growth decreased during positive phases of the PDO and increased during negative phases of the PDO.

Finally, they compared their ponderosa pine chronology to two previously created western juniper chronologies to determine their substitutability as climatic proxies in dendroecological studies. Both types of trees were able to record periods of severe drought. Western juniper, however, was more sensitive to moisture, while ponderosa pine was more sensitive to temperature. Because of this difference, their interchangeability as climatic proxies is limited (Pohl *et al.* 2002).

2.1.4 Knapp *et al.* (2004)

Knapp *et al.* (2004) studied the occurrences and spatial patterns of sustained droughts in the interior Pacific Northwest using tree-ring data from the period 1733–1980. Their primary objective was to demonstrate that drought frequency, particularly for severe droughts, can be affected by the spatial variability of climatic transition zone boundaries. A secondary objective was to determine whether a drought core region exists in the interior Pacific Northwest.

Their tree-ring data consisted of 18 western juniper tree-ring chronologies collected from northern California, southwestern Idaho, northern Nevada, and central and eastern Oregon. They defined moderate drought years based on radial growth rates that

were 20% below average and severe drought years based on radial growth rates that were 40% below average. They mapped November to May precipitation to identify approximate precipitation amounts for each chronology. November to May precipitation was selected because radial growth of western juniper in Oregon is strongly correlated ($r^2 = 0.61$) with these months. They also examined 700-hPa height data to determine upper-level airflow (jet stream) patterns during years of severe drought. Finally, they compared widespread drought occurrences to ENSO mode and the PDO phase (Knapp *et al.* 2004).

They found that frequency of sustained droughts was much greater and duration of sustained droughts was much longer in the northwestern region of the interior Pacific Northwest. This area, therefore, was labeled a drought core region. Within a drought core region, droughts originate, expand, and persist even during years of regional drought contraction. The Pacific Northwest is typically dominated by maritime air during the wet/cool season and by interior air during the dry/warm season. The fluctuation between the two air masses directly affects radial growth of western juniper trees growing in this region. They determined that drought in the Pacific Northwest is mainly caused by the presence of a blocking high pressure cell off the Pacific coast that promotes reduced precipitation during the wet/cool season. When the blocking high pressure cell was present, marine airflow was drastically reduced. Trees were often exposed to drought conditions during these times, leading to reduced radial growth. Although the most severe and persistent droughts were concentrated in the northwestern region of the study area, four large-scale droughts (early 1790s, early 1830s, 1917–1919, and 1933–1937)

also affected the entire study area during the study period. These large-scale droughts occurred mainly during positive phases of the PDO (Knapp *et al.* 2004).

2.2 The Pacific Decadal Oscillation (PDO)

Because of its North Pacific Ocean signature and interdecadal persistence, the most dominant synoptic-scale climatic forcing mechanism in the Pacific Northwest may be the PDO. The second section of my literature review focuses on this climatic oscillation and summarizes selected PDO studies.

2.2.1 Mantua *et al.* (1997)

Mantua *et al.* (1997) studied interdecadal Pacific climatic oscillations and their effects on salmon production. They analyzed tropical and Northern Hemisphere extratropical SST and sea level pressure, winter North American land surface air temperatures and precipitation, winter Northern Hemisphere 500-mb height fields, SST along the western coast of North America, select western North American streamflow records, and salmon landings from Alaska, Washington, Oregon, and California. From these records, they identified a recurring pattern of ocean-atmosphere climatic variability centered over the midlatitude North Pacific basin. During the 20th century, the amplitude of the oscillation varied irregularly at interannual-to-interdecadal timescales. Reversals in the polarity of the oscillation occurred around 1925, 1947, and 1977. The reversals in 1947 and 1977 corresponded with drastic shifts in salmon production in the North Pacific Ocean, especially near Alaska. During the cool phase that began in 1947, Alaskan salmon landings dropped considerably. During the warm phase that began in 1977,

however, Alaskan salmon landings increased considerably. PDO oscillations did not have quite the same effect on salmon landings in the southern range. This may have been a result of anthropogenic factors (Mantua *et al.* 1997).

The climatic oscillation also affected coastal SSTs and continental air temperatures. SSTs from Alaska to southern California varied in phase with the PDO. During positive phases of the PDO, coastal central Alaska experienced an enhanced cyclonic flow of warm, moist air that led to increased precipitation, while British Columbia and Washington experienced an enhanced anticyclonic flow that created warmer and drier conditions. Pacific Northwest snowpack also decreased during warm phases of the PDO. The PDO was also positively correlated with winter precipitation in northern Mexico and southern Florida and negatively correlated with winter precipitation over much of interior North America and the Hawaiian Islands.

The PDO also affected streamflow in major coastal river systems from Alaska to California. During positive phases of the PDO, the annual discharge in the Skeena, Fraser, and Columbia Rivers was 8%, 8%, and 14% lower, respectively, than during negative phases of the PDO. During positive phases of the PDO, however, the Kenai River in the central Gulf of Alaska region was approximately 18% higher than during negative phases of the PDO (Mantua *et al.* 1997).

2.2.2 Minobe (1997)

Minobe (1997) studied interdecadal climatic oscillations over the North Pacific and North America, using instrumental data (air temperature, sea level pressure, and SST) from the North Pacific, North America, the tropical oceans, and tree-ring records

from North America. Climatic regime shifts around 1890 (cool phase), the 1920s (warm phase), the 1940s (cool phase), and the 1970s (warm phase) were detected.

Warmer temperatures coincided with a strengthened Aleutian low. As the Aleutian low deepened, advection of warmer air onto the western coast of North America increased. The opposite occurred when the Aleutian low weakened. On the western side of the Pacific basin, Japanese coastal SSTs provided further evidence for the occurrences of the regime shifts associated with the Aleutian low. The SSTs along the Japanese coast were positively correlated with atmospheric pressure associated with the Aleutian low. Strong winds from the strengthened Aleutian low likely forced the cold Oyashio current farther south along the Japanese coast. The Indian Ocean also exhibited a teleconnection with the Aleutian low. Indian Ocean SSTs were negatively correlated with atmospheric pressure associated with the Aleutian low (Minobe 1997).

To determine the dominant time scale of the climatic variability, Minobe employed the Multi-Taper method (MTM) of spectral analysis. The MTM of spectral analysis is a nonparametric statistical procedure that provides a means for spectral estimation and signal reconstruction of a time series which is believed to exhibit a spectrum containing both continuous and singular components (Percival and Walden 1993). The MTM of spectral analysis is applicable for geophysical signal analysis, including analyses of atmospheric and oceanic data (SSA-MTM Group 2006). The MTM spectrum showed a significant peak at the 95% confidence level between the periods of 50 to 70 years for boreal winter and spring. This result confirmed that individual epochs (cool or warm phases) were approximately 25 to 35 years in length, and the approximate time required for two complete phases was 50 to 70 years.

In addition to analyzing instrumental data, Minobe reconstructed air temperature based on North American tree-ring chronologies from 65 western sites. During the common period, the pattern for the reconstructed air temperature closely matched the pattern of the instrumental data. In the early period during which instrumental data were not available, several other interdecadal shifts in air temperature were detected, especially after the end of the 18th century. The MTM spectrum for the tree-ring chronology also had a statistically significant peak between the periods of 50 to 70 years in the 18th and 19th centuries (Minobe 1997).

2.2.3 Biondi *et al.* (2001)

Biondi *et al.* (2001) studied North Pacific decadal climatic variability since 1661. Six study sites were located in a direction roughly parallel to the North American coastline, from the Transverse Ranges of southern California to Sierra San Pedro Martir in northern Baja California. They selected this area because tree-ring records from this region more strongly correlate with the PDO than with ENSO. Tree-ring records from Jeffrey pine (*Pinus jeffreyi* Balf.) and bigcone Douglas-fir (*Pseudotsuga macrocarpa* (Vasey) Mayr) were gathered and processed according to standard dendrochronological procedures for paleoclimatic reconstruction. A chronology dating to 1661 was then constructed and compared to historical weather records.

They determined that the PDO oscillated on roughly a 23-year cycle and was relatively dormant from the late 1700s until the middle 1800s, and the temporal patterns of the oscillation during the 20th century were more active and varied from those of previous centuries. In the 20th century, the major PDO reversals of 1947 and 1977 were

matched by reversals in tree-growth time series. It should be noted that in their study region, a positive phase of the PDO promotes increased precipitation, while a negative phase of the PDO promotes decreased precipitation. From 1706–1977, the most dramatic PDO or ENSO shifts were focused around 1750, 1905, 1947, and 1977. The 1750 and 1947 shifts were warm-to-cool transitions. The 1750 oscillation, however, might be an isolated excursion and not a true climatic reversal. The 1905 and 1977 shifts were cool-to-warm transitions. The 1905 cool-to-warm transition reported in this study is not widely reported elsewhere in the literature, and may have been a regional occurrence. Finally, they suggested the La Niña that followed the intense El Niño of 1997–1998 might have been the beginning of a cool PDO phase (Biondi *et al.* 2001).

2.2.4 Gedalof and Smith (2001)

Gedalof and Smith (2001) compiled a transect of six tree-ring chronologies from stands of mountain hemlock (*Tsuga mertensiana* (Bong.) Carrière) growing in near-treeline areas from southern Oregon to the Kenai Peninsula, Alaska. The chronologies were compiled from existing sources and newly collected tree-ring series. Summer temperature was the dominant factor that controlled the radial growth of their trees.

The individual site chronologies were compiled into a single series using factor analysis, a statistical technique that is used to explain variability among observed random variables in terms of fewer unobserved random variables called factors. The leading eigenvector (that represented 44% of radial growth variability) was retained and compared to mean winter (December to February), spring (March to May), and annual indices that represented ENSO and the PDO. A partial correlation analysis was then

conducted and indicated that the spring PDO index was most strongly correlated with mountain hemlock radial growth. The correlation analysis also indicated that ENSO did not contribute any unique information about the leading eigenvector that was not also revealed by the PDO index. When compared with historical data from local meteorological stations, the mountain hemlock tree-ring record provided a record of spring PDO variability comparable to that found from meteorological stations (Gedalof and Smith 2001).

The leading eigenvector was used in a simple linear regression to construct a proxy mean spring PDO index back to A.D. 1600. Negative PDO regimes prevailed from 1662–1679, 1696–1711, 1734–1757, 1798–1815, and 1946–1976. Positive PDO regimes prevailed from 1680–1695, 1712–1733, 1758–1797, 1816–1839, 1923–1945, and 1977–present. The PDO was in a weakened oscillatory pattern during the period 1840–1923. This suggests that much of the pre-instrumental record in the Pacific Northwest was characterized by oscillating regimes of relatively warmer and cooler SSTs in the North Pacific Ocean. A wavelet analysis, a statistical technique that divides a signal into shifted and scaled versions of the original time series, was conducted on the reconstructed series to determine the dominant frequency of variability. The analysis showed that there was variability at approximately decadal scales (10 to 20 years). The average duration of a single phase was 23 years. Almost all of the interdecadal shifts (30 to 70 years) occurred before 1840. In contrast, nearly all of the interannual shifts (< 8 years) occurred during the period 1840–1930 (Gedalof and Smith 2001).

2.3 Western Juniper Ecology and Recent Biogeography

Changes in plant community composition and structure have been intensively studied in the Pacific Northwest. Western juniper encroachment into non-traditional habitats is just one example of plant community shifts in the region. Western juniper expansion is closely linked to climatic change in the Pacific Northwest and, therefore, is salient to this study. The following section consists of summaries of selected studies that focus on western juniper expansion in the Pacific Northwest.

2.3.1 Burkhardt and Tisdale (1976)

Invasion of woody plants into herbaceous habitats has been a problem in the western U.S. since the beginning of Euro-American settlement. From an agricultural and land-use aspect, the negative aspects of woody plant invasion include reduced forage production, greater difficulty in handling livestock, increased erosion, and decreased water yields. Burkhardt and Tisdale (1976) studied the causes of western juniper invasion in southwestern Idaho. They suggested that livestock grazing, climatic change, and a reduction in fire frequency have promoted western juniper invasion.

They chose a 200,000 ha area located on top of the Owyhee Plateau in southwestern Idaho for their study site. The area, dominated by sagebrush-grass and western juniper communities, was first occupied by Euro-American settlers in the 1860s. Mature stands of western juniper typically dominate the ridges and rimrocks of their study area, while young western junipers have invaded downslope into the herbaceous communities. The fire history of the study area, mechanisms of seed dispersal, and

physical and biotic characteristics that affect the establishment of western juniper were investigated.

They performed a systematic search of the area to determine the influence of fire on vegetation. Once the reconnaissance was complete, four areas of approximately 260 ha were selected for a detailed study. Each of the four areas consisted of a mosaic of climax and expansion western juniper stands. A reference tree-ring chronology was constructed from cross-sections of 50 trees (Burkhardt and Tisdale 1976).

The pattern of invasion and topography of the study area suggested that downslope seed movement was an important method of western juniper expansion. They released 225 g of radioactive tracer seeds to test this hypothesis. Seed displacement was tracked during subsequent growing seasons with a Geiger-Muller counter. Because western juniper invasion within the study area was occurring mainly in mountain big sagebrush (*Artemisia tridentata* Nutt. ssp. *vaseyana* (Rydb.) Beetle)/ Poaceae communities, studies of western juniper seedling establishment and growth were limited to these communities. Forty-five sample areas were then selected for intensive study. Sites that represented a considerable diversity in range conditions were chosen to allow for possible effects of past grazing use. To obtain a comparable seed source, each of the 45 study areas was located downslope from and close to a climax western juniper stand. Within each study area, vegetation within macroplots of 30.5 x 30.5 m was sampled. The number of western juniper on all plots was counted, and 25% were aged and measured for height. Understory shrub density and grass cover was determined within each macroplot. Relevant site characteristics were recorded that included percent bare ground,

soil texture, soil moisture, soil bulk density, topographic position, elevation, and aspect (Burkhardt and Tisdale 1976).

Fire evidence was found in every climax western juniper stand examined. Very little fire evidence was found in seral sites. Most fires predated Euro-American settlement, with some occurring as early as the 1600s. Fires burned some portion of the Plateau every year before settlement occurred. From 1840–1910, a fire occurred in one of the four study areas every four years. A decline in fire frequency occurred around 1910. Reasons for the decline in fire frequency are likely related to fire-suppression and fire-prevention programs implemented by state and federal governments, the introduction of livestock grazing, the construction of roads and trails which act as firebreaks, and a warmer and drier climate since 1870 which likely reduced fuel production. A fire interval of 30 to 40 years could maintain a sagebrush/bunchgrass community free of western juniper (Burkhardt and Tisdale 1976).

The radioactive seeds were distributed in all directions, but winter dispersal was strictly downslope. Dispersal occurred more rapidly during summer months. This was probably related to increased small animal activity that may have also been a cause for uphill seed dispersal. Larger mammals likely assisted dispersal via kicking or rolling the seeds. Overall, however, seed dispersal occurred primarily downhill and could have promoted new stands of trees downslope from climax stands (Burkhardt and Tisdale 1976).

On northern exposures, the density of older western junipers and the number of western juniper seedlings were positively correlated. Also, soil bulk density and seedling response were positively correlated. Generally, the deeper and less well-drained soils of

valley bottoms favored seedling establishment; whereas, the shallower, but well-drained, soils of upper slopes favored growth after establishment. This relationship suggests that western juniper establishment may have occurred more readily in soil conditions different from those most favorable for western juniper growth. The amount of bare ground was negatively correlated with seedling establishment and seedling density, and the growth rate of western junipers was positively correlated with shrub density. This relationship was likely a function of temperature, because extreme surface temperatures can easily result in seedling mortality. Summer soil surface temperature under sagebrush and mature trees averages 33 °C and 26 °C respectively, compared to 60 °C on bare ground. Most seedlings were found under the crowns of nurse plants (either sagebrush or another western juniper).

Seedling establishment was negatively correlated with the amount of sunlight, while seedling growth was positively correlated with the amount of sunlight. Site factors favorable for the establishment and growth of most herbaceous species were also favorable for the establishment and growth of western juniper seedlings. Competition with herbaceous species seemed to have little effect on western juniper establishment. Interestingly, there was little relationship between seedling survival and precipitation amounts in this study (Burkhardt and Tisdale 1976).

2.3.2 Miller and Rose (1995)

Miller and Rose (1995) studied the historic expansion of western juniper in southeastern Oregon. Western juniper began to increase in density and distribution in the late 1800s when it invaded sagebrush, aspen, and riparian communities. Their study area

was located on Steens Mountain, Oregon. Plot locations were selected in an attempt to reflect sagebrush-grassland communities in different stages of western juniper invasion. Twenty-two 0.4 ha plots were located within the western juniper belt of Steens Mountain. An additional six 0.1 ha plots were located in six separate quaking aspen (*Populus tremuloides* Michx.) stands undergoing various stages of western juniper invasion (Miller and Rose 1995).

Density was recorded for trees greater than 0.5 m tall. Tree height, minimal and maximal crown diameter, basal area, establishment location of juveniles, and male and female reproductive status were recorded. In each plot, a 10-tree subsample was randomly selected for aging in each of four height classes. Cross-sections were taken from trees to determine their age. In the quaking aspen plots, densities of western junipers and quaking aspens, as well as age and height of western junipers, were determined (Miller and Rose 1995).

Very few older western junipers were found. The first signs of an increase in western juniper density occurred in the 1880s. Relatively steady establishment continued into the 1950s. In the 1960s, western juniper density increased at a geometric rate. The greatest densities of western juniper were found in the quaking aspen plots, where very few aspens remained. Western juniper seedlings that established beneath sagebrush grew faster than young trees growing without the shade of a nurse plant. In western junipers over 0.5 m tall, 32% expressed predominantly male-only or female-only characteristics, 38% expressed both male and female characteristics, and 30% contained neither fruits nor cones. Approximately 75% of western junipers that produced heavy crops of berries

or cones were > 50 years old. Trees < 20 years old rarely expressed reproductive characteristics (Miller and Rose 1995).

A five-fold increase in western juniper pollen during the late-20th century, an abundance of younger trees, and the limited distribution of trees > 130 years old suggest that western juniper has greatly expanded on Steens Mountain during the past 100 years. Expansion coincided with Euro-American settlement. Climatic change (the end of the Little Ice Age), altered fire regimes, livestock grazing in the late 1800s, and an increase in sagebrush cover were primary factors that likely assisted the expansion of western juniper (Miller and Rose 1995). Fire-frequency intervals of 30 to 40 years would be adequate to keep western juniper from invading a sagebrush-grassland community. The reduction of fine fuels by livestock grazing, however, greatly reduced the potential for wildfires. Also, quaking aspen is considered a fire-dependent species. In the absence of fire, it cannot compete with western juniper. The accelerated increase in western juniper density and invasion is probably closely related to the continued absence of fire, abundant woody plant cover, and an increase in western juniper seed rain (Miller and Rose 1995).

2.3.3 Miller and Rose (1999)

Miller and Rose (1999) documented the fire history and successional development of a western juniper woodland on a sagebrush steppe in south central Oregon. Plants associated with western juniper in this area include mountain big sagebrush and Idaho fescue (*Festuca idahoensis* Elmer), found in moderate to moderately deep soils, and low sagebrush (*Artemisia arbuscula* Nutt.) and Sandberg's bluegrass (*Poa sandbergii* Vasey), found in stony, shallow clay soils on the benchlands. Fire suppression began in the area

in 1908, but suppression efforts were minimal until the late 1940s (Miller and Rose 1999).

A 5,000 ha study area was chosen in the Fremont National Forest in the upper Chewaucan River basin near Paisley, Oregon. From a grid, 250 study points were systematically selected. Plant community, percent slope, aspect, elevation, and evidence of presettlement juniper establishment were documented at each point. Each site was also categorized as an early ($\leq 5\%$), middle (6 to 20%), late (21 to 35%), or closed ($> 35\%$) woodland transition stage, based on western juniper canopy coverage. Eight plots were randomly selected in each of the early, middle, and closed woodland transition stages in the mountain big sagebrush steppe community. Eight plots were also randomly selected in the early low sagebrush steppe community. The early woodland transition stage was the only woodland transition stage present in the low sagebrush steppe community.

Western juniper density, height, and canopy cover were measured at each of the 32 study sites in a circular plot with a radius of 20 m in the mountain big sagebrush communities and 30 m in the low sagebrush steppe communities. Each tree was counted, and tree and shrub canopy cover were estimated. All western junipers within the study plots were cored or cross-sectioned, and the number of standing dead trees, stumps, and downed logs was recorded for each plot (Miller and Rose 1999).

Expansion began during the period 1875–1885 in both low sagebrush and mountain big sagebrush communities. Mean age of the trees across the study area was 68 years. Presettlement western junipers (> 130 years old) accounted for $< 1\%$ of the total population. Western juniper density has increased in the low sagebrush steppe

communities since the 1870s, but not as much as in mountain big sagebrush steppe communities. This is related to slow western juniper recruitment and growth rates in the low sagebrush steppe communities. Two patterns of woodland development, open and closed, occurred across the study area. Open woodlands accounted for 42% and 46% of the land area for mountain big sagebrush communities and low sagebrush communities, respectively. Saplings were common and shrub cover was still a dominant component in the open woodlands. In the closed woodlands, saplings were absent and the skeletons of dead shrubs characterized the understory. Western juniper establishment in closed woodlands peaked during the period 1885–1915. Establishment in open stands occurred more gradually and continued throughout the 20th century (Miller and Rose 1999).

Ten ponderosa pine cross-sections from four of the study sites were used to determine fire history. Ponderosa pines were used because thin-barked western junipers typically do not survive fires. Samples were crossdated to assign accurate dates to each fire scar. A large fire was defined as one recorded in three or more clusters in the same year. Seasonality of fires was estimated from the position of the fire scar within the annual growth ring. The fire history in the fuel-limited low sagebrush steppe community was determined using cross-sections from 12 burned western juniper stumps and logs found in the Ennis Butte basin. It was assumed that synchronous fire dates on three or more samples distributed across the area indicated a fire that burned across the low sagebrush community. Before 1871, a fire occurred somewhere within the study area once every 7.7 years. None of the fire-scarred trees, however, was scarred by fire during the last 99 years (Miller and Rose 1999).

Western juniper establishment coincided with increases in domestic livestock, reduction in fire frequency, and increased radial tree growth. Livestock grazing may have enhanced western juniper expansion through the reduction of fine fuels, alteration of plant community structure (i.e. sagebrush cover increases in the presence of heavy grazing and reduced fire occurrence, thus more nurse plants for western juniper are available), and reduced competition with herbaceous species. Prior to 1871, there was a 100% probability of a fire occurring every 45 years in mountain big sagebrush steppe communities. Mean fire-return intervals were considerably longer in the low sagebrush communities because of lower productivity and fuel accumulations. A fire-return interval of 15 years would likely inhibit western juniper encroachment into mountain big sagebrush steppe communities. After the end of the Little Ice Age in the middle 1800s, winters became milder and precipitation increased above the current long-term average until 1916. Radial growth increased during that period, and western juniper establishment peaked across the study area (Miller and Rose 1999).

2.3.4 Soulé *et al.* (2003)

Soulé *et al.* (2003) examined changes in canopy cover for adult western juniper in central Oregon from the 1960s–1994 via repeat aerial photography. They compared eight sites, four that consisted of research natural areas with little anthropogenic disturbance and four matched sites that had undergone typical rangeland disturbance. The sites were considered disturbed if they contained exotic plants such as cheatgrass (*Bromus tectorum* L.).

Aerial photographs from the 1960s–1994 were scanned for each site. The photographs were coded into juniper or non-juniper areas, and the total area of juniper coverage on each photograph was determined. Next, the effects of climate on tree growth were analyzed through a dendrochronological analysis. Approximately 100 trees per site were randomly sampled along systematic transects with at least two cores extracted per tree. The rings on all cores were crossdated and two chronologies were constructed for each site (Soulé *et al.* 2003).

The results revealed an average doubling of cover for mature western juniper over a 27- to 35-year period across the eight sites. Afforestation on the disturbed sites was greater, however, mainly because of livestock grazing. Comparatively younger woodlands exhibited greater relative increases in western juniper coverage. October to June precipitation was the climatic factor responsible for the greatest amount of variance in tree growth. October to June precipitation remained unchanged (or decreased) during the study period, and mean radial growth was above average at all sites during the period of study. Increases in radial growth, however, largely occurred from 1978–1994 after a drought in 1977 (Soulé *et al.* 2003).

Several factors promoted afforestation at all sites. First, fire suppression allowed young, extremely fire-intolerant western junipers to reach maturity. Second, favorable (wetter) climatic conditions during portions of the 20th century afforded western juniper more favorable growing conditions. Third, as new trees reached reproductive maturity, the effects of biological inertia increased the chances of continued afforestation. Fourth, livestock grazing favored expansion as competitive grasses were removed, fine fuels were reduced, shrub growth increased, and western juniper seed rain increased. Finally,

western junipers may have become much less sensitive to dry conditions in the latter part of the 20th century because of the drought-ameliorating effects of elevated atmospheric CO₂ levels. As a consequence, western juniper canopy-cover reductions in response to drought were possibly reduced (Soulé *et al.* 2003).

Chapter 3

Site Description

3.1 Introduction

“The Oregon desert is the “high desert” and is not so hot as Iran, not so wind-combed as the Sahara, and its nights are usually cold. It may be snow-covered in winter.”

-E.R. Jackman, native High Desert Oregonian, 1964

Samples for this study were collected on Bureau of Land Management lands around Frederick Butte (43°37'08" N, 120°27'55" W) in the High Desert of central Oregon. Frederick Butte is located primarily in Deschutes County, Oregon, but the southern extent of the butte crosses into Lake County, Oregon. The elevation of the Frederick Butte summit is 1722 m. The samples were collected from two sites (Frederick Butte North and Frederick Butte South) at lower elevations (approximately 1370 m) on the lava plains located around the base of Frederick Butte. The slope of the study sites is negligible. The Level III and Level IV Ecoregions for the study area are the Northern Basin and Range and the High Lava Plains, respectively (United States Environmental Protection Agency 2006). The area is situated on the edge of the *Juniperus occidentalis* Zone, an ecotone between ponderosa pine forest and sagebrush-steppe (Driscoll 1964). In this ecotone, the precipitation regime changes drastically from the wet Cascades in western Oregon to the dry High Desert in eastern Oregon (Franklin and Dyrness 1988, Pohl *et al.* 2002). Where climate is more limiting to tree growth, mean sensitivity of tree rings tends to be higher (Fritts 1976). Because of this, the area can act as a very sensitive climatic-change indicator region.

3.2 Geology

3.2.1 Physiography

Central Oregon is located within the Intermontane Plateau physiographic region and is divided into several physiographic divisions, provinces, and sections. The major physiographic provinces in central Oregon are the High Cascades, the High Lava Plains, and the Basin and Range (Catchings and Mooney 1988). Frederick Butte, a volcanic butte that arose during the Pliocene epoch (5.3–1.8 mya), is located in the High Lava Plains physiographic province of central Oregon (Figure 3.1). Frederick Butte is one of many buttes and cinder cones interspersed throughout the High Lava Plains. The High Lava Plains province is approximately 80 km wide and 250 km long, and consists of a continuous plateau that averages just over 1,600 m above sea level (Walker and Nolf 1981). The plateau is characterized by extensive lava flows that are interrupted by cinder cones and lava buttes. Undrained basins with playas are also common (Franklin and Dyrness 1988). The High Lava Plains are bordered by the Blue Mountains to the north, the Basin and Range to the south, the Owyhee Uplands to the east, and the Cascade Mountains to the west (Catchings and Mooney 1988, Orr *et al.* 1992).

3.2.2 Geomorphology

Much of present-day Oregon was covered by warm seas from the Carboniferous Period through the Cretaceous Period (354–65 mya). This was also a period of increased volcanism in Oregon (Baldwin 1964). During the Eocene epoch (55.5–33.7 mya), the Coast and Cascade Ranges began to rise and the sea receded westward from central and eastern Oregon (Baldwin 1964, Orr *et al.* 1992).

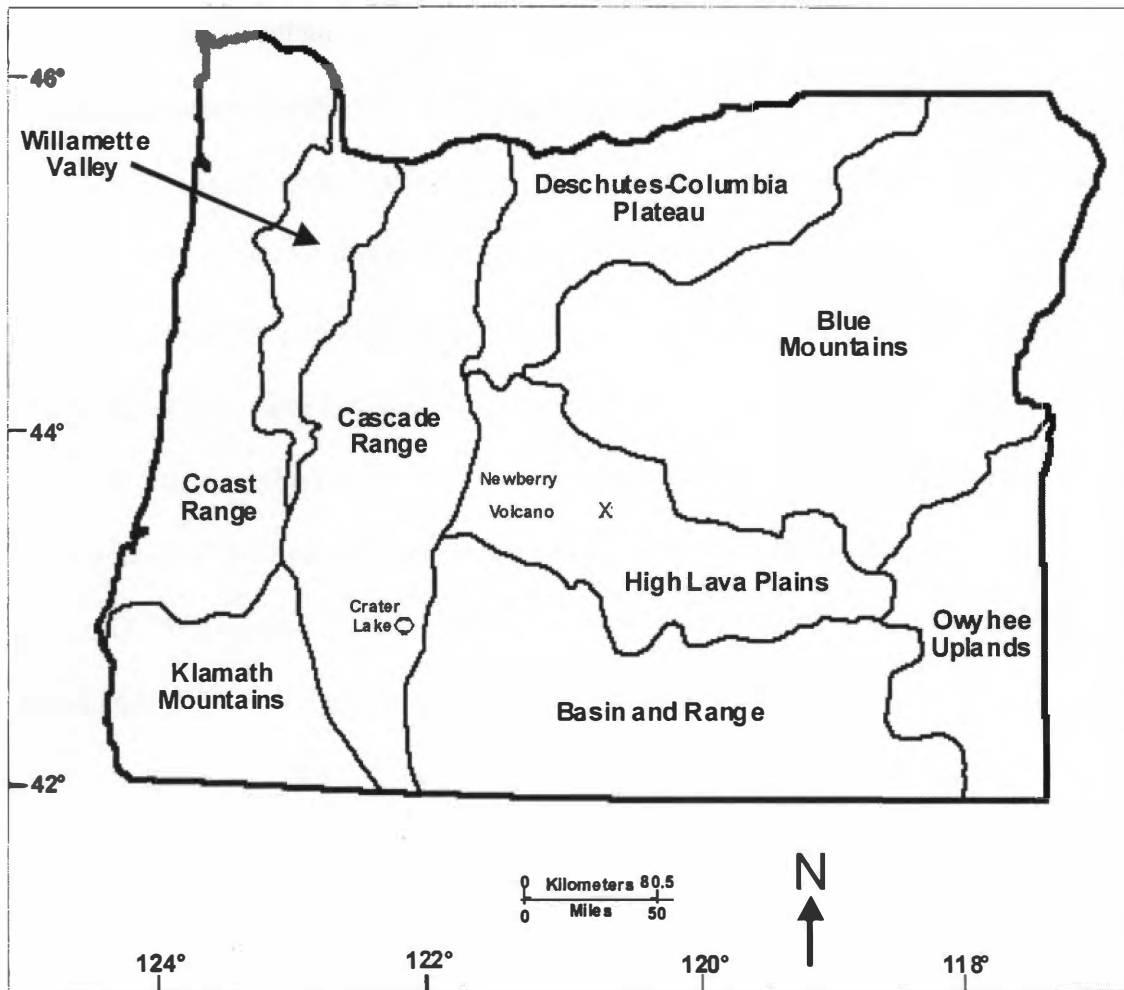


Figure 3.1 The High Lava Plains and other physiographic provinces of Oregon. The study area is marked with an "x".

Thick layers of lava extruded over much of Oregon during the Miocene epoch (23.8–5.3 mya) as the forces of crustal stretching and the movement of tectonic plates initiated faulting, widespread volcanism, and the development of the Basin and Range horst and graben topography characteristic of present-day south central Oregon (Catchings and Mooney 1988, Orr *et al.* 1992). Multiple eruptions occurred for millions of years along a broad northwestern trending zone of normal and strike-slip faults known as the Brothers Fault Zone (Catchings and Mooney 1988). This fault zone was created by the same tectonic forces that have rotated Oregon in a clockwise motion throughout the Cenozoic era (65 mya–Present) (Catchings and Mooney 1988, Gutmanis 1989, Orr *et al.* 1992). Today, the area is covered by up to 5 km of volcanic and sedimentary debris that overlie crystalline basement rocks.

Two types of lava occur in this province. The predominant darker basaltic lava originated deep within the crust, likely appeared during the early stages of eruptions, and rose to extremely high temperatures before cooling. The less common lighter-colored rhyolitic lava originated within shallow chambers, likely occurred later in the eruption cycle, and achieved relatively lower temperatures than the basaltic lava (Catchings and Mooney 1988, Gutmanis 1989, Orr *et al.* 1992). The most recent volcanism occurred closest to the northwestern terminus of the Brothers Fault Zone, near Newberry Crater (Catchings and Mooney 1988, Gutmanis 1989). Lava flows become increasingly older toward the southeastern terminus of the Brothers Fault Zone, near Harney Basin (Walker and Nolf 1981, Catchings and Mooney 1988, Gutmanis 1989). The oldest exposed rocks in the High Lava Plains province are aphyric and phyric basalts (with plagioclase phenocrysts) and andesite. These rocks formed from lava that extruded from the Brothers

Fault Zone during the Miocene epoch and compose a large complex of volcanic rock known as the Steens Basalt (Walker and Nolf 1981).

The orogenesis of the Coast and Cascade Ranges continued during the Miocene epoch, and the rainshadow of the Cascade Range began to influence the climate of eastern Oregon during this time (Baldwin 1964). The Cascade Range rainshadow has contributed to the poorly developed network of streams and the overall lack of deep canyons and gullies in central Oregon. The formation of the High Cascades began with the growth of broad shield volcanoes during the early Pliocene epoch (5.3–1.8 mya). Basaltic and andesitic flows from these volcanoes further contributed to the physical and climatic division between eastern and western Oregon (Myhrum and Ferry 2002).

Major glaciation occurred during the Pleistocene epoch (1.8 mya–10,000 years ago). Colder temperatures during this epoch led to increased alpine glaciation in the Blue Mountains, the Cascade Range, and along Steens Mountain (Orr *et al.* 1992).

Continental glaciation to the north caused extensive flooding in Oregon during the Pleistocene epoch, as ice dams along the upper drainage of the Columbia River periodically failed and released huge floods that scoured the Columbia River channel (Orr *et al.* 1992). Several presently dry basins contained lakes during the Pleistocene epoch (Franklin and Dyrness 1988, Orr *et al.* 1992). New episodes of Pleistocene volcanism produced Newberry Crater, located near the northwestern terminus of the Brothers Fault Zone at the High Cascade/High Lava Plains/Basin and Range physiographic boundary (Catchings and Mooney 1988, Gutmanis 1989). Newberry Crater lies in Paulina Peak, the largest shield volcano in the High Lava Plains province (Franklin and Dyrness 1988). Eventual climatic warming marked the end of the

Pleistocene epoch, and it was during this time that an ice-free corridor opened through Canada to Alaska and Asia across Beringia. The land bridge offered a passage for intercontinental mammalian migration, and prehistoric humans may have first entered North America during this time (Orr *et al.* 1992).

The Holocene epoch (10,000 years ago–Present) is marked by two major volcanic eruptions that affected central Oregon. Mt. Mazama, a High Cascade peak, erupted 6,600 years ago and deposited ash over most of central Oregon (Myhrum and Ferry 2002). During the eruption, Mt. Mazama lost 760 to 1100 m of its height. The large caldera that remained later filled with water and formed Crater Lake. An eruption of Newberry Crater 4,000 years ago deposited pumice and ash over an extensive area to the north and east of Paulina Peak, the mountain that contains Newberry Crater (Franklin and Dyrness 1988).

3.2.3 Soils

Most soil development in central Oregon began during the Pliocene epoch and has continued into the present. There are three widespread soil great groups in the High Lava Plains physiographic province: Haplargids, Camborthids, and Vitrandepts. Less abundant great groups found in the High Lava Plains include Durargids, Argixerolls, Haploxerolls, Natrargids, Haplaquolls, Haplaquepts, Haplorhents, Durorthids, and Rockland, a miscellaneous land type that consists of rock outcrops and other rocky surfaces (Franklin and Dyrness 1988, Myhrum and Ferry 2002). In many areas, volcanic ash and Quaternary sediments (alluvium, lake deposits, and eolian sediments eroded from

the volcanic uplands) cover the volcanic flows of central Oregon (Sowder and Mowat 1965, Franklin and Dyrness 1988).

The study sites are located within the Beden-Ninemile soil unit in central Oregon (Myhrum and Ferry 2002). These are generally cool, well-drained, organic-poor soils that typically formed in residuum with ash that was largely produced during eruptions of Mt. Mazama and Newberry Volcano. Soil temperatures are typically cooler as ash content and elevation increase (Myhrum and Ferry 2002). The unit is approximately 55% Beden soils, 25% Ninemile soils, and 20% soils of minor extent.

The northern extent of Frederick Butte is characterized by soils of the Stookmoor-Westbutte complex. These soils are typically located on north-facing slopes. Stookmoor soils are associated with hills and lava plains and are moderately deep and somewhat excessively-drained. Stookmoor soils are ashy, frigid Vitritorrandic Haploxerolls. The parent material is ash. The typical profile of Stookmoor soils is grayish brown sandy loam (0–15 cm), grayish brown and pale brown sandy loam (15–61 cm), and basalt (below 61 cm). The pH of the profile is neutral to moderately alkaline (Myhrum and Ferry 2002). Westbutte soils are typically associated with hills and are moderately deep and well-drained. They are loamy-skeletal, mixed, frigid Pachic Haploxerolls. The parent material is colluvium, derived from basalt or tuff, with ash on the surface. The typical profile of Westbutte soils is very dark grayish brown stony loam (0–23 cm), dark brown very cobbly loam (23–53 cm), brown very cobbly clay loam (53–76 cm), and welded tuff (below 76 cm). The pH of the profile is neutral to mildly alkaline (Myhrum and Ferry 2002). Both soils have a depth to bedrock of approximately 51 to 102 cm.

The Redcliff-Rock outcrop complex surrounds Frederick Butte on all sides except for the northeastern slope. These soils are often associated with south-facing slopes, and are moderately deep and well-drained. Redcliff soils are loamy-skeletal, mixed, mesic Aridic Haploxerolls. The parent material is colluvium and residuum derived from basalt. The typical profile of Redcliff soils is brown very gravelly loam (0–48 cm), dark yellowish brown extremely gravelly clay loam (48–63.5 cm), and fractured rhyolite (below 63.5 cm). Depth to bedrock is approximately 51 to 102 cm. The pH of the profile is neutral (Myhrum and Ferry 2002).

The Beden stony sandy loam complex mantles a large area to the northeast of Frederick Butte. These soils are associated with lava plains and hills and are shallow and well-drained. Beden soils are loamy, mixed, frigid Lithic Argixerolls. The parent material is ash over residuum derived from basalt or welded tuff. The typical profile of Beden stony sandy loam soils is grayish brown and brown stony sandy loam (0–28 cm), brown loam (28–38 cm), brown clay loam (38–46 cm), and basalt (below 46 cm) (Myhrum and Ferry 2002). Depth to bedrock is approximately 25 to 51 cm. The pH of the profile is neutral to mildly alkaline (Myhrum and Ferry 2002).

3.3 Oregon Climate

3.3.1 General Overview Along a West–East Transect

Climate in Oregon varies across the state because of topographic variations and the influence of different air masses (Franklin and Dyrness 1988). Coastal regions are usually cool, cloudy, and wet, the mountains are generally cool to cold and often wet and/or snowy, and the areas in rainshadows to the east of the Cascades are commonly

sunny and dry in the summer and cold in the winter (Franklin and Dyrness 1988, Taylor and Hannan 1999).

The generalized climate for coastal Oregon is marine west coast, with mild-to-cool summers. This is a mesothermal climate in which the mean temperature of the warmest month is $> 10^{\circ}\text{C}$ (but $< 22^{\circ}\text{C}$), the mean temperature of the coldest month is $> 0^{\circ}\text{C}$ (but $< 18^{\circ}\text{C}$), and four months experience mean temperatures $> 10^{\circ}\text{C}$ (Köppen 1931). The higher-elevation areas of the Oregon Cascades tend to be colder than adjacent lowlands, as altitude and exposure to sun become the major climatic controls. In many other respects, however, the climate of highland locations is closely related to that of the adjacent lowlands, particularly with regard to wet and dry seasons. The generalized climate for the dry regions east of the Cascades is cold midlatitude steppe, where the mean annual temperature is $< 18^{\circ}\text{C}$. In this climate, potential evapotranspiration exceeds precipitation, which is greater than half, but not equal to, the natural moisture demand (Köppen 1931). Temperatures here fluctuate more widely than temperatures west of the Cascades (Franklin and Dyrness 1988).

3.3.1.1 Oregon Climatic Zones

The National Oceanic and Atmospheric Administration (NOAA) has divided Oregon into nine climatic zones (Figure 3.2). Each zone represents an area with similar annual temperature and precipitation totals (Climate Diagnostics Center 2006). Across the state, precipitation totals for winter are typically greater than precipitation totals for

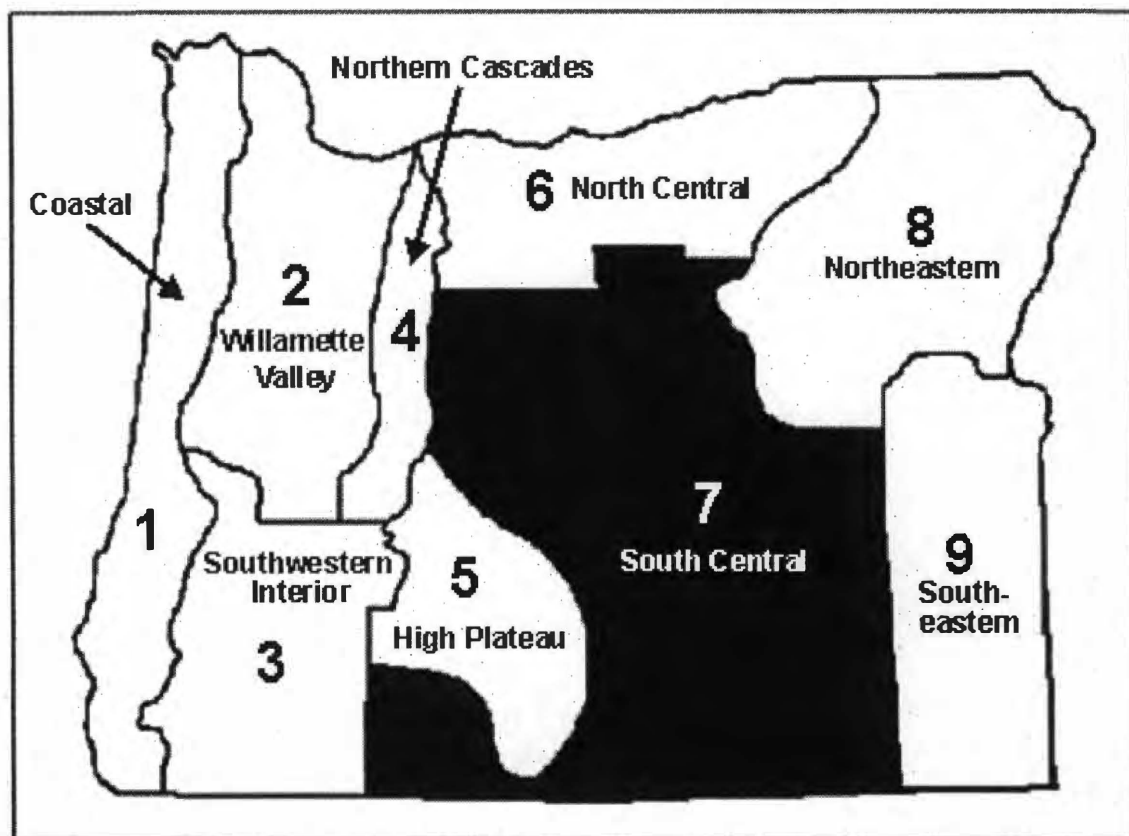


Figure 3.2 Oregon climatic zones. Frederick Butte is located in Zone 7.

summer (Bradley 1976, Western Regional Climate Center 2006), while temperatures tend to fluctuate dramatically and are greatly affected by the Pacific Ocean and elevation gradients. The study sites are situated in Zone 7, the High Lava Plains-South Central Area. This region is a high desert prairie that receives little rainfall (Taylor and Hannan 1999). Temperatures are characterized by warm summers and cool winters.

3.3.2 Climate of Frederick Butte

Climatic data (1971–2000) recorded at the Brothers, Oregon, climate station (elev. 1,414 m) were chosen to describe the climate of the study sites. This station, although not in existence quite as long as the Bend, Oregon, climate station, was chosen because of its close proximity (approximately 25 km NNW) to the study sites.

3.3.2.1 Temperature

Summer temperatures around Frederick Butte tend to be quite warm. The Brothers climate station, nevertheless, generally records some of the coldest temperatures in Zone 7 (Taylor and Hannan 1999). The monthly mean temperature at Brothers, Oregon, is 5.9 °C with monthly mean maximum and minimum temperatures of 14.2 °C and –2.4 °C, respectively (National Oceanic and Atmospheric Administration 2002b, Oregon Climate Service 2006). The average summer temperature (June, July, and August) is 14.8 °C, and the average winter temperature (December, January, and February) is –2.3 °C (National Oceanic and Atmospheric Administration 2002b, Oregon Climate Service 2006). The average growing seasons at ≥ 0 °C and ≥ -2.2 °C are 36 and 57 days, respectively. The median dates of the last and first frosts (0 °C) are July 13 and

August 13, respectively (Oregon Climate Service 2006). Frost-free days, however, can occur from June to September (Oregon Climate Service 2006). The hottest day recorded from 1971–2000 was 37.2 °C on August 6–8, 1972. The coldest day recorded from 1971–2000 was –34.4 °C on December 23, 1983 (Oregon Climate Service 2006). The mean hottest and coldest years from 1971–2000 were 1998 and 1979, respectively (National Oceanic and Atmospheric Administration 2002b).

3.3.2.2 Precipitation

The Brothers climate station is similar to most other Zone 7 climate stations in that it receives the highest amounts of precipitation in the winter months with a secondary maximum that occurs during late spring and early summer. Within Oregon, this precipitation pattern only occurs east of the Cascades (Henry 1906). Precipitation is primarily cyclonic in origin (Franklin and Dyness 1988). Mean annual precipitation is 23 cm, of which 31% falls between November to January (National Oceanic and Atmospheric Administration 2002b, Oregon Climate Service 2006). February and September are generally the driest months of the year. The secondary maximum usually occurs in May and June and accounts for 22% of the mean annual precipitation (National Oceanic and Atmospheric Administration 2002b, Oregon Climate Service 2006). The area receives approximately 54 cm of snowfall annually (Oregon Climate Service 2006). Snowfall accounts for approximately 23% of total annual precipitation. The peak season for snowfall is November to January, during which approximately 64% of total annual snowfall occurs. June to September is generally a snow-free period, but, depending on

temperature and available atmospheric moisture, snowfall can occur during these months (Figure 3.3).

3.3.3 Typical Factors That Affect Oregon Climate

The climate of Oregon is affected by a variety of complex factors, many of which experience cyclical changes (Brubaker 1980). The Pacific Ocean is one influential factor. Seasonality, large-scale atmospheric and oceanic circulations, and the topography of the region are other important factors. A rainshadow dominates the climate east of the Cascade Mountains, including the climate of Frederick Butte.

These factors, however, do not act alone in producing the climate of Oregon. An example of the interactions of these climatic factors may begin with a moist onshore flow from the Pacific Ocean. Once the moist air mass encounters the Coastal Range or the Cascades, it may experience orographic lifting and produce large amounts of precipitation on the windward side of the mountains, while the leeward side of the mountains remains relatively dry (Oregon Climate Service 2006).

3.3.3.1 Seasonal Climatic Regimes

The climatic diversity of Oregon becomes even more complex as the seasons change. During summer months, Oregon is typically dominated by a surface high-pressure cell centered over the North Pacific Ocean. Prevailing westerly winds decrease in intensity, and storms are usually diverted far to the north (Taylor and Hannan 1999). Also during summer, inland temperatures tend to be warmer than those along the coast.

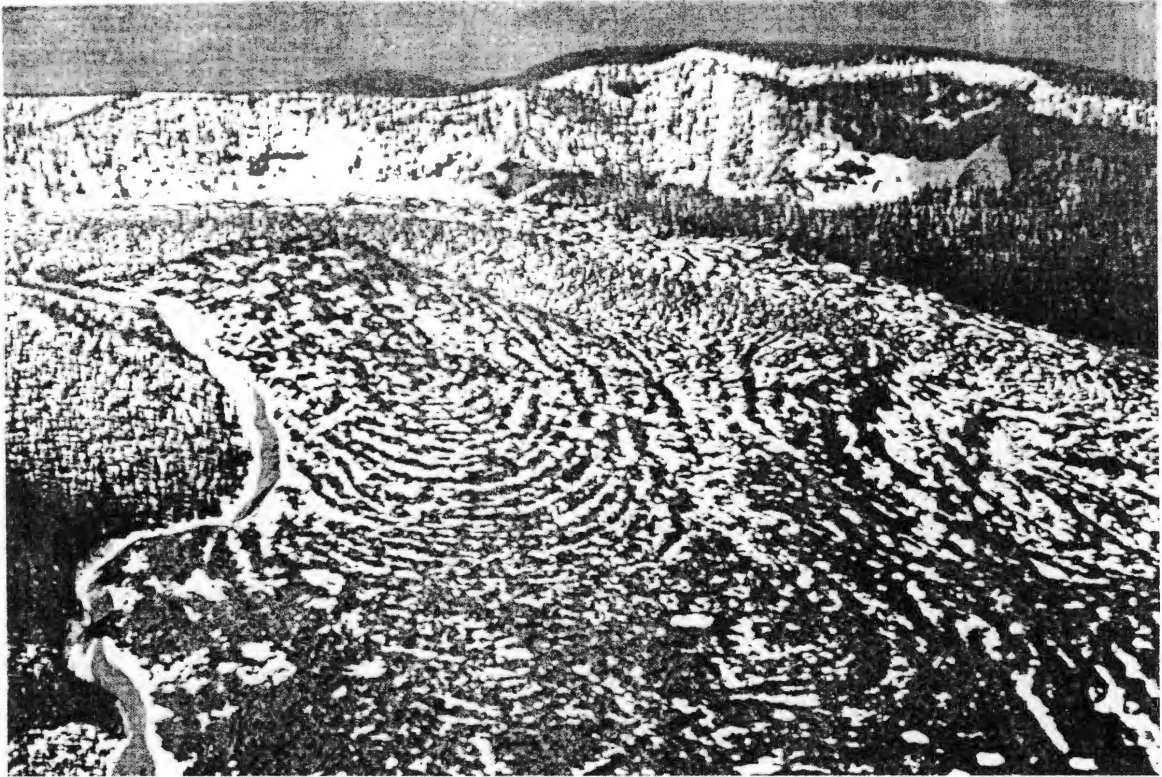


Figure 3.3 Early snow on a Newberry Crater lava flow (photo courtesy of Jim Anderson, Oregon Museum of Science and Industry, Portland, Oregon).

With the seasonal change to autumn, the subsolar point migrates southward toward the Equator, and the surface high-pressure cell located off the coast of Oregon weakens and also migrates southward (Taylor and Hannan 1999). Southward-flowing ocean currents weaken and are eventually supplanted by strengthened northward-flowing currents. This effectively stops oceanic upwelling along the Oregon coast (Taylor and Hannan 1999). As autumn gives way to winter, cyclones once again are ushered inland by strengthened westerlies in the absence of the blocking surface high-pressure cell (Henry 1906, Franklin and Dyrness 1988). The likelihood of precipitation in Oregon drastically increases. The cycle continues with the coming of spring, when the storm

track begins its northward progression, and the chances of precipitation are reduced (Taylor and Hannan 1999).

3.3.3.2 Air Masses

Oregon is affected by air masses that originate in several neighboring regions (Figure 3.4), but the air mass types with the greatest influence on the climate of Oregon are moist, maritime air masses that originate in the Pacific Ocean. Maritime influences are strongest near the coast, but even eastern Oregon can periodically receive still-moist Pacific air (Oregon Climate Service 2006). The maritime effect fosters a large percentage of the precipitation in Oregon, and it also moderates terrestrial temperatures. The Pacific air masses are especially dominant during the winter months. Compared to the Pacific air masses, air masses that originate in the Gulf of Alaska, the Great Basin, and from continental polar outbreaks can bring colder temperatures to Oregon. Air masses that originate in the Great Basin and polar regions are usually very dry, whereas the flow from the Gulf of Alaska area tends to usher in cool, moist air. The Great Basin, however, also produces some very dry and hot air masses during the summer (Taylor and Hannan 1999).

Subtropical air is responsible for creating some of the wettest months in Oregon. This warm, moist flow is sometimes referred to as the “Pineapple Express” because it generally originates near Hawaii (Taylor and Hannan 1999). Finally, another southerly type of flow, originating in California, generally brings warmer air to Oregon. If this occurs during the summer months, thunderstorms may occur, especially in eastern



Figure 3.4 Air masses that affect Oregon.

Oregon (Henry 1906, Taylor and Hannan 1999). The normally predominant trajectories of these air masses are generally disrupted during positive phases of ENSO and the PDO.

3.4 Land Use and Fire History

3.4.1 Land Use

After the last glacial maximum when altered climate still filled the High Desert with large freshwater lakes, more Native Americans (Figure 3.5) lived, fished, and hunted in this area than in any other part of Oregon (Jackman and Long 1964). The Klamath Lakes, Warm Springs, Paiute, Molalla, Cayuse, and Sahaptin Indians lived, hunted, fished, or gathered food around central Oregon (Myhrum and Ferry 2002). The pursuit of beaver pelts brought the first Europeans into the area. In 1825, Peter Skene Ogden of the Hudson's Bay Company was the first Euro-American to see central Oregon. Euro-American settlers began to arrive in large numbers after President Abraham Lincoln signed the Homestead Act in 1862 (Jackman and Long 1964). By 1911, the High Desert was heavily populated with new settlers, but the population gradually declined into the 1930s (Eddleman 1989). Livestock grazing, the introduction of alien plant species, abandonment of disturbed agricultural land, fire suppression, and drought led to major changes in the central Oregon landscape during this period (Eddleman 1989, Miller 1989).

By the end of the 1890s, competition for forage between herds of sheep was intense, and over-grazing often resulted in barren landscapes. Early-settlement cattle grazing peaked around 1910 (Figure 3.6). Sheep populations also increased dramatically during this period (Figure 3.7). The horse population peaked around 1917 and many



Figure 3.5 Native American petroglyph in the Oregon High Desert (photo courtesy of Lake County, Oregon, Chamber of Commerce).

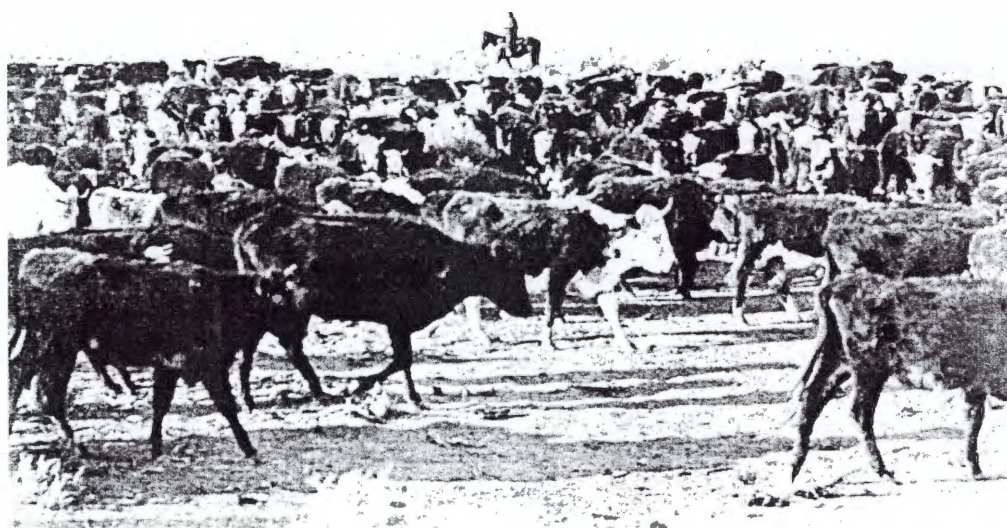


Figure 3.6 Oregon High Desert cattle drive (photo courtesy of the Schminck Memorial Museum, Lakeview, Oregon).

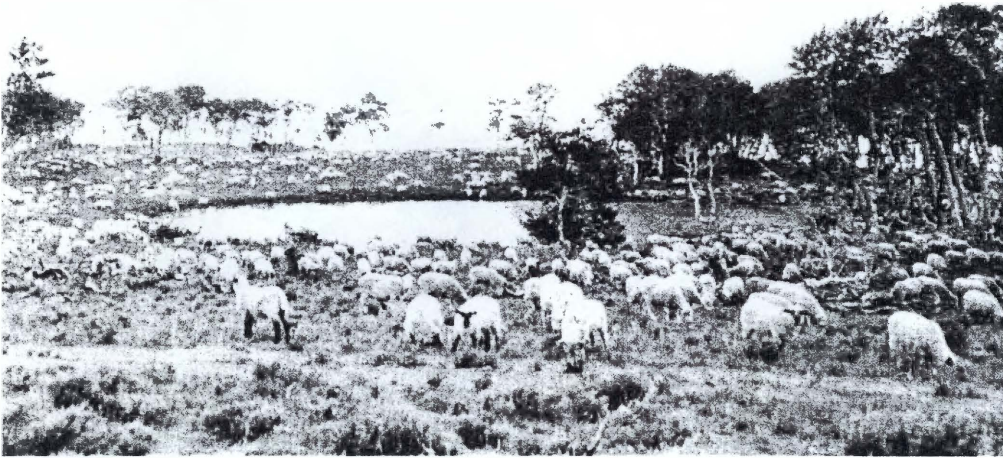


Figure 3.7 Sheep in central Oregon (photo courtesy of Bill Cyrus, Hillsboro, Oregon).

horses were eventually abandoned as settlements failed (Figure 3.8) and people moved away (Eddleman 1989). Native vegetation was not adapted to such intense grazing because native herbivores simply did not exert such a heavy burden on the ecosystem. Domestic overgrazing in the High Desert, therefore, resulted in a reduction in native grasses and forbs and an increase in alien grasses and invasive woody species such as western juniper. This period of abusive grazing coincided with a reduction in fire frequency because of active fire suppression and the loss of fine fuels as a result of livestock grazing (Weaver 1959, Burkhardt and Tisdale 1976, Vale 1981, Eddleman 1989, Kauffman and Sapsis 1989, Miller and Rose 1995, 1999, Wall *et al.* 2001, Soulé *et al.* 2003, 2004).

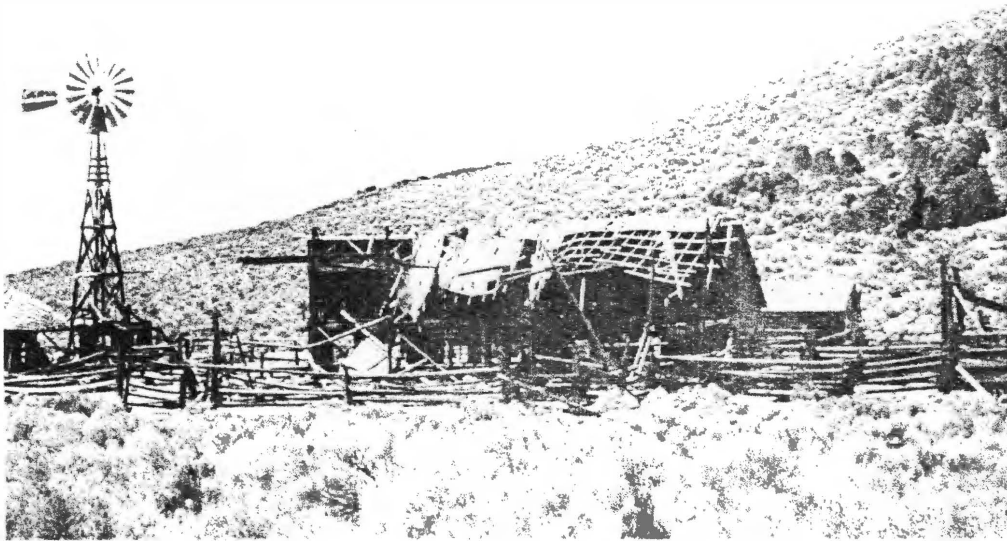


Figure 3.8 An abandoned homestead in the Oregon High Desert (photo courtesy of Merritt Parks, Fort Rock, Oregon).

A severe drought from the middle 1920s through the early 1930s ended the period of overgrazing and forced many homesteaders to abandon their settlements. The drought, coupled with overstocked rangelands and intense livestock grazing, left many native sagebrush/grassland areas in states of almost pure sagebrush and weeds. Erosion quickly became an issue, especially with the increased amount of newly abandoned agricultural fields (Eddleman 1989). Cheatgrass, introduced from Asia in the 1890s, quickly began to colonize disturbed areas in central Oregon. Cheatgrass seeds utilize awns for dispersal, and domestic animals readily distributed the alien seeds throughout disturbed areas. Cheatgrass easily resists reestablishment of native species and has proven to be very resilient in central Oregon where it still persists today (Eddleman 1989). Since the 1930s,

land managers have attempted to control overgrazing by domestic livestock. This has not proven to be an easy task, however, as previous changes in plant species and community structure still influence the successional direction of vegetation on the High Desert (Eddleman 1989).

Today, Deschutes County is the outdoor recreation capital of Oregon, and Bend, the Deschutes County seat, is the hub of this industry (Oregon Climate Service 2006). The county is predominantly livestock country, with beef cattle, llamas, sheep, dairy herds, horses, and swine. Much of the cropland in Deschutes County is irrigated, and alfalfa and other types of hay are the major crops (Myhrum and Ferry 2002). Mint, wheat, oats, barley, onions, and potatoes are also grown (Taylor and Hannan 1999). Lake County is home to the 109,265 ha Hart Mountain Antelope Refuge. Irrigated cropland is less extensive in Lake County, and grazing lands and dry-land farming are the predominant forms of agriculture (Taylor and Hannan 1999). The land immediately adjacent to the study area is primarily rangeland, and provides year-round forage for wildlife and livestock and habitat for many wild animals (Myhrum and Ferry 2002).

3.4.2 Fire

Nearly all plants and animals native to the High Desert evolved to survive fire (Kauffman and Sapsis 1989), yet, for many years, fire has been viewed as destructive, unnecessary, and undesirable. Prior to Euro-American settlement, fires were ignited by lightning and Native Americans (Foster 1917, Leopold 1924, Bork 1984, Morrison and Swanson 1990, Wallin *et al.* 1996). Fires ignited by Native Americans were likely just as important as lightning-ignited fires in shaping central Oregon vegetation communities.

Native Americans set fire to their surroundings to assist with the gathering of food, to improve travel routes, and to aid in the defense of their settlements (Eddleman 1989). Fire was a dominant ecological factor in the Oregon High Desert during pre-Euro-American settlement (Kauffman and Sapsis 1989). Fire frequencies of 20 to 80 years were normal (Miller 1989), and generally increased with increasing elevation. Return intervals for some higher elevation areas, however, are as short as 10 years (Eddleman 1989, Kauffman and Sapsis 1989). At lower elevations, biomass accumulation (i.e., fuel for fires) was limited by precipitation. In western juniper-dominated ecosystems, the presettlement fire-return interval was likely 10 to 30 years (Kauffman and Sapsis 1989).

Since Euro-Americans began settling the country, spreading throughout traditionally vegetated landscapes, fire suppression has been viewed as necessary to help prevent the loss of crops, property, homes, lives, and natural vegetation. Fire suppression has led to the alteration of traditional fire regimes in many western locations (Weaver 1959, Grissino-Mayer 1995, Grissino-Mayer and Swetnam 2000, Heyerdahl *et al.* 2001, 2002, Weisberg and Swanson 2003). In the absence of periodic fire, fuels have accumulated to critical levels in many forested ecosystems (Dieterich 1983, Everett *et al.* 1994, Grissino-Mayer and Swetnam 2000, Weisberg and Swanson 2003, Grissino-Mayer *et al.* 2004). If a fire occurs in an area with an increased accumulation of fuel, it may quickly crescendo into an uncontrollable stand-replacing crown fire (Swetnam 1993, Veblen *et al.* 2000). The result is usually devastating and property losses may be great.

Fire is an important disturbance mechanism (Weaver 1959, Franklin *et al.* 1971, Morrison and Swanson 1990, Agee 1993, Everett *et al.* 1994, Rorig and Ferguson 1999, Weisberg and Swanson 2003) that removes overstory and understory vegetation, affects

nutrient cycling, and facilitates regeneration of native plant species (Kauffman and Sapsis 1989). In the western United States, the practice of fire suppression has caused many changes in forest stand composition and structure (Dieterich 1983, Everett *et al.* 1994, Wall *et al.* 2001). Several native plants, such as many in the genus *Pinus*, possess a variety of adaptations to survive fire and numerous species even depend on fire for regeneration (Weaver 1959, Kauffman and Sapsis 1989). The serotinous cones borne by many *Pinus* species often require heat before they will open and disperse their seeds. Fire naturally provides the heat required to open serotinous cones, scars the seedcoat, increases soil pH, and provides a mineral seedbed. All of these factors help facilitate germination. In the absence of fire, seeds from many of these dominant trees fail to germinate. If a seed, however, happens to germinate in the absence of fire, the seedling will face almost insurmountable competition from established fire-intolerant species.

Rabbitbrush (*Chrysothamnus* spp.), native bunchgrasses, and perennial forbs vigorously sprout from subsurface tissues after a fire, and antelope bitterbrush (*Purshia tridentata* Pursh DC.) seeds are able to germinate from buried rodent caches after a fire (Kauffman and Sapsis 1989). Soil nitrogen has also been found to increase by up to 20 times after a fire. A large influx of a limiting nutrient such as nitrogen can lead to increased flowering and seed production in native plants. During the crucial post-fire period, native plants have the greatest odds of establishment because of reduced competition from fire-intolerant species.

When fire is excluded, native plants are often supplanted, animals that rely on fire-dependent trees, shrubs, and herbs for food or shelter move away or die, composition and structural changes occur, and the ecosystem becomes even more likely to burn

because of the excessive build-up of fuels (Dieterich 1983, Kauffman and Sapsis 1989). Absence of fire also assists in the encroachment of fire-intolerant trees and sagebrush into areas typically dominated by grasses and shrubs (Burkhardt and Tisdale 1976, Vale 1981, Young and Evans 1981, Kauffman and Sapsis 1989, Miller and Rose 1995, 1999, Hadley 1999, Soulé and Knapp 2000, Wall *et al.* 2001, Soulé *et al.* 2003, 2004).

Today, much of the High Desert bears little resemblance to the landscape observed by the early Euro-American trappers and settlers (Kauffman and Sapsis 1989). Recently, however, policies and management guidelines have changed because of the realization that fire is a crucial ecological factor in many ecosystems. It is now widely accepted that periodic fire is necessary to improve the current composition and productivity of bunchgrass prairies in central Oregon (Kauffman and Sapsis 1989). A prescribed fire study at the John Day Fossil Beds National Monument in central Oregon demonstrated that native grasses have very high fire-survival rates ($> 90\%$ for many species), and encroaching big sagebrush and western juniper (< 2 m in height) had survival rates of $< 10\%$. This study helped to effectively restore the area to a bunchgrass prairie (Kauffman and Sapsis 1989). In many instances, the practice of fire suppression has now shifted to a practice of fire management (Arno and Sneek 1977, Bork 1984), which has facilitated an increase in prescribed burning whenever possible (Weaver 1959, Wright *et al.* 1979, Veblen *et al.* 2000, Wall *et al.* 2001).

Fire suppression and excessive livestock grazing, however, are not the only causes of an anomalous fire regime. Climate also plays a major role in controlling wildfire activity (Burkhardt and Tisdale 1976, Vale 1981, Grissino-Mayer 1995, Miller and Rose 1995, 1999, Grissino-Mayer and Swetnam 2000, Veblen *et al.* 2000, Heyerdahl

et al. 2001, Weisberg and Swanson 2003). Moisture in both the air and soil directly affects the moisture content of fuel (Heyerdahl *et al.* 2001). The drier the fuel, the more likely it will ignite. Climate significantly influences forest composition and structure, which, in turn, influences the amount of fuel produced, the fuel size, and the spatial arrangement of fuel (Grissino-Mayer and Swetnam 2000, Heyerdahl *et al.* 2001). Lightning ignition frequency and short-term weather phenomena are other climatically related factors that affect forest fire occurrence (Grissino-Mayer and Swetnam 2000). Future climatic changes could further alter the frequency, severity, and areal extent of wildfires, as well as the length and timing of the fire season (Swetnam and Betancourt 1990, Grissino-Mayer and Swetnam 2000, Westerling *et al.* 2006). A better understanding of natural fire regimes, as well as the factors that shape these regimes, is crucial in helping us manage these forested ecosystems (Dieterich 1983, Heyerdahl *et al.* 2001, 2002).

3.4.3 Climate/Fire Relationships

Anytime a drought occurs in the western United States, especially if it occurs immediately following a period of sufficient precipitation, the likelihood of fire increases. Holmes *et al.* (1986) demonstrated the statistical relationship between climate and fire using a technique known as superposed epoch analysis. They showed that, leading up to large fire events, precipitation regimes may change from drought (two years prior to the fire year) to abundant precipitation (one year prior to the fire year) to drought again (during the fire year). The increase in precipitation just before the fire year serves to boost primary production in winter annuals. This, in turn, leads to an increase of fine

fuels required for fire ignition and spread (Baisan and Swetnam 1990, Grissino-Mayer 1995). The abundant fuel is dried during the drought year, and an ignition source, such as lightning, can start the fire (Bork 1984, Morrison and Swanson 1990, Wallin *et al.* 1996). Lightning is closely linked to the occurrence of fires in the Pacific Northwest (Morris 1934, Bork 1984, Morrison and Swanson 1990, Wallin *et al.* 1996, Rorig and Ferguson 1999), and is particularly potent during dry periods.

Fire regimes in much of the western United States are affected by broad-scale climatic oscillations such as ENSO and the PDO. Swetnam and Betancourt (1990) were the first to discover the link between ENSO and wildfires in the Southwest. El Niño events typically bring above-average winter and spring precipitation and increased moisture availability to vegetation in the Southwest. If an El Niño event is followed by a strong La Niña event, the newly produced fine fuels are desiccated and fire probability increases. Kitzberger *et al.* (2001) found similar results in the southwestern United States and Patagonia, Argentina. A comparison of fire and climatic histories of the two areas showed very similar fire and ENSO-anomaly regimes. In both regions, El Niño events typically increase precipitation and available moisture to plants. If an El Niño event is followed by a drought, wildfire probability increases (Kitzberger *et al.* 2001). Grissino-Mayer *et al.* (2004) discovered a similar pattern in the San Juan Mountains, Colorado, where warm phases of ENSO or the PDO, followed by a strong drought, also increase the likelihood of wildfires (Grissino-Mayer *et al.* 2004). In Oregon, however, positive-phase ENSO events typically bring below-average precipitation (Heyerdahl *et al.* 2002). In much of the Pacific Northwest, La Niña and cold-phase PDO are the catalysts behind increased precipitation and primary production, and the likelihood of wildfire increases

when a wet period is followed by a strong El Niño event or warm-phase PDO (Heyerdahl *et al.* 2002).

3.5 The Ecology and Biogeography of Western Juniper

“Sunshine and thin air are abundant... Upon these commodities the tree subsists, crouching, stubbornly clinging, while a single root offers foothold, its gnarled branches picturesque and beautiful in their tufts of gray-green leaves... When they succumb, their trunks last almost as long as the granite boulders among which they are cast....”

-Julia Ellen Rogers, naturalist, describing western juniper, 1917

Western juniper is a member of the cypress family (Cupressaceae). The tree is native to the western U.S., but is encroaching into areas outside its native habitat. Its native range reaches from Susanville, Lassen County, California, northward through the northwestern tip of Nevada and eastern and central Oregon to southwestern Idaho and southeastern Washington (Figure 3.9) (Vasek 1966, Young and Evans 1981). Western juniper reaches its greatest abundance in central Oregon where extensive open stands are common (Berry 1924, Dealy 1990). A parapatric subspecies, *Juniperus occidentalis* Hook. ssp. *australis* Vasek, is separated geographically from subspecies *J. occidentalis* Hook. ssp. *occidentalis*, and grows in the southern part of the western juniper range, mainly in California. Western juniper has one of the strongest responses to changes in climate of all tree species (Knapp *et al.* 2001b) and is, by far, the tree species most suitable for this project. Its extensive geographic range, proven longevity, minimal biological lags, high sensitivity to moisture fluctuation, and its low sensitivity to temperature variability and nutrient deposition (Knapp *et al.* 2001a, 2001b, 2002, Pohl *et al.* 2002, Knapp *et al.* 2004) are qualities important for reconstructions of precipitation and teleconnection variability that have regional implications.



Figure 3.9 Native Range of western juniper.

Western juniper is a xerophyte that usually grows on sites that receive < 35 cm annual precipitation (Knapp *et al.* 2002). It is a sabinoid juniper with light-green foliage and denticulate leaf margins (Figure 3.10) (Vasek 1966). Its leaf characteristics contribute to a high competitive ability and enable the species to grow in a semi-arid environment. Leaves have no stomata on their exposed sides. Most all stomata are located on the cupped side of leaves and compressed next to the stem (Miller 1989). The location of stomata, coupled with a waxy cuticle on leaf surfaces, protects western junipers from excessive evaporative water loss related to wind, high temperature, and low humidity (Miller 1989). The radial growth of western juniper largely depends on winter and spring precipitation (Young and Evans 1981, Knapp *et al.* 2002, 2004). Northern populations grow in a continental climate, whereas southern populations grow in a similar climate but with less extreme winter conditions (Dealy 1990).

The distribution of subspecies *J. occidentalis* Hook. ssp. *occidentalis* generally follows the Columbia River Basalts (Young and Evans 1981). Soils are usually stony but can be nearly free of cobbles (Berry 1924, Dealy 1990). Soils are usually 25 to 38 cm deep but can be > 122 cm (Dealy 1990). Traditionally, these are areas where few, if any, other tree species can survive (Figure 3.11) (Sowder and Mowat 1965).

The range of elevation for western juniper is 185 to 3,050 m. Relict stands are usually confined to rocky surfaces and high ridges, as well as pumice sands with sparse vegetation. Western juniper is largely a fire-intolerant tree, and these rocky surfaces serve as protective “islands” for western juniper (Kauffman and Sapsis 1989, Dealy 1990). These areas have low amounts of available fuel, preventing large-scale fires from occurring frequently (Burkhardt and Tisdale 1976). Most recent expansion has occurred

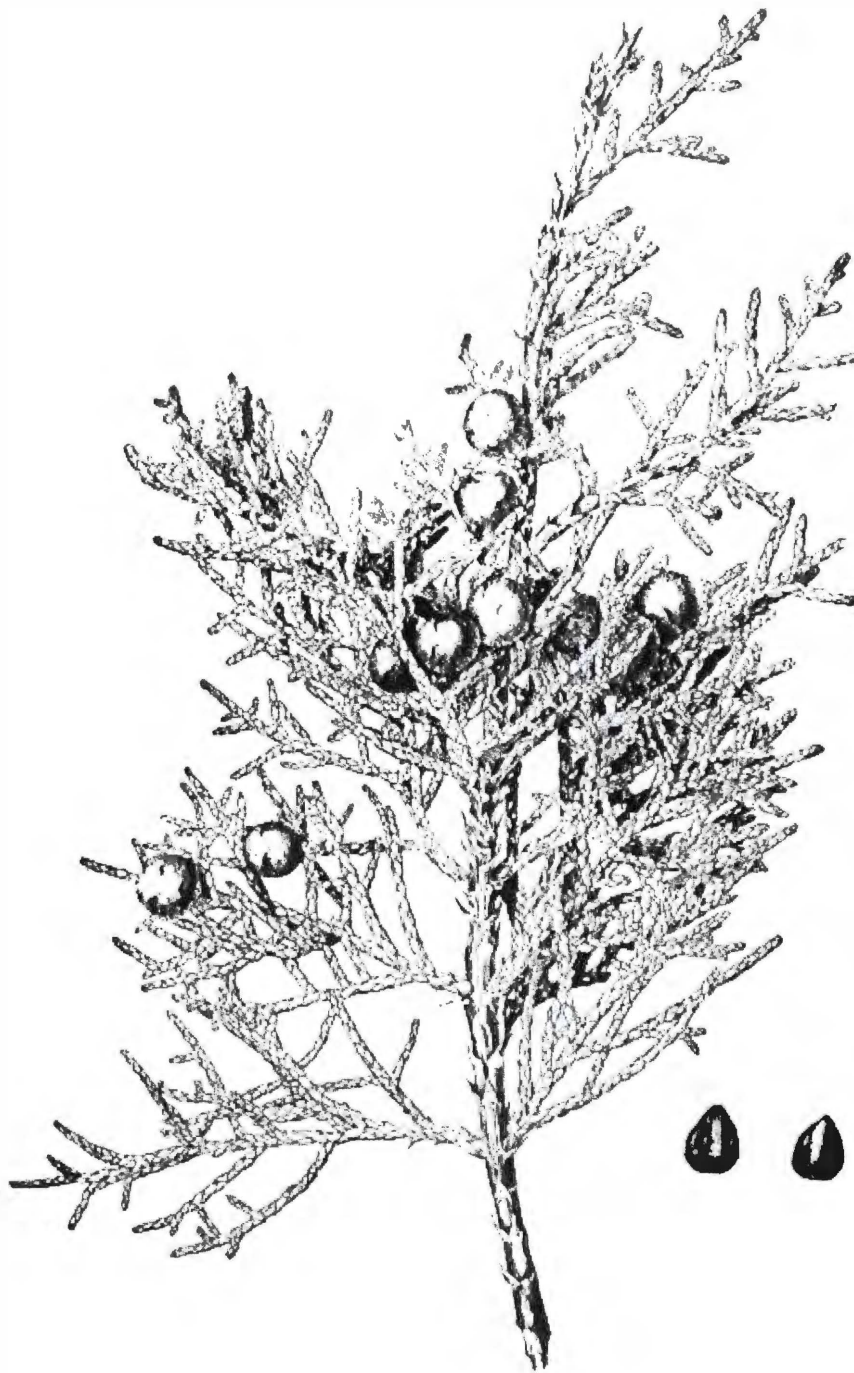


Figure 3.10 Western juniper stem with berries and seeds (adapted from Berry 1924).

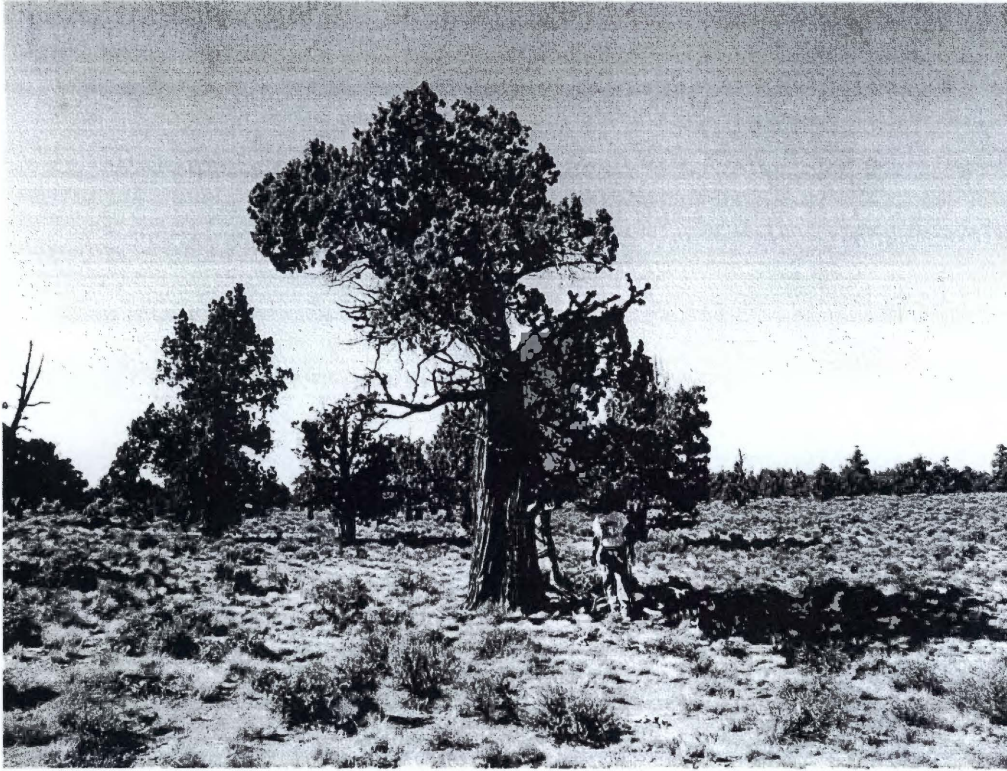


Figure 3.11 *Juniperus occidentalis* Hook. ssp. *occidentalis* in its native habitat (photo courtesy of Henri D. Grissino-Mayer, The University of Tennessee, Knoxville).

on sagebrush sites downslope from these rocky outcroppings (Burkhardt and Tisdale 1976, Miller and Rose 1999, Soulé *et al.* 2004).

3.5.1 Associated Flora

Western juniper woodlands consist of a single-species overstory in many northern stands. The study area is one such example. In some stands, however, the species can be found growing with other trees such as white fir (*Abies concolor* (Gordon) Lindl. ex Hildebr.), mountain hemlock, ponderosa pine, curl-leaf mountain mahogany (*Cercocarpus ledifolius* Nutt.), lodgepole pine (*Pinus contorta* Douglas ex Loudon), and

Douglas-fir (*Pseudotsuga menziesii* (Mirb.) Franco) (Sowder and Mowat 1965, Franklin and Dyrness 1988, Dealy 1990). Major western juniper associations in central Oregon include *Juniperus/Artemisia/Agropyron*, *Juniperus/Artemisia/Festuca*, *Juniperus/Artemisia/Festuca/Lupinus*, *Juniperus/Festuca*, *Juniperus/Artemisia/Agropyron/Chaenactis*, *Juniperus/Artemisia/Agropyron/Astragalus*, *Juniperus/Artemisia/Purshia*, *Juniperus/Agropyron*, and *Juniperus/Agropyron/Festuca* (Driscoll 1964, Dealy 1990). The *Juniperus/Artemisia/Agropyron* association is found on well-drained, loamy soils and is designated as the climatic climax association (Franklin and Dyrness 1988). Western juniper is recognized as the dominant species in the Juniper Steppe Woodland (*Juniperus/Artemisia/Agropyron*), and is considered a secondary species in the Juniper-Pinyon Woodland (*Juniperus/Pinus*) (Driscoll 1964, Little 1971, Griffin and Critchfield 1972).

Big sagebrush is the most common plant associated with western juniper (Sowder and Mowat 1965, Franklin and Dyrness 1988, Dealy 1990), but western juniper is also found growing with other shrubs, grasses, and forbs, many of which are well-adapted to fire (Burkhardt and Tisdale 1976). Other commonly associated shrub species are rubber rabbitbrush (*Chrysothamnus nauseosus* (Pallas ex Pursh) Britt.), green rabbitbrush (*C. viscidiflorus* (Hook.) Nutt.), antelope bitterbrush, low sagebrush, gray horsebrush (*Tetradymia canescens* DC.), smooth horsebrush (*Tetradymia glabrata* Gray), wax currant (*Ribes cereum* Douglas), and prickly phlox (*Leptodactylon pungens* (Torr.) Nutt.) (Sowder and Mowat 1965, Wright *et al.* 1979, Franklin and Dyrness 1988, Dealy 1990). Big sagebrush is occasionally displaced wholly or to codominance by antelope-bitterbrush (Franklin and Dyrness 1988). Less commonly associated shrub species are

stiff sagebrush (*Artemisia rigida* (Nutt.) Gray), spiny hopsage (*Atriplex spinosa* (Hook.) Collotzi), broom snakeweed (*Gutierrezia sarothrae* (Pursh) Britt. & Rusby), and desert gooseberry (*Ribes velutinum* Greene). Suffrutescents are represented by *Eriogonum* spp. (Franklin and Dyrness 1988, Dealy 1990).

Grass and grass-like species commonly associated with western juniper are bluebunch wheatgrass (*Agropyron spicatum* (Pursh) Scribn. & J.G. Sm.), introduced Asian cheatgrass, Idaho fescue, prairie Junegrass (*Koeleria cristata* Pers.), Sandberg bluegrass, bottlebrush squirreltail (*Sitanion hystrix* (Nutt.) J.G. Sm.), and Thurber's needlegrass (*Stipa thurberiana* (Piper) Barkworth) (Wright *et al.* 1979, Franklin and Dyrness 1988, Dealy 1990). Less commonly associated grass and grass-like species are threadleaf sedge (*Carex filifolia* Nutt.), Ross' sedge (*C. rossii* Boott), sixweeks fescue (*Festuca octoflora* Walt.), needle and thread (*Stipa comata* Trin. & Rupr.), and pubescent western needlegrass (*S. occidentalis* Thurb. ex S. Wats. var. *pubescens* (Vasey) Maze, Taylor & MacBryde) (Franklin and Dyrness 1988, Dealy 1990).

Forb species commonly associated with western juniper are western yarrow (*Achillea millefolium* L. ssp. *occidentalis* DC.), milkvetch (*Astragalus* spp.), maiden blue-eyed Mary (*Collinsia parviflora* Lindl.), obscure crypthantha (*Cryptantha ambigua* (Gray) Greene), lineleaf fleabane (*Erigeron linearis* (Hook.) Piper), woolly sunflower (*Eriophyllum lanatum* (Pursh) Forbes), spreading groundsmoke (*Gayophytum diffusum* Torr. & Gray), lupine (*Lupinus* spp.), agoseris (*Agoseris* spp.), and tufted phlox (*Phlox caespitosa* Nutt.) (Franklin and Dyrness 1988, Dealy 1990). Less commonly associated forb species are small bluebells (*Mertensia longiflora* Greene) and Hooker's silene

(*Silene hookeri* Nutt.). Forbs, however, usually are not major components of relatively undisturbed areas (Franklin and Dyrness 1988).

3.5.2 Associated Fauna

The dry western juniper woodlands and sagebrush steppe rangeland provide habitat for many wildlife species. Shrubs provide nesting sites, camouflage, thermal protection, and barriers against winter winds. Shrubs are also important food sources for animals in the winter because snow may cover lower-lying plants (Myhrum and Ferry 2002). Bunchgrasses offer protection for newborn animals and, along with various forbs, provide forage in spring, summer, and fall.

Associated mammals include mule deer (*Odocoileus hemionus* Rafinesque), antelope (*Antilocapra americana* Ord), coyote (*Canis latrans* Say), badger (*Taxidea taxus* Shreber), yellow-bellied marmot (*Marmota flaviventris* Audubon & Bachman), Belding's ground squirrel (*Spermophilus beldingi* Merriam), brush rabbit (*Sylvilagus bachmani* Waterhouse), mountain cottontail (*Sylvilagus nuttallii* Bachman), and black-tailed jackrabbit (*Lepus californicus* Gray) (Myhrum and Ferry 2002). The area provides habitat for avian species such as sage grouse (*Centrocercus urophasianus* Bonaparte), golden eagle (*Aquila chrysaetos* Linn.), prairie falcon (*Falco mexicanus* Schlegel), American kestrel (*Falco sparverius* Linn.), red-tailed hawk (*Buteo jamaicensis* Gmelin), Swainson's hawk (*Buteo swainsoni* Bonaparte), ferruginous hawk (*Buteo regalis* Gray), sage thrasher (*Oreoscoptes montanus* Townsend), sage sparrow (*Amphispiza belli* Cassin), western meadowlark (*Sturnella neglecta* Audubon), Brewer's sparrow (*Spizella*

breweri Cassin), and mountain bluebird (*Sialia currucoides* Bechstein) (Myhrum and Ferry 2002).

3.5.3 Life History of Western Juniper

Early growth is typically controlled by site conditions. Young trees are pyramidal in form, single-stemmed, hearty, and insect and disease resistant (Dealy 1990). Western juniper seedlings seem to favor areas with ample soil moisture and that lack intense sunlight. These conditions, however, do not necessarily favor growth of mature western junipers (Burkhardt and Tisdale 1976). Seedlings have been found to grow better under the protection of a nurse plant (such as *Artemisia* spp.) than in open spaces, where surface temperatures can be 45 to 57% higher than temperatures beneath a nurse plant (Burkhardt and Tisdale 1976, Miller and Rose 1995). Seedlings place an abundance of energy into vertical root structure in search of water. Saplings have narrowly conical crowns and many small branches that persist to a point near the ground (Berry 1926).

As a tree matures, its vertical root system becomes extensive and is capable of penetrating deep into bedrock (Dealy 1990). The lateral root system can also be extensive, and western junipers are often able to exploit soil resources at great distances from the trunk (Miller 1989). Soil nutrients absorbed by western juniper are typically recycled beneath the canopy. This results in soil nutrient levels that are often greater immediately beneath the tree canopy than in the soils between trees or adjacent to grasses (Miller 1989). The height of mature trees usually ranges from 4 to 10 m, and growth throughout the range tends to be poor compared to that of other conifers. The ratio of monoecious to dioecious trees is approximately 1:1. Mature trees produce white blooms

and blue-black berries with one to three grooved seeds (Berry 1926). Abundant fruit production in western juniper occurs nearly every year (Sowder and Mowat 1965, Dealy 1990), but it takes two years for fruit to mature, and viability of the seed is low, usually below 17% (Vasek 1966). In the latter stages of its life, western juniper has a ragged, dead-topped, gnarled appearance (Sowder and Mowat 1965, Dealy 1990). It is capable of reaching ages > 1,000 years. Old-growth stands in central Oregon are typically between the ages of 200 to 400 years (Dealy 1990).

Western juniper is wind and shade intolerant. The species has difficulty competing with other tree species on upper slopes (Dealy 1990). Western juniper establishment on upper slopes apparently occurs when a stand is opened by disturbance. The species is also fire intolerant (Franklin and Dyrness 1988). Seedlings, saplings, and poles are highly susceptible to fire. Only mature western junipers can survive relatively intense fires because they have little fuel near the trunk and fairly thick bark (Sowder and Mowat 1965, Kauffman and Sapsis 1989, Dealy 1990). Old-growth stands remain today because they have not been exposed to intense fire. The principal damaging agent to western juniper is juniper fomes (*Fomes juniperinus* (H. Schrenk) Sacc. & P. Syd.), a heartwood white pocket rot that causes significant damage and loss (Sowder and Mowat 1965, Dealy 1990, Knapp and Soulé 1999). Heart rot, however, cannot become established in western juniper unless the tree has already been wounded in some way (Knapp and Soulé 1999). Branch-deforming mistletoe (*Phoradendron juniperinum* Engelm. ex Gray) and stem rusts (*Gymnosporangium kernianum* Bethel and *G. betheli* Kern) (Sowder and Mowat 1965, Dealy 1990), and the juniper bark beetle (*Phloeosinus serratus* LeConte) (Dealy 1990) are also known to damage western juniper. Few

herbivores graze on western juniper, but mule deer have been known to occasionally feed on the foliage (Sowder and Mowat 1965).

3.5.4 Western Juniper Invasion

Although western juniper has more than doubled its range since the beginning of the 20th century, the species likely had a much wider distribution 2,000 to 4,000 years ago. Only 400 years ago, the distribution of western juniper likely resembled the present distribution. A decline in range likely occurred approximately 200 years ago (Miller 1989). The most recent western juniper expansion began in the 19th century and coincided with Euro-American settlement. Evidence indicates that just before the most recent expansion began, stands resembled savannas or open woodlands, with fire restricting the oldest trees to steep and/or rocky areas (Burkhardt and Tisdale 1976, Miller and Rose 1995, West and Young 2000).

Invasion downslope of relict stands is an important factor in recent afforestation (Burkhardt and Tisdale 1976, Soulé *et al.* 2003). Western juniper seeds typically spread downslope in the winter, aided by gravity-assisted berry dispersal and water runoff (Burkhardt and Tisdale 1976, Soulé *et al.* 2003). In summer and fall, seed dispersal is found both downslope and upslope (Burkhardt and Tisdale 1976). Gnawed seed remains and seed-laced scat from both mountain cottontails and ground squirrels (*Spermophilus* spp.) have been found in abundance during summer (Burkhardt and Tisdale 1976). Robins (*Turdus migratorius* Linn.) have been observed feeding on juniper berries in the fall (Young and Evans 1981). Juniper seeds in their feces are broadcast in all directions from an established stand of trees. Animal dispersal is likely a major factor related to the

spread of western juniper, both upslope and downslope (Sowder and Mowat 1965, Burkhardt and Tisdale 1976).

A number of factors have contributed to the expansion of western juniper into areas once dominated by big sagebrush, perennial bunchgrass, and other species:

- a reduction in fires because of the implementation of fire suppression, development of roads and other fire barriers (Sowder and Mowat 1965, Burkhardt and Tisdale 1976, Young and Evans 1981, Eddleman 1989, Miller 1989, Miller and Rose 1995, Knapp and Soulé 1998, Miller and Rose 1999, Soulé and Knapp 2000, Soulé *et al.* 2003, 2004),
- an increase in livestock grazing, which reduces the amount of fine fuels for fire, increases the number of sagebrush nurse plants, and removes competing vegetation (Sowder and Mowat 1965, Burkhardt and Tisdale 1976, Eddleman 1989, Kauffman and Sapsis 1989, Miller 1989, Miller and Rose 1995, Knapp and Soulé 1998, Miller and Rose 1999, Soulé and Knapp 2000, Soulé *et al.* 2003, 2004),
- favorable climate (Burkhardt and Tisdale 1976, Young and Evans 1981, Eddleman 1989, Miller 1989, Dealy 1990, Miller and Rose 1995, Knapp and Soulé 1998, Miller and Rose 1999, Soulé and Knapp 2000, Soulé *et al.* 2003, 2004),
- an increased level of CO₂ in the atmosphere that appears to facilitate continued western juniper expansion during periods of below average precipitation (Knapp *et al.* 2001a, Soulé and Knapp 2000, Soulé *et al.* 2003, 2004), and

- biological inertia (i.e., trees that, because of the adverse conditions in which they grow, far exceed the generally accepted maximum age for this species) (Schulman 1954, Miller and Rose 1995, Knapp and Soulé 1998, Soulé and Knapp 2000, Soulé *et al.* 2003, 2004).

This expansion is changing stand composition. Once western juniper becomes established in a new area, the trees purge their understories of almost all herbaceous and shrub vegetation. The understories of invading western juniper growing on big sagebrush sites are almost completely bare of shrub and herbaceous vegetation, rendering the stands virtually fireproof (Young and Evans 1981). This reduction in ground cover also potentially reduces range productivity, increases erosion, and alters water balances (Burkhardt and Tisdale 1976, Young and Evans 1981, Soulé *et al.* 2003). Research suggests that fire frequencies of 15 to 50 years would be sufficient to halt western juniper expansion into a sagebrush-grassland community (Miller and Rose 1995, 1999). Because of the practice of fire suppression, however, fire intervals in the Pacific Northwest currently exceed this recommended fire frequency by a large margin.

3.5.5 Special Uses and Economic Value

Western juniper has little commercial value. Locally, it is used for fence posts because of its durability, and early Euro-American settlers used the wood as a fuel source (Rogers 1917, Berry 1924). Experienced woodworkers familiar with western juniper are often able to successfully cut and dry thin boards without incurring the twisting and warping common to the species. Even still, western juniper lumber is used sparingly, usually only in furniture and small craft items (Dealy 1990). Native Americans once

wove the stringy bark into clothing and matting (Rogers 1917). The species is, however, valuable for wildlife cover and food (primarily berries), and for avian nesting sites (Dealy 1990).

Chapter 4

Methods

4.1 Field Methods

4.1.1 Site Selection

Frederick Butte has experienced substantially less domestic livestock grazing, organized fire suppression, and timber harvesting than most woodlands in central Oregon, largely because of the relative difficulty in accessing these sites by humans and livestock. The relative lack of disturbance was an important factor in choosing the study area. The area is located in the rainshadow of the Cascade Mountains, and precipitation is the primary limiting factor of tree growth in the area. This is important because ring widths can be crossdated only if an environmental factor is critically limiting, persists temporally, and affects a wide enough geographic area to cause ring widths to vary the same way in multiple trees (Fritts 1976). Western junipers that grow in this area are remarkably long-lived (some are over 1,000 years old) and particularly sensitive to annual variations in precipitation. The rate of decomposition in the Frederick Butte area is relatively slow, and very old dead and downed remnant wood is abundant and readily available for analysis. The high resin and terpenoid content in western juniper is primarily responsible for the persistence of dead wood (sometimes over 1,000 years) in many dry, open sites (Miksicek 1987). This combination of longevity and sensitivity makes it possible to derive ring-width indices from the trees at the Frederick Butte study sites that are more reliable than indices based on younger trees from less arid sites (Schulman 1954). Reconstructions from this area may provide some very broad-scale

interpolations of climate, both spatially and temporally, that may help answer some very important climatic questions.

4.1.2 Collection of Cross Sections

Cross sections (Figure 4.1) were used for this study because most of the samples were collected from the remnant wood of stumps, logs, and snags. Some of the remnant wood was refuse from previously sawn fence-post lumber, but most cross sections came from long-dead juniper stems found lying on the soil surface. Only a few partial sections from living trees were collected. Sample location, slope, condition of the specimen, and a sketch of the cross section were recorded for all samples on standard field sample forms. The lean of the specimen sampled (angle and direction), diameter at breast height (dbh), tree height, and crown density were noted when appropriate. On August 5 and 6, 2001, 31 cross sections were collected at Frederick Butte South. On August 6 and 7, 2001, 47 cross sections were collected at Frederick Butte North. All cross sections were cut from western juniper stumps, snags, logs, and trees with a chainsaw (Figures 4.2 and 4.3). After collection, many of the cross sections were in multiple pieces because of various degrees of natural deterioration. All cross sections, therefore, were wrapped with 80-gauge shrinkwrap to ensure their stability during transit.

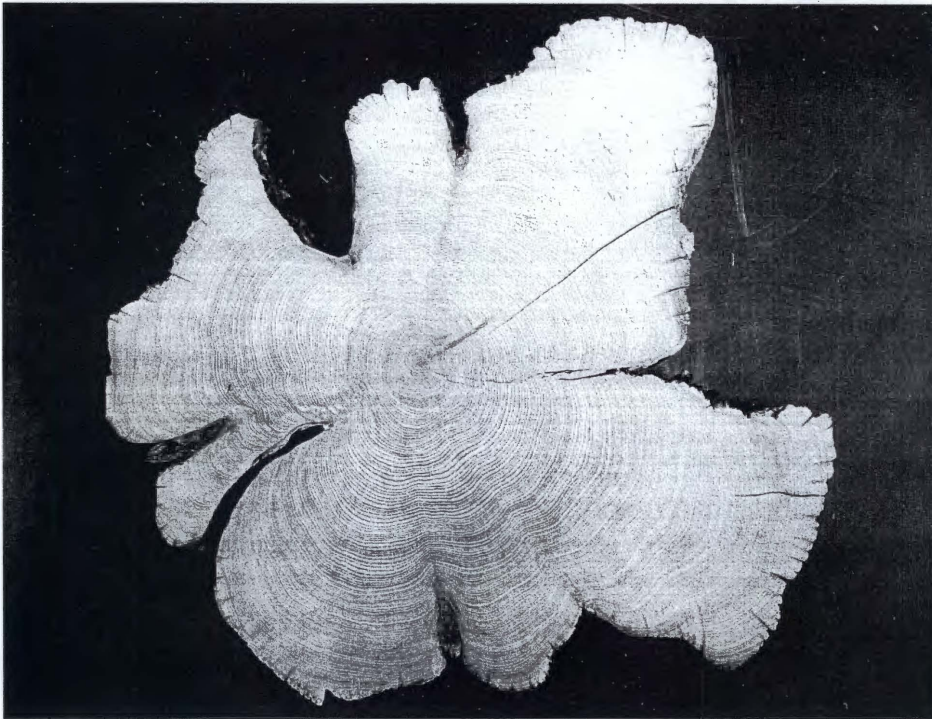


Figure 4.1 Western juniper cross section.



Figure 4.2 Sample collection from a fallen western juniper (photo courtesy of Henri D. Grissino-Mayer, The University of Tennessee, Knoxville).



Figure 4.3 Chain-sawed cross section of western juniper (photo courtesy of Henri D. Grissino-Mayer, The University of Tennessee, Knoxville).

4.2 Laboratory Methods

4.2.1 Sample Preparation and Selection

All cross sections were placed in the University of Tennessee Herbarium freezer at -40°C for 48 hrs to kill any fungi and/or insects. Unstable cross sections were glued onto plywood. When necessary, cross sections were cut into manageable pieces using an industrial band saw. Cross sections were processed in the Laboratory of Tree-Ring Science at the University of Tennessee, Knoxville, using standard dendrochronological techniques (Stokes and Smiley 1996). All cross sections were sanded with a hand-held belt sander using ANSI 40-grit (500 to 595 μm) to ANSI 400-grit (20.6 to 23.6 μm)

sandpaper to ensure maximum ring clarity under standard 10X magnification (Orvis and Grissino-Mayer 2002). Twenty-five of the most promising cross sections (i.e., the ones with the clearest ring structure and greatest temporal sample depth) were selected for this dendroclimatological study (Figure 4.4).

4.2.2 Crossdating

Accurate crossdating is the key to all dendrochronological studies (Douglass 1946). Crossdating involves the comparison of signature patterns of wide and narrow growth rings from one specimen with corresponding growth ring patterns from another specimen. Individual cross sections, beginning with the specimens collected from living trees, were crossdated using the skeleton plot method (Stokes and Smiley 1996).

Skeleton plotting is a graphical method of illustrating the growth ring patterns of an individual tree or a group of trees. I constructed and compared skeleton plots for each individual cross section and then used the individual skeleton plots to assemble a master skeleton plot. The master skeleton plot was used to confirm the dates of the cross sections and to detect missing and false rings.

4.2.3 Measurement

Upon completion of crossdating, ring-width series were developed by measuring each growth ring on every cross section to the nearest 0.001 mm (1.0 μm) with a Velmex measuring system. Ring-width measurements were recorded with Measure J2X software.

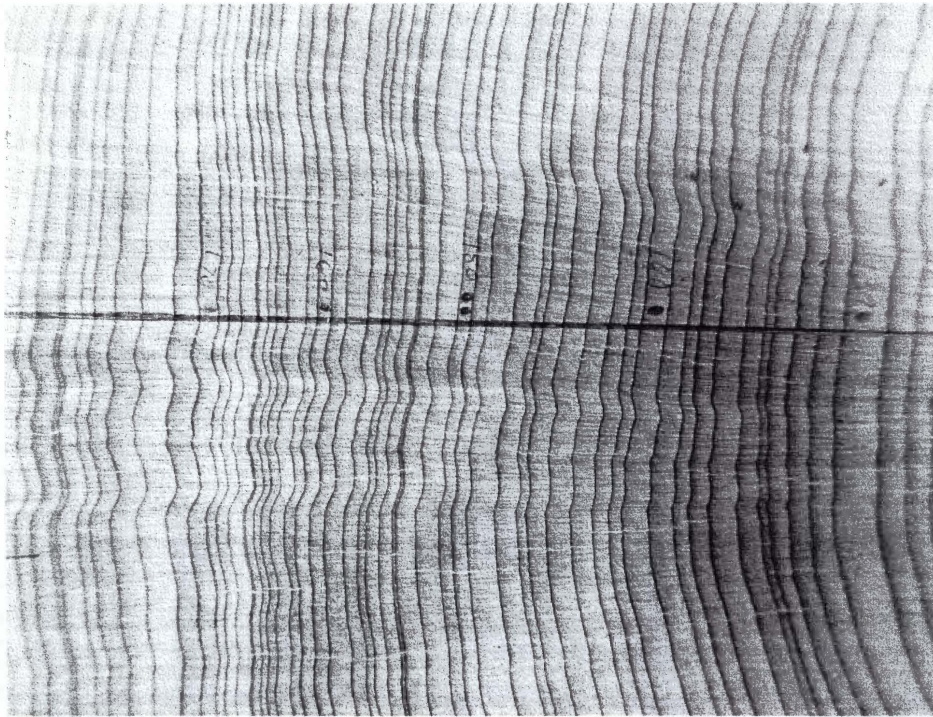


Figure 4.4 Magnification of western juniper annual growth rings.

4.2.4 Quality Control with COFECHA

Ring-width measurements and crossdating were statistically verified with the program COFECHA (Holmes 1983). COFECHA is a software package that reduces dendrochronological error through identification of data that need further examination. COFECHA is especially important in a dendroclimatological study because it assists in maximizing the amount of correct climatic information in the tree rings by minimizing the “noise” that is introduced by incorrect crossdating and inaccurate measurement (Holmes 1983, Grissino-Mayer 2001).

Cross sections were entered into COFECHA as undated series. COFECHA then compared overlapped and successive segments (50-year segments, lagged 25 years) from each of the 25 cross sections with a nearby reference chronology that spanned A.D. 870–

1996. This reference chronology was developed from cores taken from living trees in the early 1980s and updated recently by Meko *et al.* (1996). COFECHA then flagged segments that had low correlations with the anchor chronology. This is an important step in determining the locations of potential false and missing rings that might be causing misdated segments in the ring-width series. If COFECHA identified a potentially misdated segment, the sample was re-checked for the presence of the problematic ring. Upon confirmation, the software program EDRM was used to delete or insert false or missing rings, respectively. Finally, if significant dating was achieved as noted by a statistically significant correlation coefficient ($p < 0.01$), the series were visually inspected and confirmed before final calendar dates were assigned.

4.2.5 Standardization and Chronology Development

Raw ring-width measurement standardization and chronology development were conducted by the software program ARSTAN (Cook 1985). Standardization of the ring widths removes trends attributable to natural tree physiological processes (e.g., differences in size and age) (Fritts 1976). Standardization is beneficial because it removes much of the “noise” that may cloud any climatic signals present in the growth rings. The chronology was produced using conservative standardization techniques (i.e. negative exponential curve, linear regression of negative slope, or horizontal line). This detrending option was chosen to preserve potential low-frequency, long-term climatic trends (Briffa *et al.* 1996). Use of a more flexible detrending technique (e.g., spline curve) would likely remove any low-frequency climatic signals present in the growth rings (Knapp *et al.* 2001a). Chronology indices were computed around a bi-weight,

robust mean which minimizes potential effects of particularly wide or narrow rings (i.e., outliers).

To assess the temporal and statistical robustness of my chronology, I compared it to other long western juniper tree-ring chronologies from the western United States. To determine the statistical quality of the Frederick Butte chronology, I rank-ordered all long western juniper chronologies, including the Frederick Butte chronology, by average mean sensitivity, standard deviation, and first-order autocorrelation, then summed the ranks for each chronology. Finally, the values from the chronology were converted to z-scores (i.e., standard deviation units) to assist in the determination of marker years (i.e., years of significantly above- or below-average radial tree growth) and trends in radial tree growth. This method assigns a mean of zero to a chronology. The values that fall between the standard deviation units of ± 1.1 account for 75% of the values within a chronology. Of the remaining 25% of values, the upper 12.5% (all values > 1.1 standard deviations) corresponds with years of anomalously above-average radial tree growth, and the lower 12.5% (all values < -1.1 standard deviations) corresponds with years of anomalously below-average radial tree growth.

4.2.6 Analyzing the Climatic Response

For the climatic analyses, I selected the standard version of the ARSTAN-generated chronologies because this version best preserves low-frequency trends (Knapp *et al.* 2004). Precipitation is the climatic variable that most affects the growth of western junipers in central Oregon (Knapp *et al.* 2002, Soulé 2003). This study, therefore, focused on climatic analyses of precipitation and synoptic-scale climatic oscillations that

affect precipitation. Climatic response models of tree growth were developed using 1920–2000 monthly precipitation data for climatic Zone 7 (south central Oregon) (National Climatic Data Center 2006), the 1948–2000 PDO index (the leading principal component of monthly SST anomalies in the North Pacific Ocean) (Climate Diagnostics Center 2006), and the 1950–2000 Niño 3 index (monthly Pacific (5° north–5° south, 150° west–90° west) SST and SST anomaly data) (Climate Prediction Center 2006). The data cover historical and current periods and are updated every month.

The statistical package SAS (Schlotzhauer and Littell 1987) was used for all statistical analyses. Pearson's product-moment correlation analyses were used to isolate those months (chosen from February of the previous year through December of the year of tree growth) that a climatic variable had a statistically significant effect on tree growth. Seasons (i.e., groups of months) were then determined for each climatic variable based on the months during which the climatic variable exhibited the most significant relationship with tree growth. Seasonalization is important because it illustrates the period during which a climatic variable has the greatest effect on tree growth (Grissino-Mayer and Butler 1993, Grissino-Mayer 1995). Once the climatic data were seasonalized, a Pearson's product-moment correlation analysis was conducted for the season during which each climatic variable had the most significant effect on tree growth. The precipitation season was truncated to 12 months, even though some other months were statistically significant and added to the statistical strength of the season. This truncation was performed to confine the precipitation season to one water year, in this case, July of the previous year to June of the following year.

If a strong seasonal response was present, a regression equation was developed that predicted the selected climatic variable for the full length of the tree-ring chronology. Standard regression diagnostics (studentized residuals and Cook's *d*) assisted with the removal of outliers and ensured that violations of least squares regression were minimized. During the removal of outliers, not more than 10% of the sample size was removed from any of the data sets. Oftentimes, I found outliers during years in which precipitation was higher than normal (e.g., 1941, 1942, 1950, 1956, 1958, and 1984), perhaps related to short-duration extreme precipitation events in which most precipitation was lost as runoff. If this were the case, the runoff would not have been available for uptake by trees, thus causing large discrepancies between annual precipitation and total radial tree growth (Grissino-Mayer 1995). The Durbin-Watson statistic and a first-order autocorrelation test were used to detect the presence of autocorrelation in the residuals of the regression analyses.

Chapter 5

Results

5.1 Quality Control

Of the 25 series from 24 trees measured for development of the Frederick Butte western juniper chronology, all were retained because of the accurate visual and graphical crossdating between series. When testing for dating accuracy, none of the 538 50-year segments from the 25 measurement series were flagged by COFECHA as being possibly misdated. All segments correlated highest at the dated position, and all correlations were higher than the minimum needed for statistical significance ($r > 0.3281$ with $p < 0.01$).

5.2 Western Juniper Chronology

The 25 measured series yielded a continuous tree-ring chronology spanning A.D. 797 to 2000 (Figures 5.1–5.7). Figure 5.1 illustrates the entire span of the chronology, while Figures 5.2–5.7 show the chronology divided into successive 200-year increments which better illustrate the variability in radial growth. In Figures 5.2–5.7, sample depth is indicated at the top of each graph. When compared to other western juniper chronologies in the western United States, the Frederick Butte chronology ranked among the most robust temporally. The span of 1,204 years makes the Frederick Butte chronology the third longest western juniper chronology in the United States (Table 5.1). Sample depth in the chronology is highest (21 series) between A.D. 1269–1274 (Figure 5.7). The

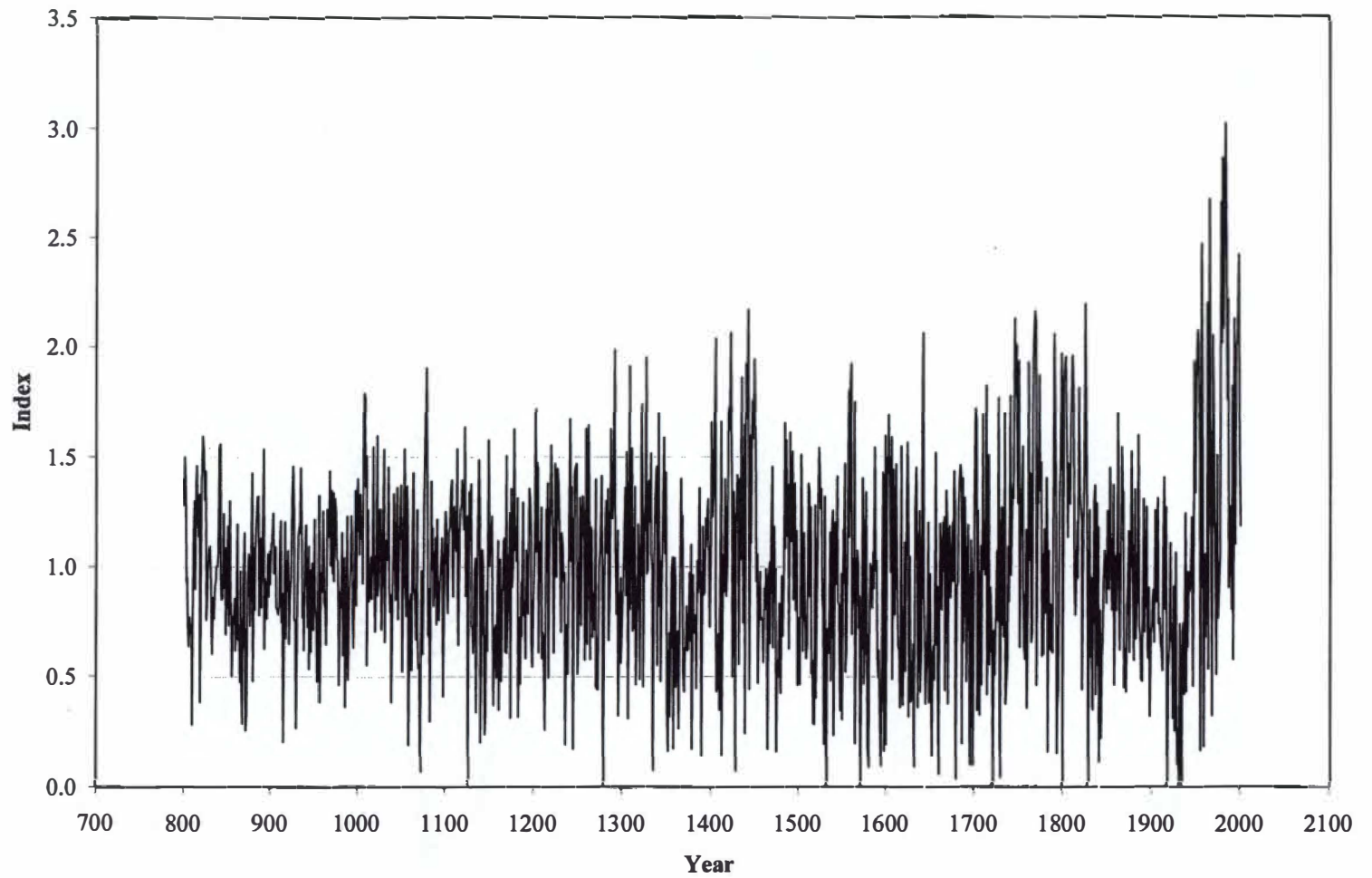


Figure 5.1 Frederick Butte western juniper chronology.

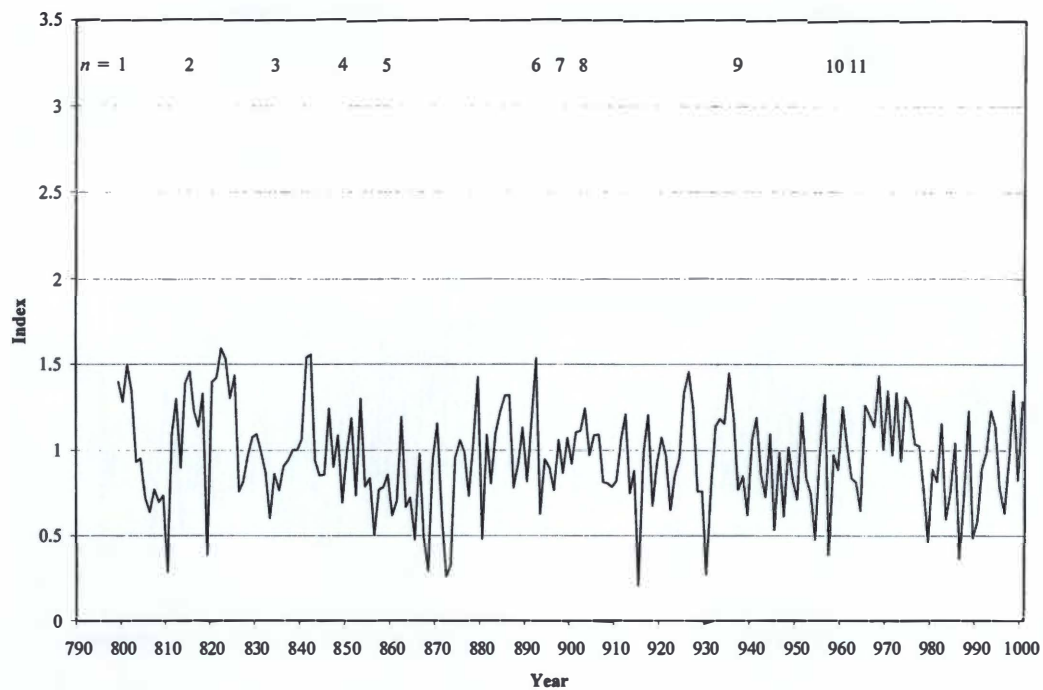


Figure 5.2 Frederick Butte western juniper chronology (A.D. 799–1000).

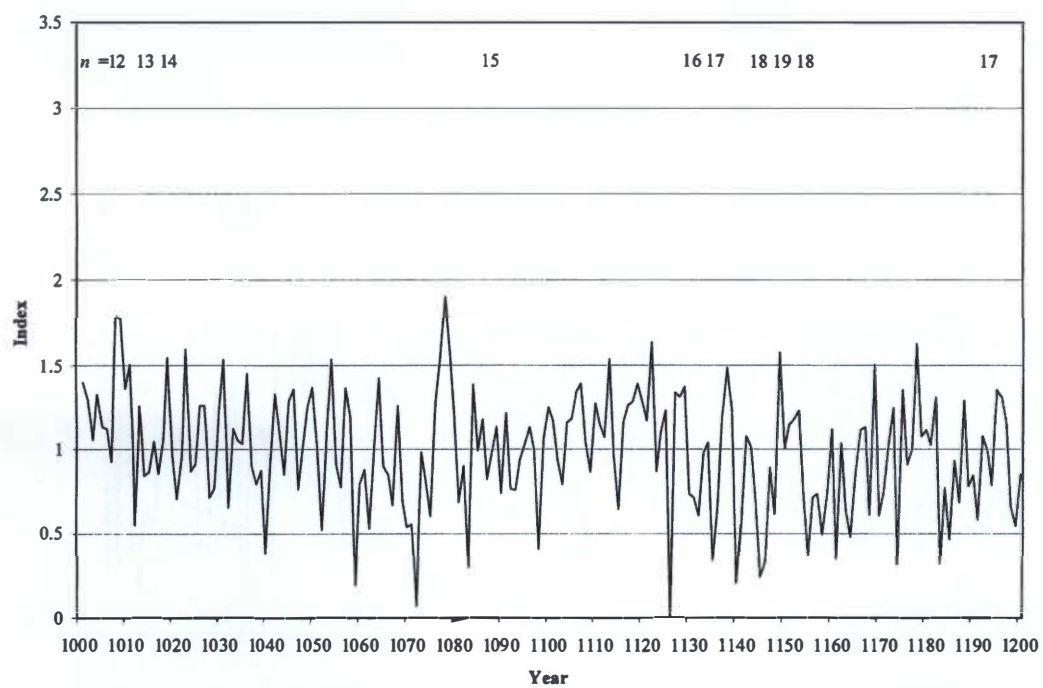


Figure 5.3 Frederick Butte western juniper chronology (A.D. 1001–1200).

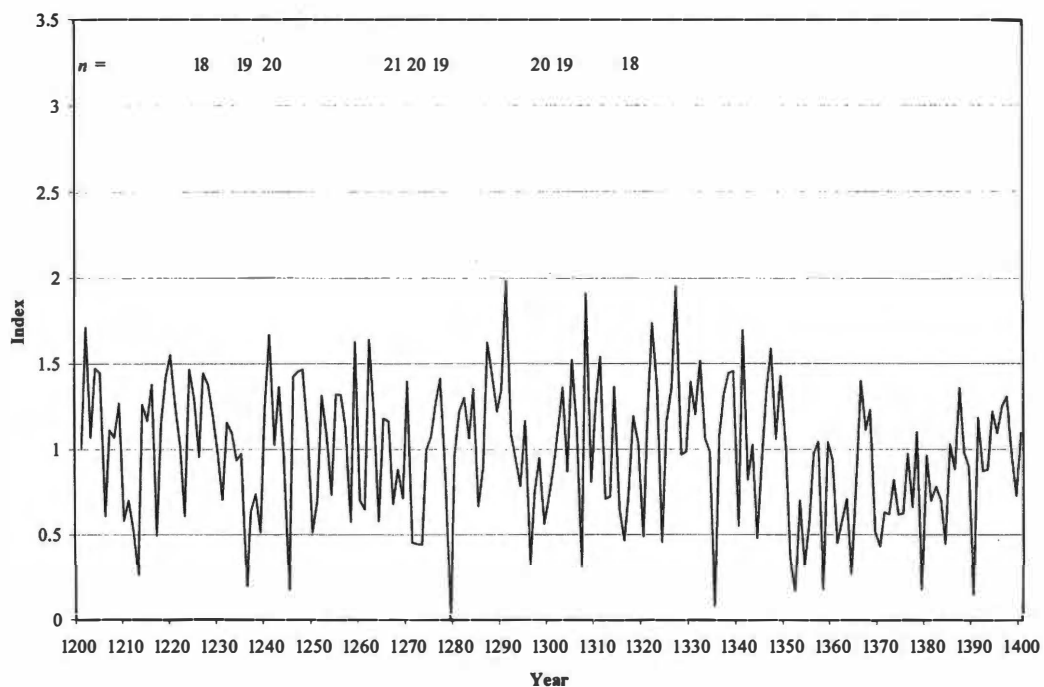


Figure 5.4 Frederick Butte western juniper chronology (A.D. 1201–1400).

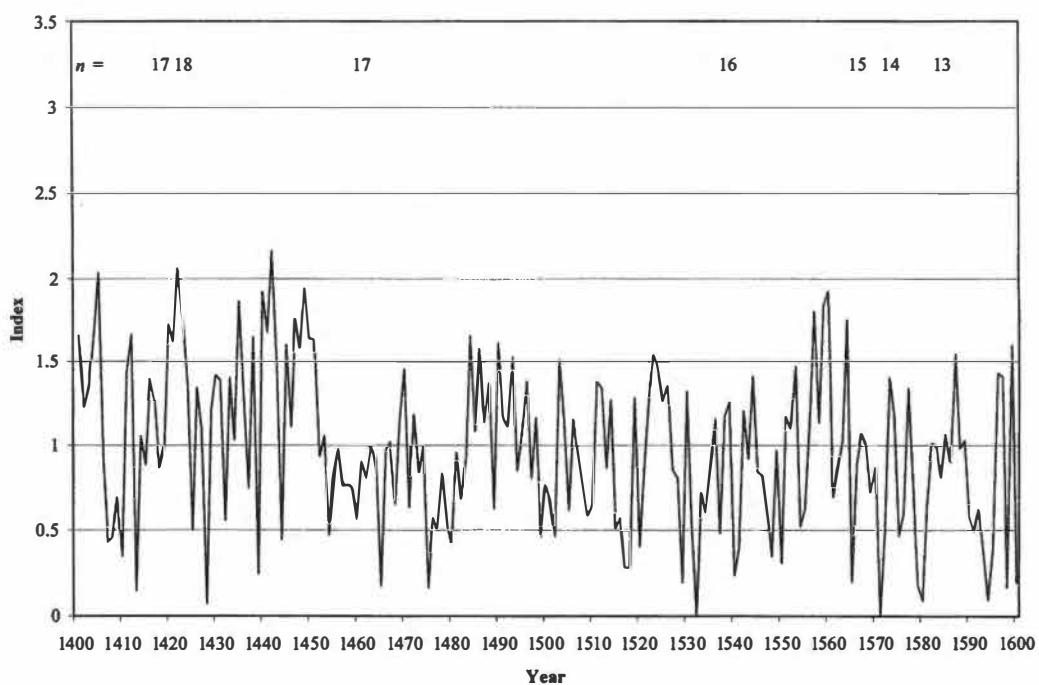


Figure 5.5 Frederick Butte western juniper chronology (A.D. 1401–1600).

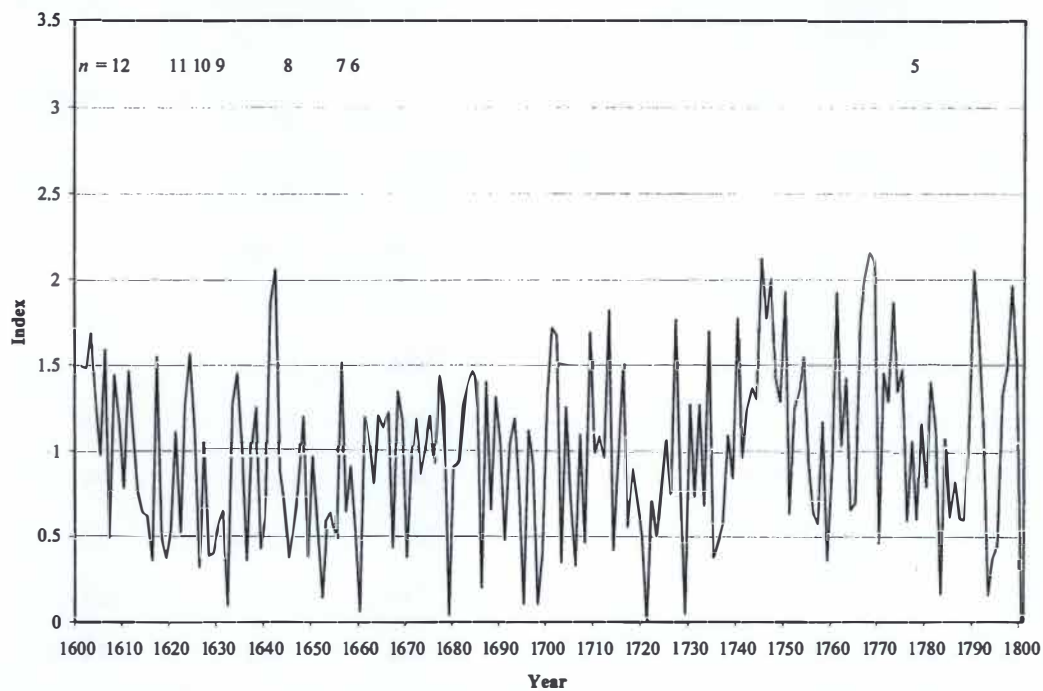


Figure 5.6 Frederick Butte western juniper chronology (A.D. 1601–1800).

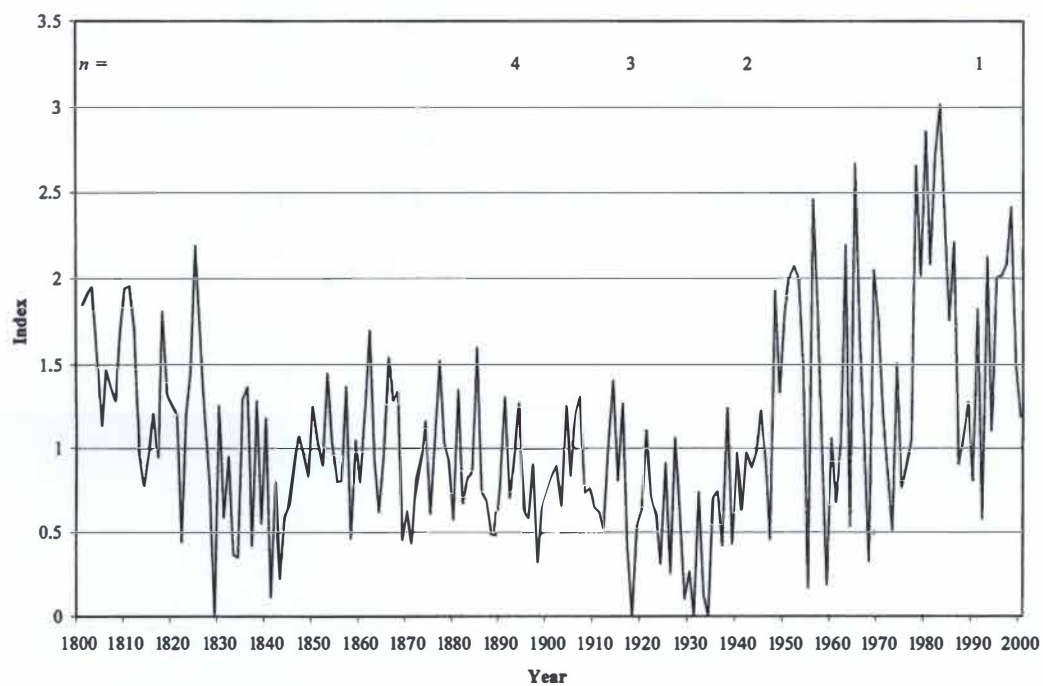


Figure 5.7 Frederick Butte western juniper chronology (A.D. 1801–2000).

Table 5.1 The longest western juniper tree-ring chronologies in the western United States (International Tree-Ring Data Bank 2006).

Site Name	Inner Date (A.D.)	Outer Date (A.D.)	Length (years)	Dated Series
1. Carson Pass, CA	420 B.C.	1999	2,420	56
2. Table Rock, OR	530	1996	1,467	31
3. Frederick Butte, OR*	797	2000	1,204	25
4. Horse Ridge, OR	830	1996	1,167	66
5. Frederick Butte, OR	870	1996	1,127	36
6. Jackson Meadow, CA	930	1999	1,070	39
7. Jackson Mountains, NV	975	1998	1,024	62
8. Sardine Point, CA	1010	1999	990	47
9. Steens Mountain, OR	1017	1998	982	29
10. Frederick Butte, OR	1097	1982	886	76
11. Kaiser Pass, CA	1140	1981	842	56
12. Boles Creek, CA	1152	1998	847	43
13. Jackson Mountains, NV	1267	1984	718	72
14. Horse Ridge, OR	1281	1982	702	66
15. Hager Basin Reservoir, CA	1310	1980	671	59
16. Little Juniper Mtn., OR	1377	1982	606	66
17. Calamity Creek, OR	1396	1982	587	49
18. Spring Canyon, OR	1405	1982	578	59

*The chronology created in this study.

Frederick Butte chronology ranked fourth overall in statistical quality when compared to the previously constructed chronologies (Table 5.2). The Frederick Butte chronology also has the highest interseries correlation ($r = 0.86$) of any western juniper chronology in the United States.

Of the 25 series in this chronology, 23 are over 300 years in length, and 10 of these series exceed 500 years in length. Eleven series have inner-ring dates prior to A.D. 1000, including two exceptional samples, FBS 004 and FBN 050. FBS 004 is 784 years in length, with an inner-ring date of A.D. 797 (Figure 5.8). FBN 050, with 1,062 rings, is the longest series within the Frederick Butte chronology (Figure 5.9). The average length of the 25 series is 542 years. The average mean sensitivity for these series is 0.53, the average standard deviation is 0.37, and the average first-order autocorrelation is 0.58 (summaries for all series are presented in Appendix A). The years A.D. 797 and 798 were not included in the graphical representations or climatic reconstructions of the chronology because the ring widths for those years were anomalously wide and were based on only one sample.

5.3 Climatic Analyses

Pearson's product-moment correlation analyses showed that, of all the climatic variables analyzed in this study, Oregon Zone 7 precipitation had the strongest overall relationship with radial tree growth (Figure 5.10). The PDO and ENSO also showed significant relationships with radial tree growth during some months (Figures 5.11–5.13). All statistically significant climatic variables were positively correlated with annual radial tree growth. The season during which Oregon Zone 7 precipitation exhibited the

Table 5.2 The statistical quality of the longest western juniper tree-ring chronologies in the western United States (International Tree-Ring Data Bank 2006).

Site Name	Intercorr.	Mean Sen.	Std. Dev.	Autocorr.
1. Horse Ridge, OR	0.85	0.65	0.33	0.45
2. Table Rock, OR	0.83	0.62	0.32	0.46
3. Horse Ridge, OR	0.84	0.65	0.31	0.49
4. Frederick Butte, OR*	0.86	0.53	0.37	0.58
5. Frederick Butte, OR	0.82	0.5	0.36	0.56
6. Frederick Butte, OR	0.78	0.5	0.29	0.51
7. Little Juniper Mtn., OR	0.84	0.46	0.24	0.50
8. Jackson Mountains, NV	0.69	0.42	0.25	0.58
9. Spring Canyon, OR	0.63	0.33	0.33	0.66
10. Calamity Creek, OR	0.71	0.36	0.28	0.6
11. Jackson Mountains, NV	0.67	0.38	0.25	0.59
12. Steens Mountain, OR	0.72	0.37	0.26	0.6
13. Boles Creek, CA	0.68	0.31	0.29	0.68
14. Jackson Meadow, CA	0.63	0.28	0.28	0.74
15. Hager Basin Reservoir, CA	0.71	0.3	0.23	0.65
15. Sardine Point, CA	0.65	0.27	0.26	0.71
16. Carson Pass, CA	0.6	0.25	0.16	0.69
17. Kaiser Pass, CA	0.57	0.25	0.23	0.71

Intercorr. is the series intercorrelation, Mean Sen. is the average mean sensitivity, Std. Dev. is the average standard deviation, and Autocorr. is the average first-order autocorrelation. *The chronology created in this study.

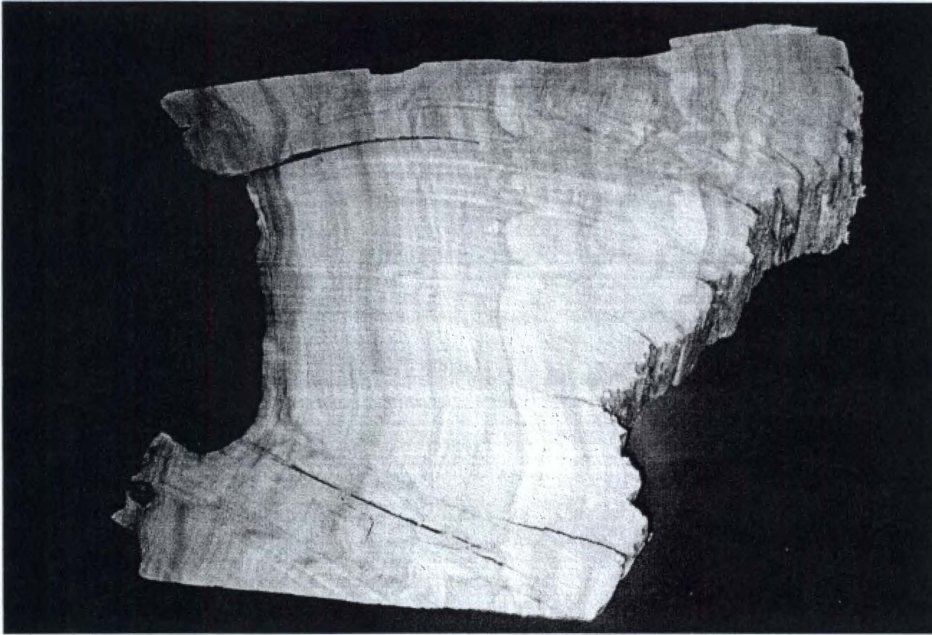


Figure 5.8 FBS 004, with an inner-ring date of A.D. 797, is the oldest series in the chronology.

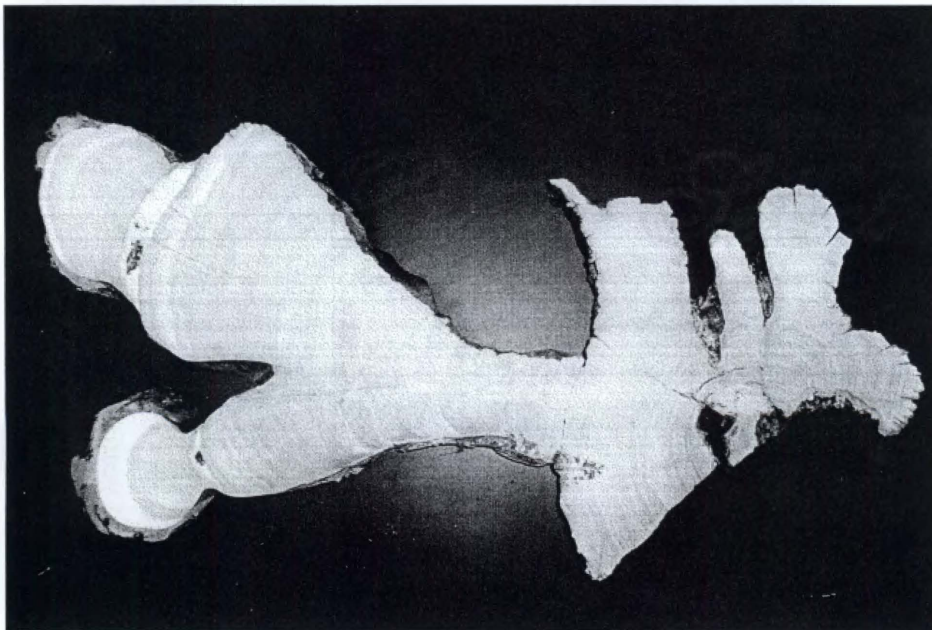


Figure 5.9 FBN 050, with 1,062 rings, is the longest series in the chronology.

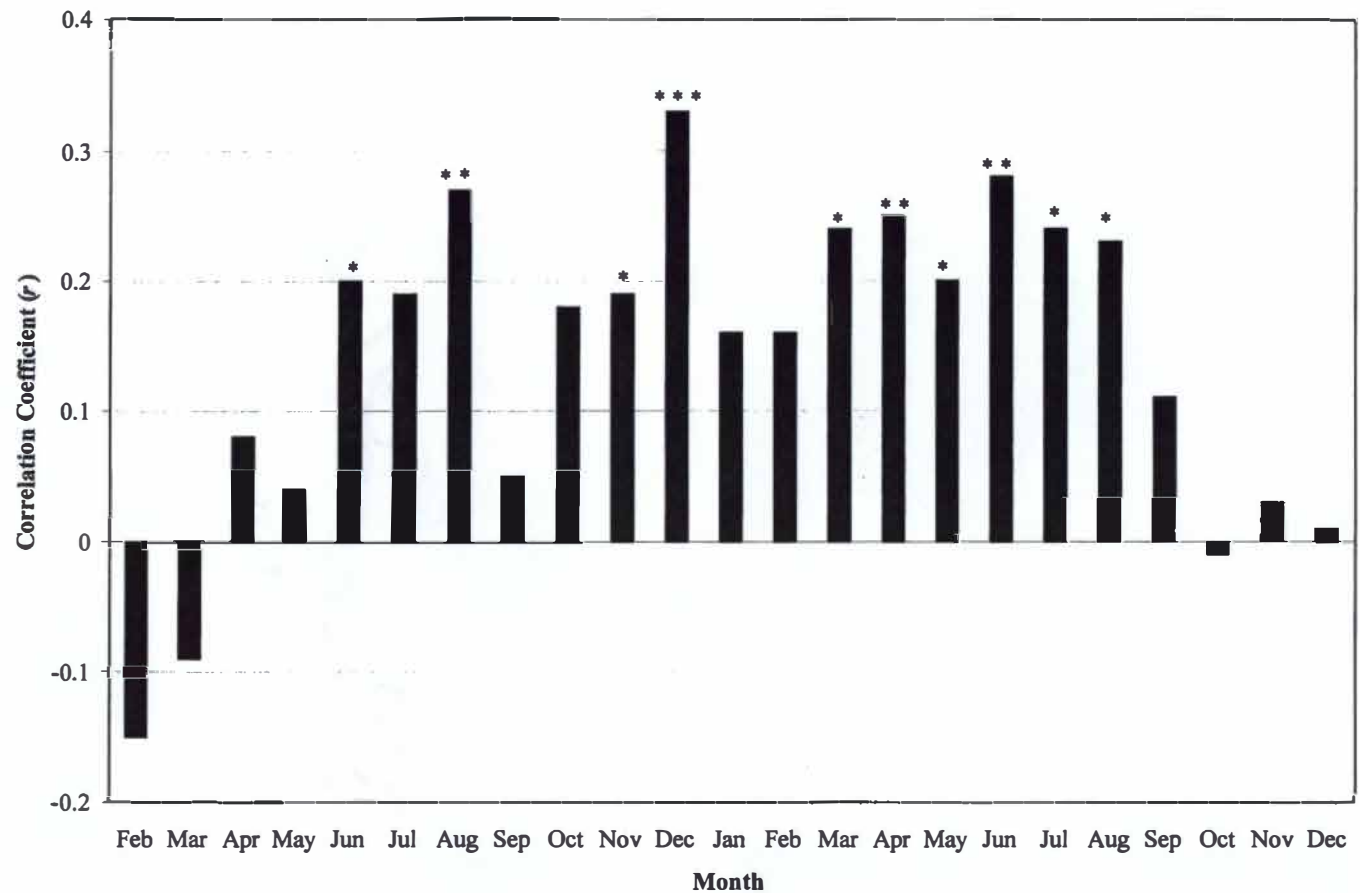


Figure 5.10 Pearson's product-moment correlation coefficients (r) between western juniper radial growth and Oregon Zone 7 precipitation data (1920–2000). The months represented are for year_{t-1} and year_t, respectively. * $p < 0.05$, ** $p < 0.01$, *** $p < 0.001$.

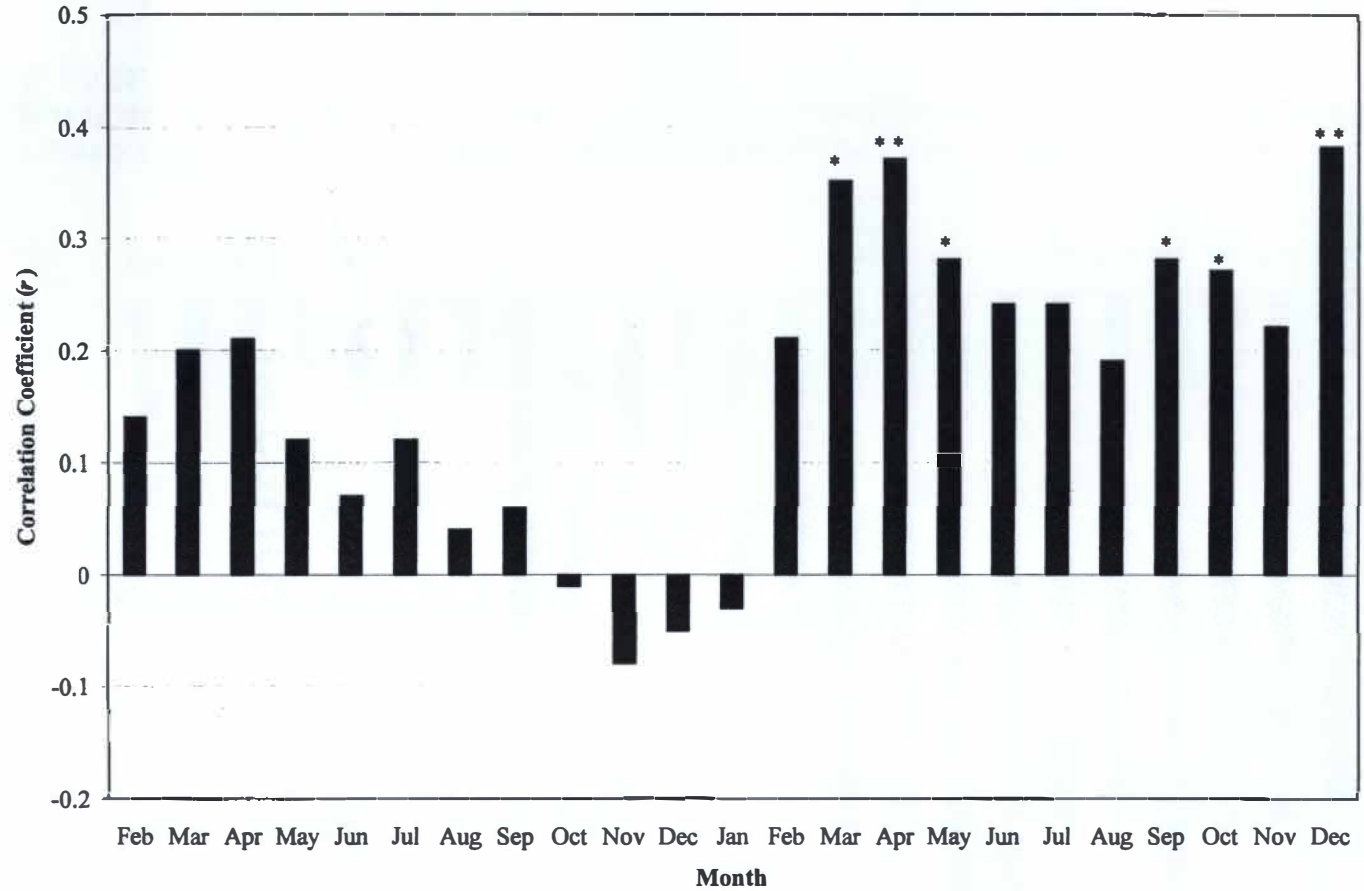


Figure 5.11 Pearson's product-moment correlation coefficients (r) between western juniper radial growth and the PDO index (1948–2000). The months represented are for year_{t-1} and year_t , respectively. * $p < 0.05$, ** $p < 0.01$.

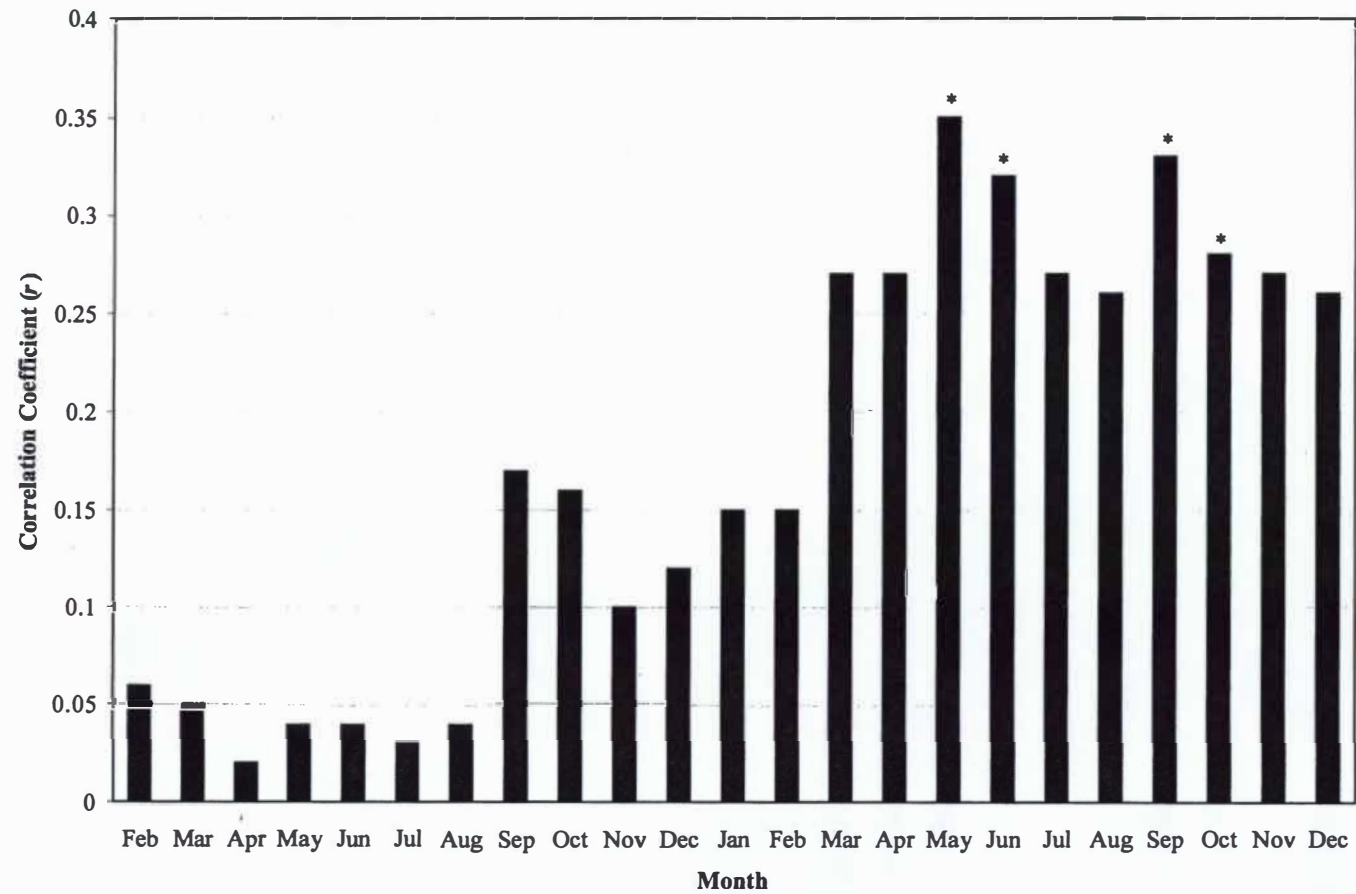


Figure 5.12 Pearson's product-moment correlation coefficients (r) between western juniper radial growth and the Niño 3 index (1950–2000). The months represented are for year_{t-1} and year_t, respectively. * $p < 0.05$.

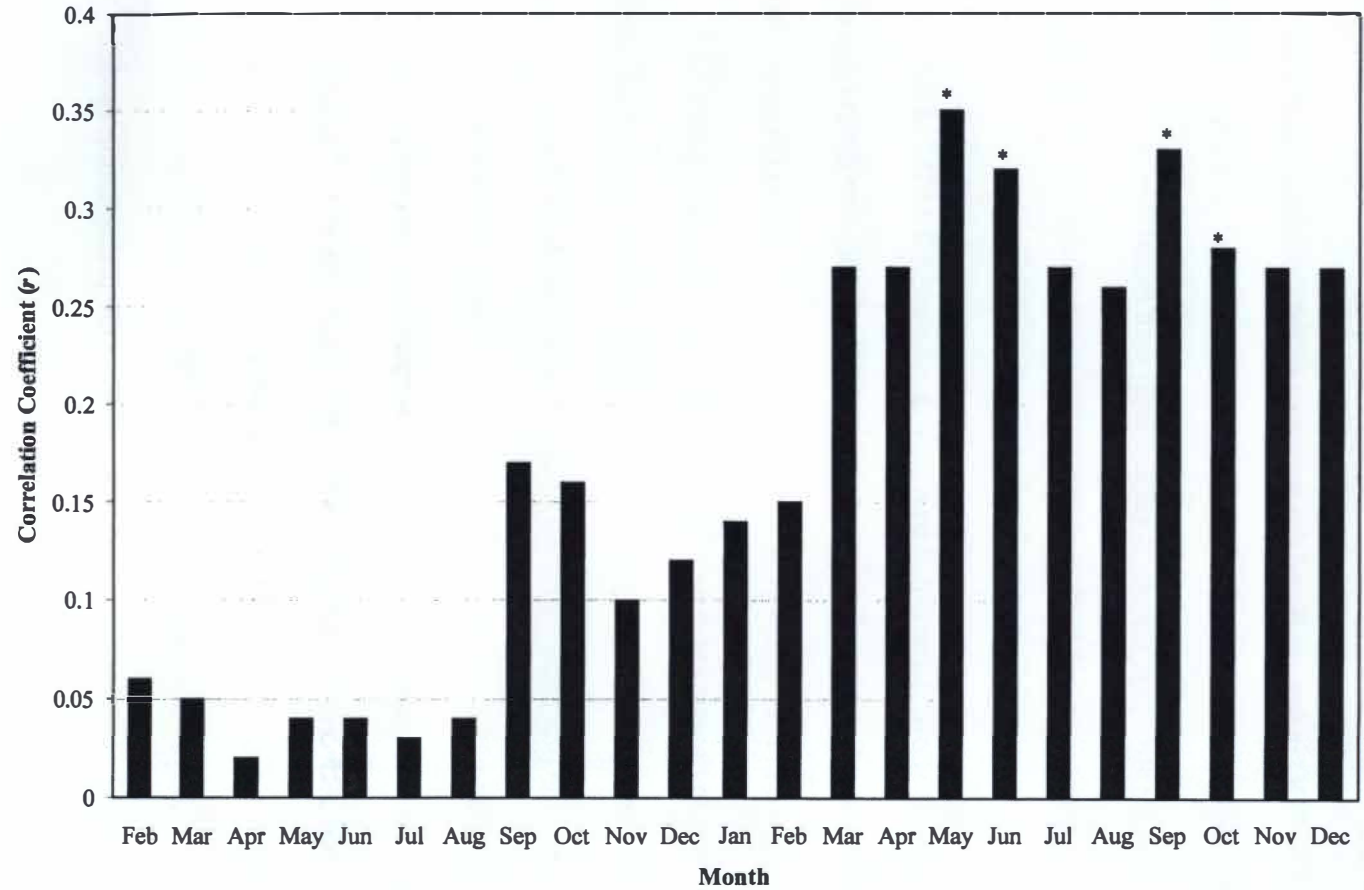


Figure 5.13 Pearson's product-moment correlation coefficients (r) between western juniper radial growth and the Niño 3 index anomaly (1950–2000). The months represented are for year_{t-1} and year_t, respectively. * $p < 0.05$.

strongest statistical relationship with radial tree growth occurred from July_{t-1} to June_t ($r = 0.68, p < 0.0001$). The PDO index exhibited the strongest statistical relationship with radial tree growth during March and April of the current year ($r = 0.37, p < 0.01$). The Niño 3 index exhibited the strongest statistical relationship with radial tree growth during May and June of the current year ($r = 0.35, p < 0.05$). The seasonal data are illustrated in Figure 5.14.

Regression models showed that radial tree growth accounted for 64% of the variance in the previous year's July to the current year's June precipitation data (Figure 5.15), 34% of the variance in the current year's March and April PDO data (Figure 5.16), and 32% of the variance in the current year's May and June Niño 3 data (Figures 5.17 and 5.18). I found that precipitation data prior to 1920, which is often afflicted with data gaps, adversely affected the precipitation model. I chose, therefore, to calibrate precipitation over the period 1920–2000. Statistical and diagnostic information for the seasonal regression models is listed in Table 5.3. For the reconstructed climatic variables, the difference between the number of years in a calibration period and the actual number of observations (n) is due to the removal of outliers. For example, the period of calibration for the precipitation model is 1920–2000 (81 years), but $n = 75$. This is because six outlying observations were removed from the precipitation model.

5.3.1 Climatic Trends

Decadal and multidecadal trends in radial tree growth, and therefore climate, are apparent throughout the chronology. To aid in the visualization of these trends, the

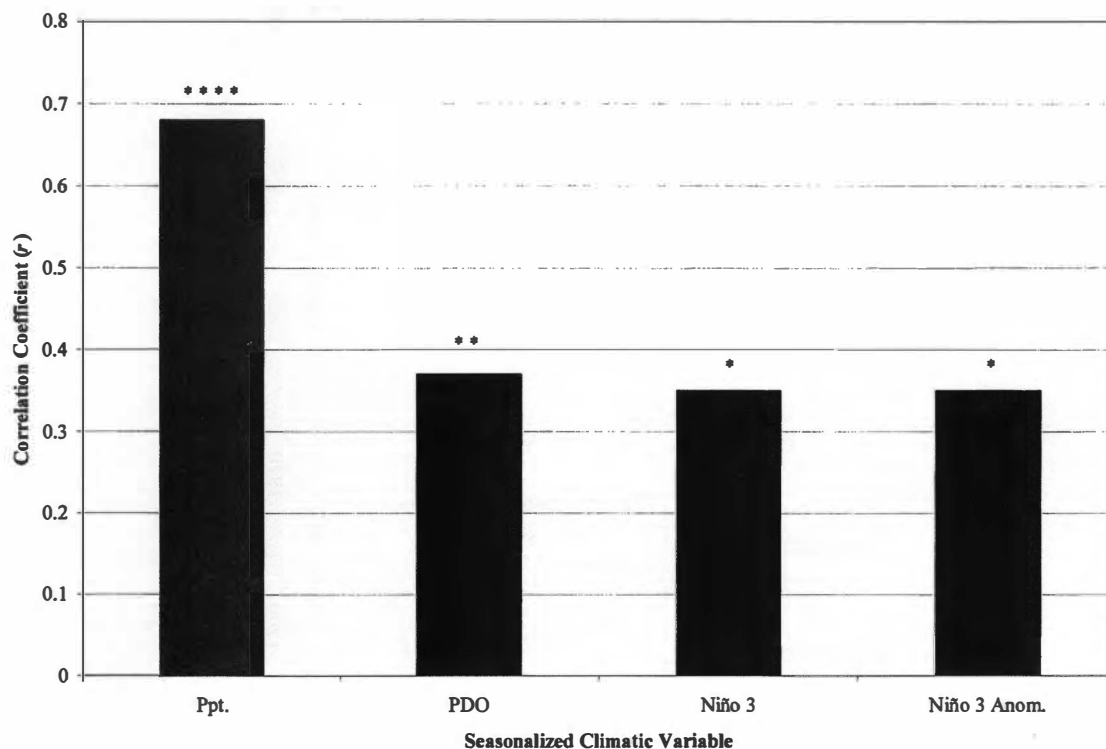


Figure 5.14 Pearson's product-moment correlation coefficients (r) between western juniper radial growth and selected seasonalized climatic variables. Ppt. is the previous July to current June precipitation data for Oregon Zone 7 (1920–2000), PDO is the current March and April PDO index (1948–2000), Niño 3 is the current May and June Niño 3 index (1950–2000), and Niño 3 Anom. is the current May and June Niño 3 index anomaly (1950–2000). * $p < 0.05$, ** $p < 0.01$, **** $p < 0.0001$.

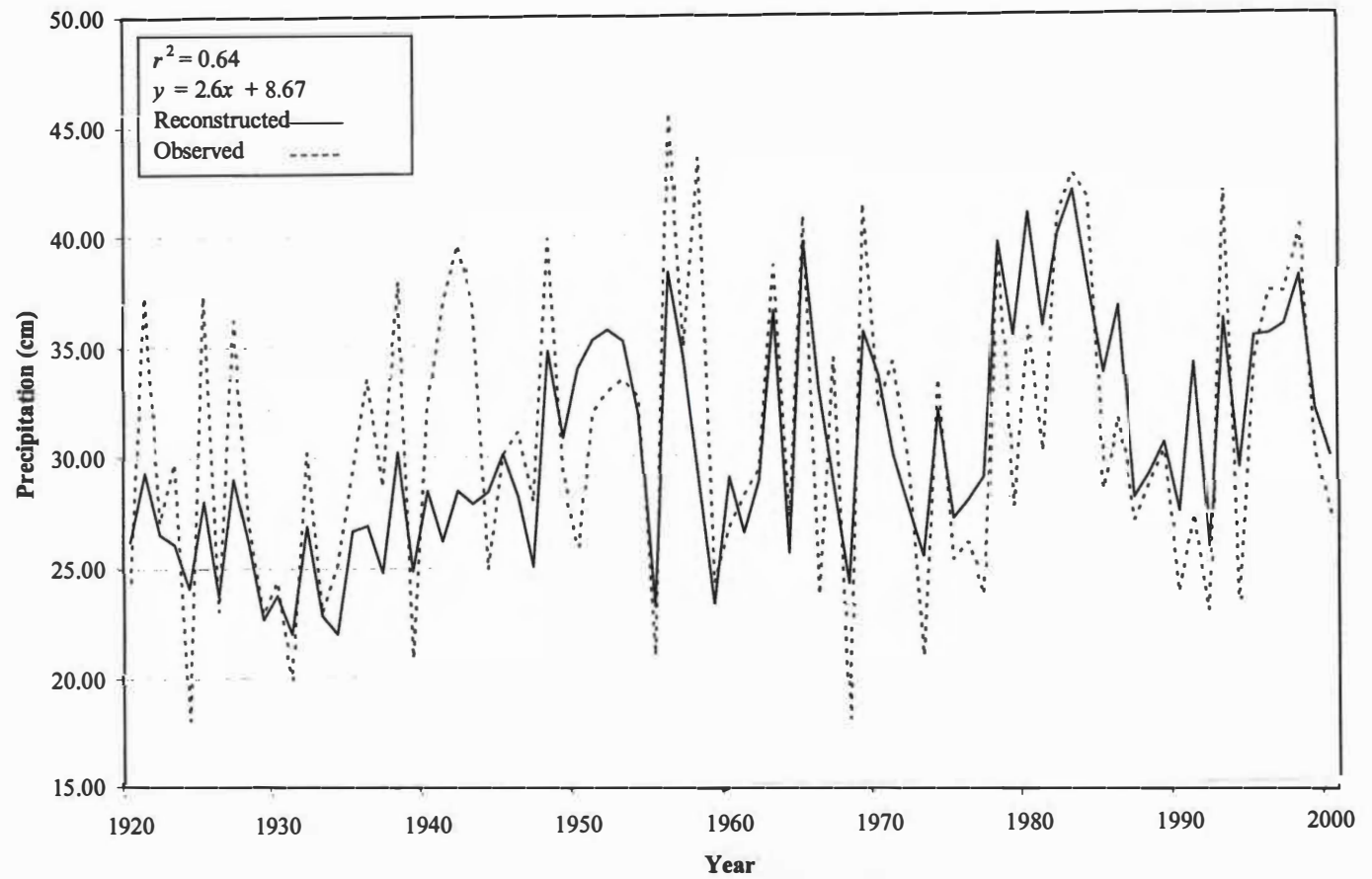


Figure 5.15 Observed and reconstructed Oregon Zone 7 precipitation (July_{t-1} to June_t).

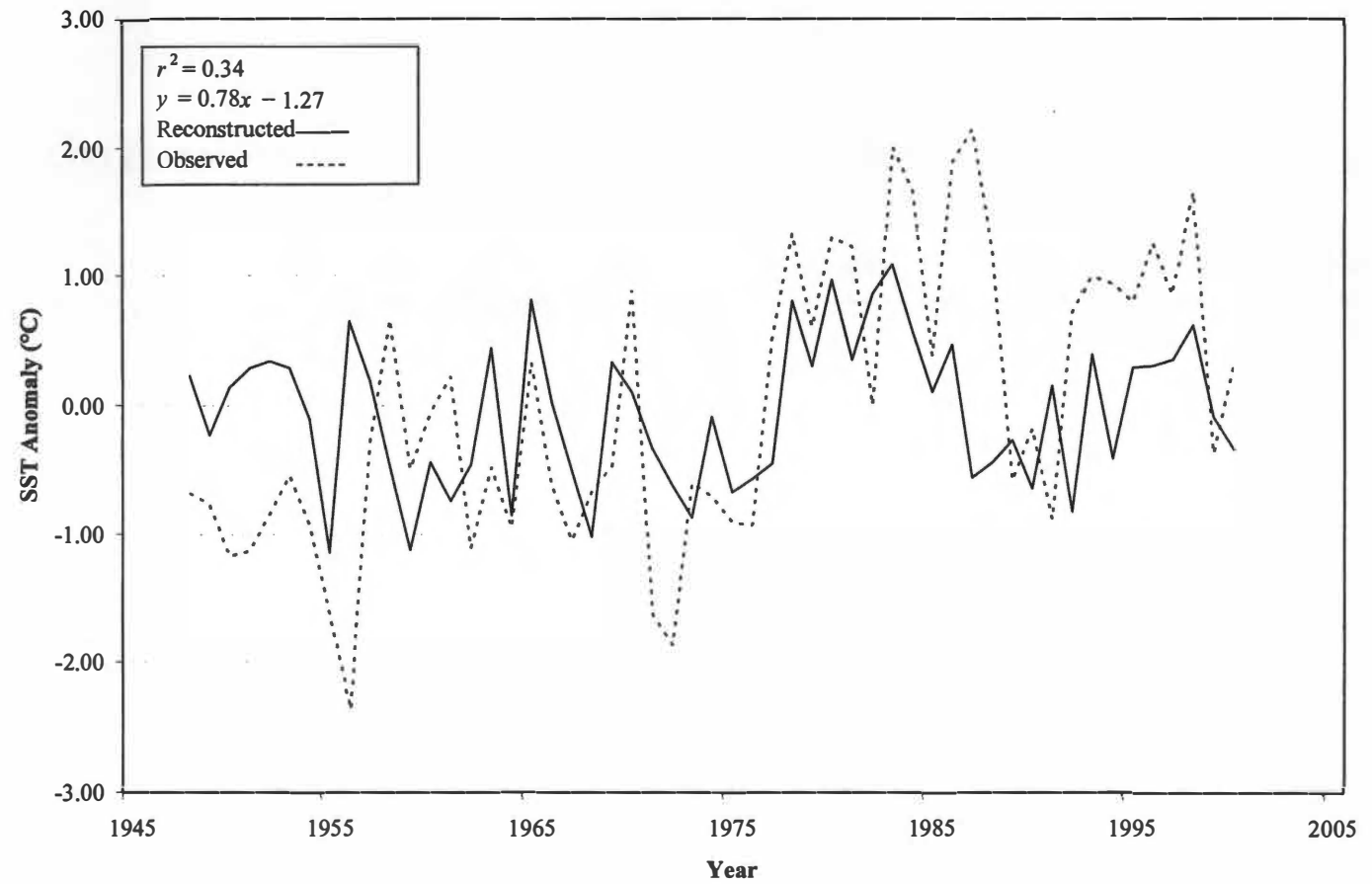


Figure 5.16 Observed and reconstructed PDO index (March_t to April_t).

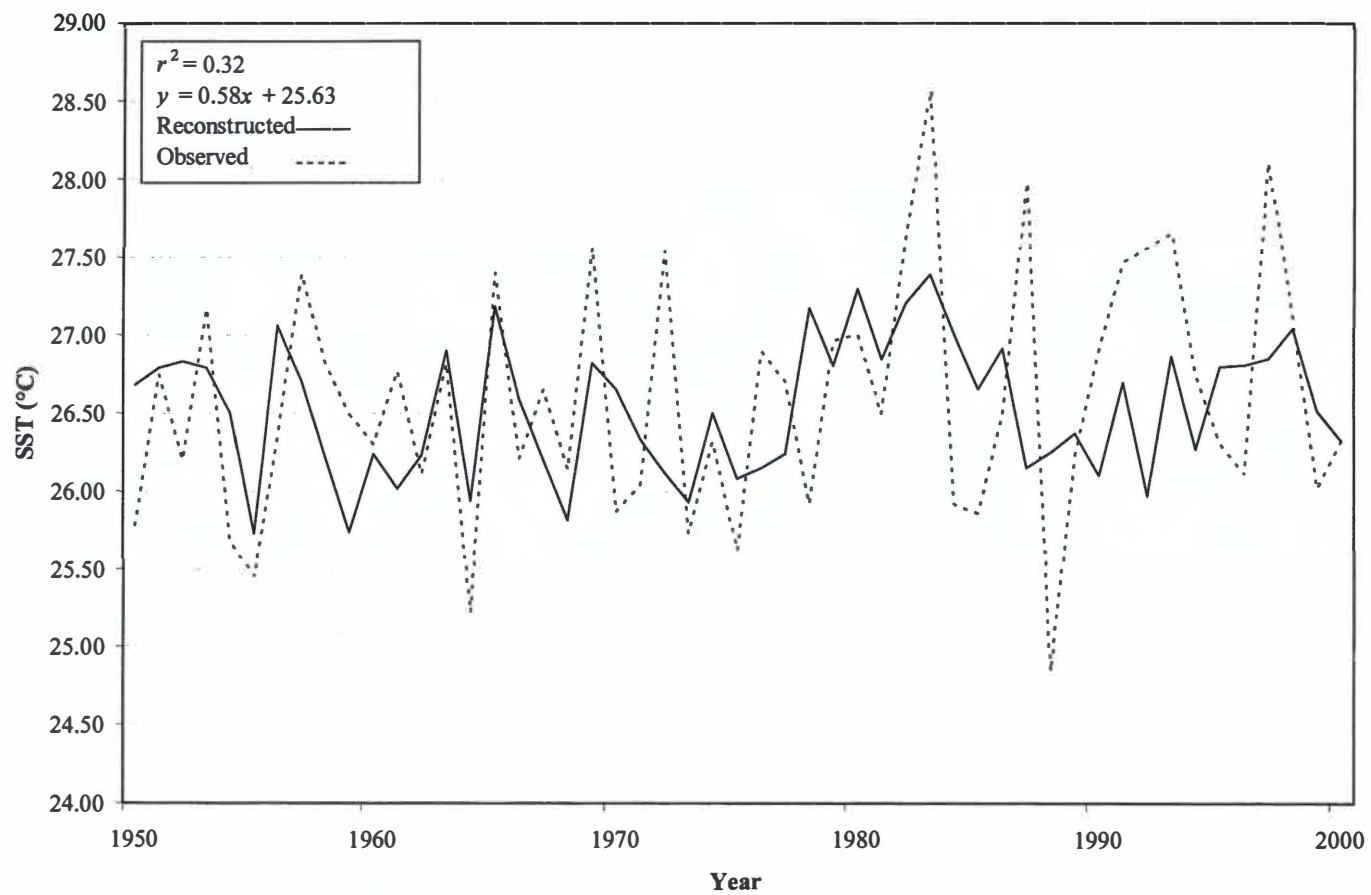


Figure 5.17 Observed and reconstructed Niño 3 index (May_t to June_t).

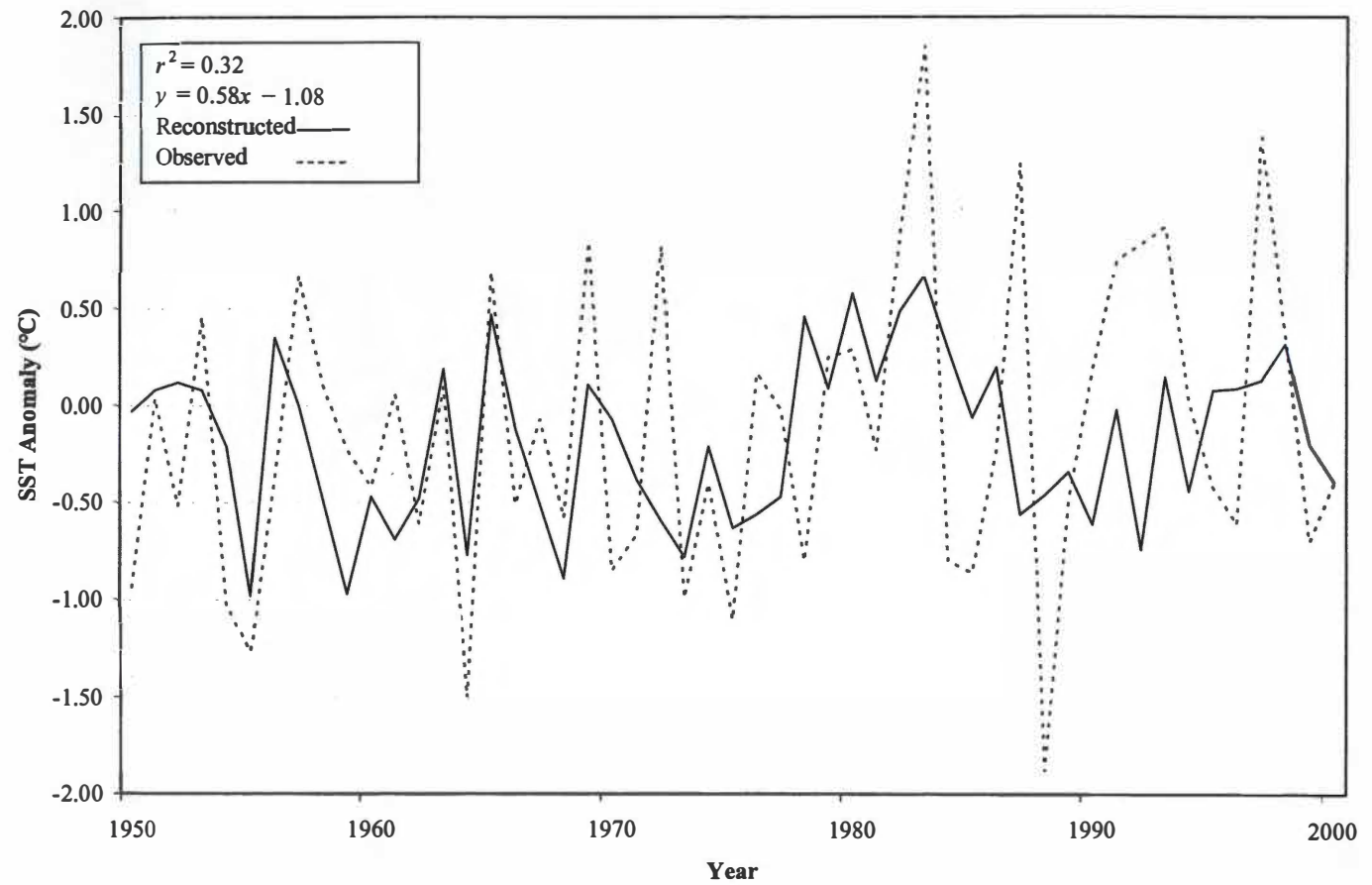


Figure 5.18 Observed and reconstructed Niño 3 anomaly (May_t to June_t).

Table 5.3 Regression statistics and diagnostics.

Statistic or Diagnostic	Zone 7 Ppt. ^a	PDO Anom. ^b	Niño 3 ^c	Niño 3 Anom. ^d
predictand	July _{t-1} to June _t	March _t to April _t	May _t to June _t	May _t to June _t
<i>n</i>	75	48	46	46
<i>F</i> value	129.76	23.99	20.64	20.67
significance prob. (<i>p</i>)	< 0.0001	< 0.0001	< 0.0001	< 0.0001
<i>r</i> ²	0.64	0.34	0.32	0.32
adjusted <i>r</i> ²	0.64	0.33	0.3	0.3
intercept	8.67	-1.27	25.63	-1.08
slope	2.6	0.78	0.58	0.58
Durbin-Watson <i>d</i>	1.89	1.55	1.77	1.77
1 st -order autocorrelation	0.05	0.21	0.09	0.09

^a Zone 7 Ppt. is the monthly precipitation data for Oregon Zone 7 (1920–2000), ^b PDO Anom. is the PDO index (1948–2000), ^c Niño 3 is the Niño 3 index (1950–2000), and ^d Niño 3 Anom. is the Niño 3 index anomaly (1950–2000).

chronology was smoothed with 10-year (Figure 5.19), 20-year (Figure 5.20), and 50-year (Figure 5.21) moving averages.

Marker years (i.e., years of extreme anomalous radial growth), listed in Tables 5.4 and 5.5, were also used to illustrate periods of above- and below-average radial growth. The chronology was divided into successive 200-year increments (Figures 5.22–5.27) to aid in the visualization of trends in marker years. In most cases, the climatic trends visible in the smoothed versions of the chronology are also visible as clusters of marker years.

The lowest average radial growth during a short-term period (2 to 9 years) occurred from A.D. 1698–1699. The highest average radial growth during a short-term period occurred from A.D. 1641–1642. The lowest average radial growth during a long-term period (≥ 10 years) occurred from A.D. 1645–1655, while the highest average radial growth during a long-term period occurred from A.D. 1440–1451. The longest sustained period of significantly below-average radial growth occurred from A.D. 1351–1390. The longest sustained period of significantly above-average radial growth occurred from A.D. 1948–1999.

The period A.D. 799–1000 (Figure 5.22) contained relatively few anomalous years of radial tree growth. Short-term periods of significantly above-average growth occurred during A.D. 801, 822–823, 841–842, and 892. Short-term periods of significantly below-average growth occurred during A.D. 810, 819, 915, 930, 954, 957, 979, 986, and 989. One long-term period of significantly below-average growth also occurred from A.D. 856–880.

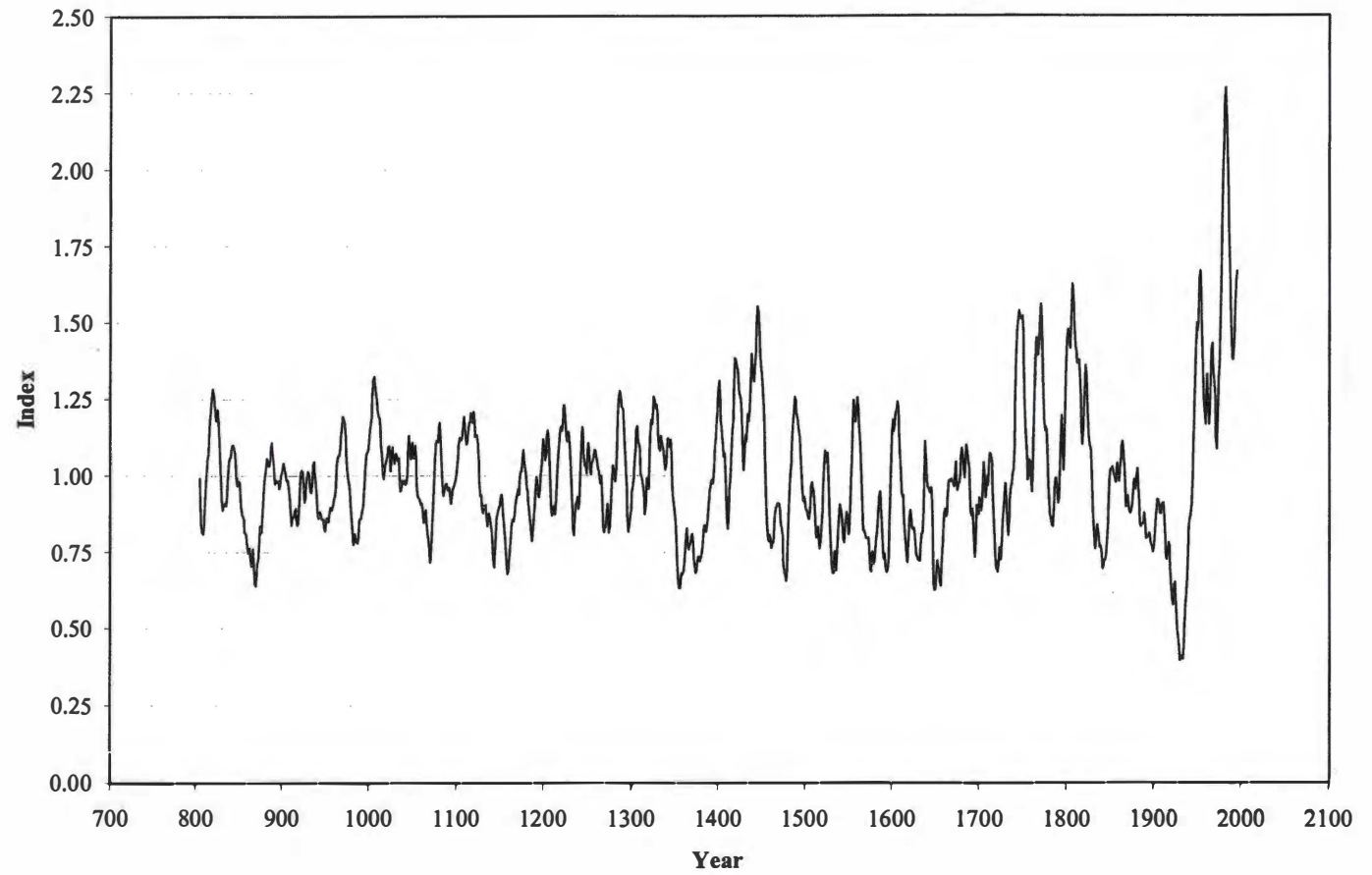


Figure 5.19 10-year moving average of the Frederick Butte western juniper chronology.

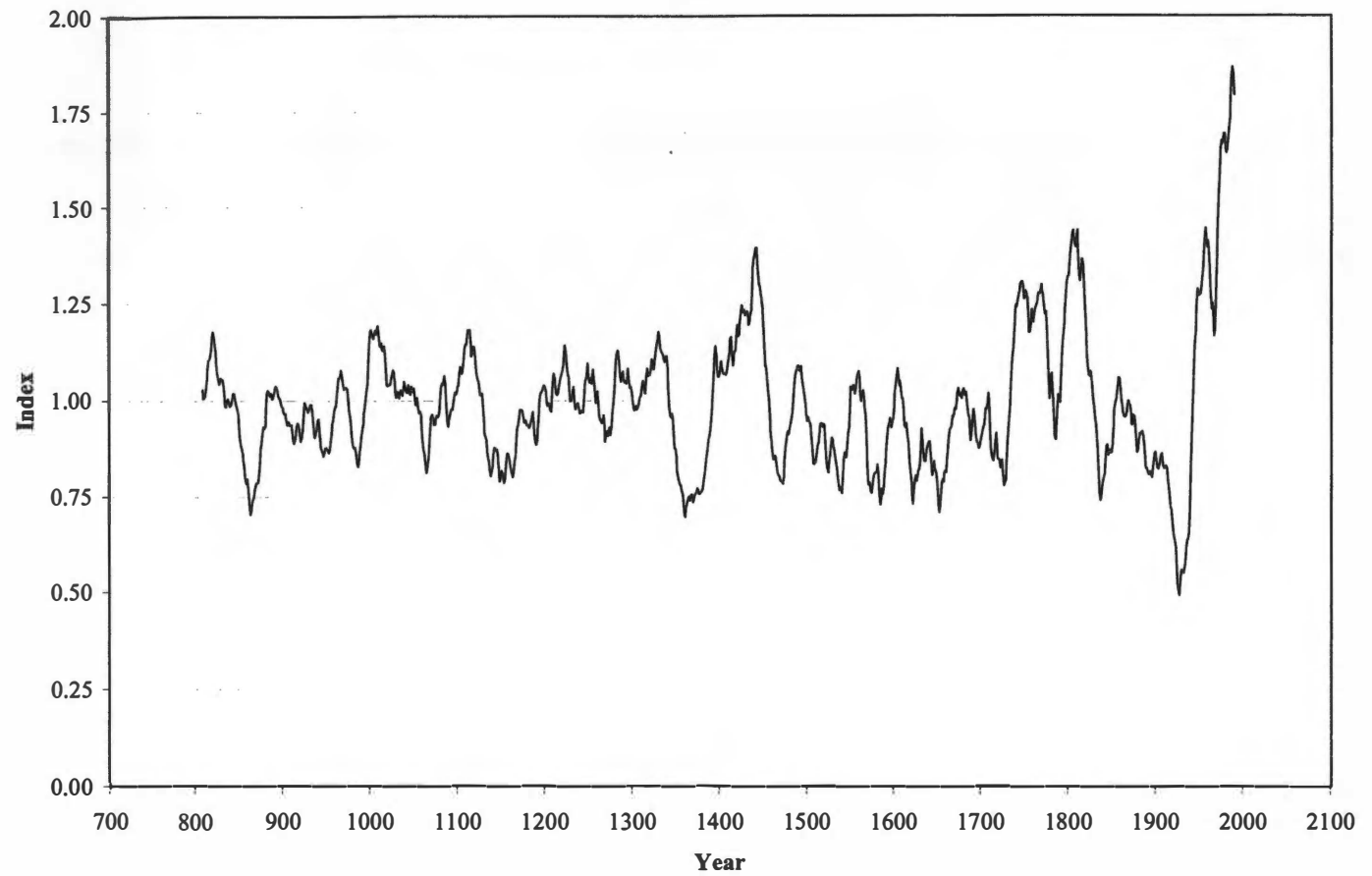


Figure 5.20 20-year moving average of the Frederick Butte western juniper chronology.

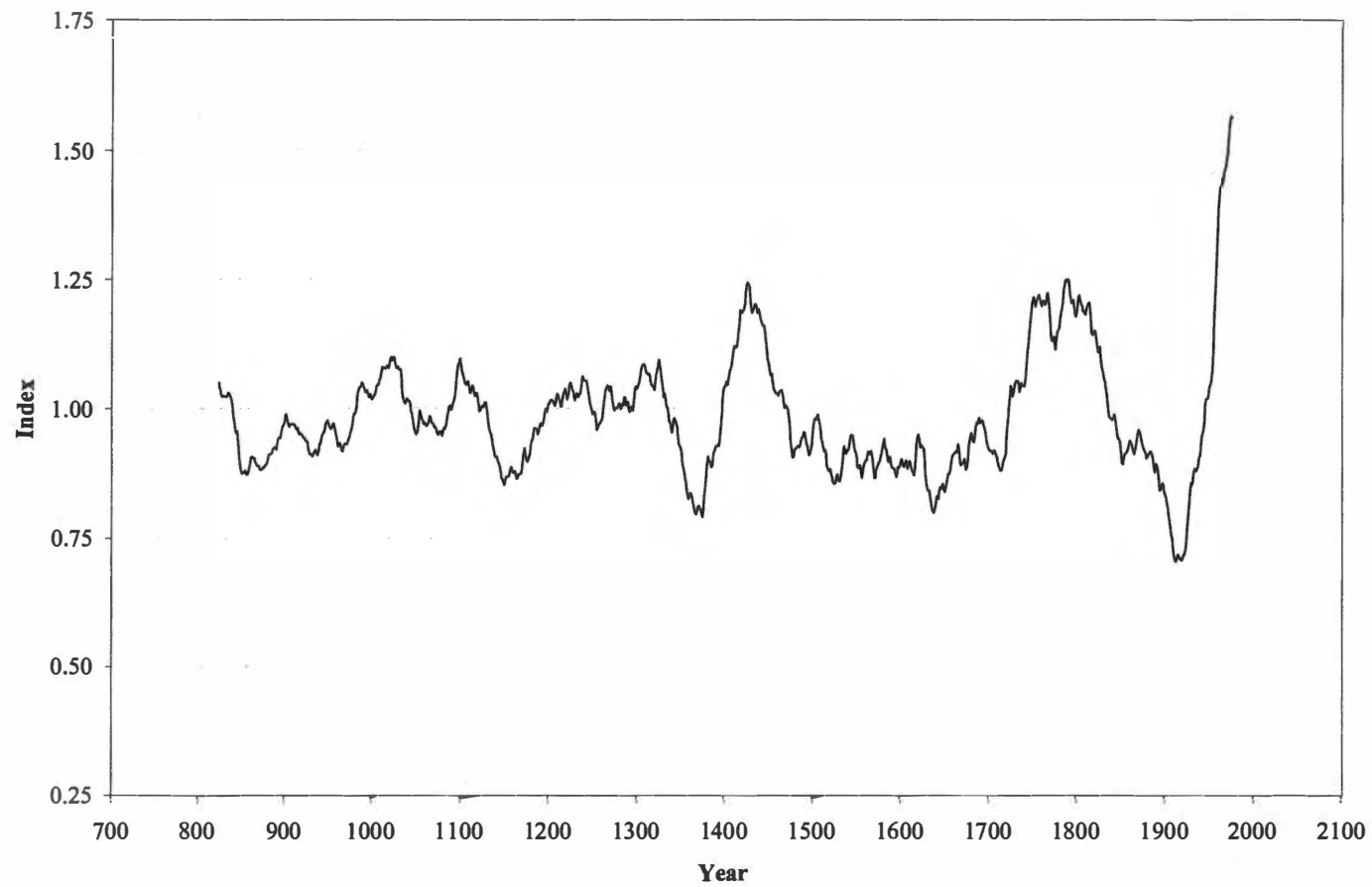


Figure 5.21 50-year moving average of the Frederick Butte western juniper chronology.

Table 5.4 Marker years of extreme above-average anomalous radial tree growth.

Century	Year
9 th	801 [*] , 822 [*] , 823 [*] , 841 [*] , 842 [*] , 892 [*]
10 th	None
11 th	1008 [†] , 1009 [†] , 1011 [*] , 1019 [*] , 1023 [*] , 1031 [*] , 1054 [*] , 1077 [*] , 1078 [‡] , 1079 [*]
12 th	1113 [*] , 1122 [*] , 1138 [*] , 1149 [*] , 1169 [*] , 1178 [*]
13 th	1202 [†] , 1204 [*] , 1220 [*] , 1241 [†] , 1259 [*] , 1262 [*] , 1287 [*] , 1291 [‡]
14 th	1305 [*] , 1308 [‡] , 1311 [*] , 1322 [†] , 1327 [‡] , 1332 [*] , 1341 [†] , 1347 [*]
15 th	1401 [†] , 1404 [†] , 1405 [‡] , 1412 [†] , 1420 [†] , 1421 [*] , 1422 [‡] , 1423 [†] , 1435 [†] , 1438 [*] , 1440 [‡] , 1441 [†] , 1442 [§] , 1443 [*] , 1445 [*] , 1447 [†] , 1448 [*] , 1449 [‡] , 1450 [*] , 1451 [*] , 1484 [†] , 1486 [*] , 1490 [*] , 1493 [*]
16 th	1503 [*] , 1523 [*] , 1524 [*] , 1557 [†] , 1559 [†] , 1560 [‡] , 1564 [†] , 1587 [*] , 1599 [*]
17 th	1601 [*] , 1602 [*] , 1603 [†] , 1606 [*] , 1617 [*] , 1624 [*] , 1641 [†] , 1642 [‡] , 1656 [*]
18 th	1701 [†] , 1702 [†] , 1709 [†] , 1713 [†] , 1716 [*] , 1727 [†] , 1734 [†] , 1740 [†] , 1745 [§] , 1746 [†] , 1747 [‡] , 1750 [‡] , 1754 [*] , 1761 [‡] , 1766 [†] , 1767 [‡] , 1768 [§] , 1769 [§] , 1773 [†] , 1775 [*] , 1790 [‡] , 1791 [†] , 1797 [*] , 1798 [‡] , 1799 [*]
19 th	1801 [†] , 1802 [‡] , 1803 [‡] , 1804 [*] , 1809 [†] , 1810 [‡] , 1811 [‡] , 1812 [†] , 1818 [†] , 1825 [§] , 1826 [†] , 1862 [†] , 1866 [*] , 1877 [*] , 1885 [*]
20 th	1948 [‡] , 1950 [†] , 1951 [‡] , 1952 [‡] , 1953 [‡] , 1954 [*] , 1956 [†] , 1957 [†] , 1963 [§] , 1965 [‡] , 1966 [†] , 1969 [‡] , 1970 [†] , 1974 [*] , 1978 [‡] , 1979 [‡] , 1980 [‡] , 1981 [‡] , 1982 [‡] , 1983 [‡] , 1984 [†] , 1985 [†] , 1986 [§] , 1991 [†] , 1993 [§] , 1995 [‡] , 1996 [†] , 1997 [†] , 1998 [†] , 1999 [*]

* ≥ 1.1 standard deviations, † ≥ 1.5 standard deviations, ‡ ≥ 2.0 standard deviations, § ≥ 2.5 standard deviations, ‡ ≥ 3.0 standard deviations, ‡ ≥ 3.5 standard deviations, ‡ ≥ 4.0 standard deviations, ‡ ≥ 4.5 standard deviations.

Table 5.5 Marker years of extreme below-average anomalous radial tree growth.

Century	Year
9 th	810 [†] , 819 [*] , 856 [*] , 865 [*] , 867 [*] , 868 [†] , 872 [†] , 873 [†] , 880 [*]
10 th	915 [†] , 930 [†] , 954 [*] , 957 [*] , 979 [*] , 986 [*] , 989 [*]
11 th	1040 [*] , 1059 [†] , 1072 [†] , 1083 [†] , 1098 [*]
12 th	1126 [†] , 1135 [†] , 1140 [†] , 1145 [†] , 1146 [†] , 1155 [*] , 1158 [*] , 1161 [*] , 1164 [*] , 1174 [†] , 1183 [†] , 1185 [*]
13 th	1212 [*] , 1213 [†] , 1217 [*] , 1236 [†] , 1239 [*] , 1245 [†] , 1250 [*] , 1271 [*] , 1272 [*] , 1273 [*] , 1279 [†] , 1296 [†]
14 th	1307 [†] , 1316 [*] , 1320 [*] , 1324 [*] , 1335 [†] , 1344 [*] , 1351 [*] , 1352 [†] , 1354 [†] , 1358 [†] , 1361 [*] , 1364 [†] , 1369 [*] , 1370 [*] , 1379 [†] , 1384 [*] , 1390 [†]
15 th	1407 [*] , 1408 [*] , 1410 [*] , 1413 [†] , 1425 [*] , 1428 [†] , 1439 [†] , 1444 [*] , 1454 [*] , 1465 [†] , 1475 [†] , 1477 [*] , 1480 [*] , 1499 [*]
16 th	1502 [*] , 1515 [*] , 1517 [†] , 1518 [†] , 1520 [*] , 1529 [†] , 1532 [†] , 1537 [*] , 1540 [†] , 1541 [*] , 1548 [*] , 1550 [†] , 1554 [*] , 1565 [†] , 1571 [†] , 1572 [*] , 1575 [*] , 1579 [†] , 1580 [†] , 1591 [*] , 1593 [*] , 1594 [†] , 1595 [*] , 1598 [†]
17 th	1600 [†] , 1607 [*] , 1616 [*] , 1618 [*] , 1619 [*] , 1622 [*] , 1626 [†] , 1628 [*] , 1629 [*] , 1632 [†] , 1636 [*] , 1639 [*] , 1645 [*] , 1649 [*] , 1652 [†] , 1655 [*] , 1660 [†] , 1667 [*] , 1670 [*] , 1679 [†] , 1686 [†] , 1691 [*] , 1695 [†] , 1698 [†] , 1699 [*]
18 th	1703 [*] , 1706 [†] , 1708 [*] , 1714 [*] , 1720 [*] , 1721 [†] , 1723 [*] , 1729 [†] , 1735 [*] , 1736 [*] , 1759 [*] , 1770 [*] , 1783 [†] , 1793 [†] , 1794 [*] , 1795 [*]
19 th	1800 [†] , 1822 [*] , 1829 [†] , 1833 [*] , 1834 [*] , 1837 [*] , 1841 [†] , 1843 [†] , 1858 [*] , 1869 [*] , 1871 [*] , 1888 [*] , 1889 [*] , 1898 [†]
20 th	1917 [*] , 1918 [†] , 1924 [†] , 1926 [†] , 1929 [†] , 1930 [†] , 1931 [†] , 1933 [†] , 1934 [†] , 1937 [*] , 1939 [*] , 1947 [*] , 1955 [†] , 1959 [†] , 1968 [†] , 1973 [*]

* ≥ 1.1 standard deviations, [†] ≥ 1.5 standard deviations, [‡] ≥ 2.0 standard deviations.

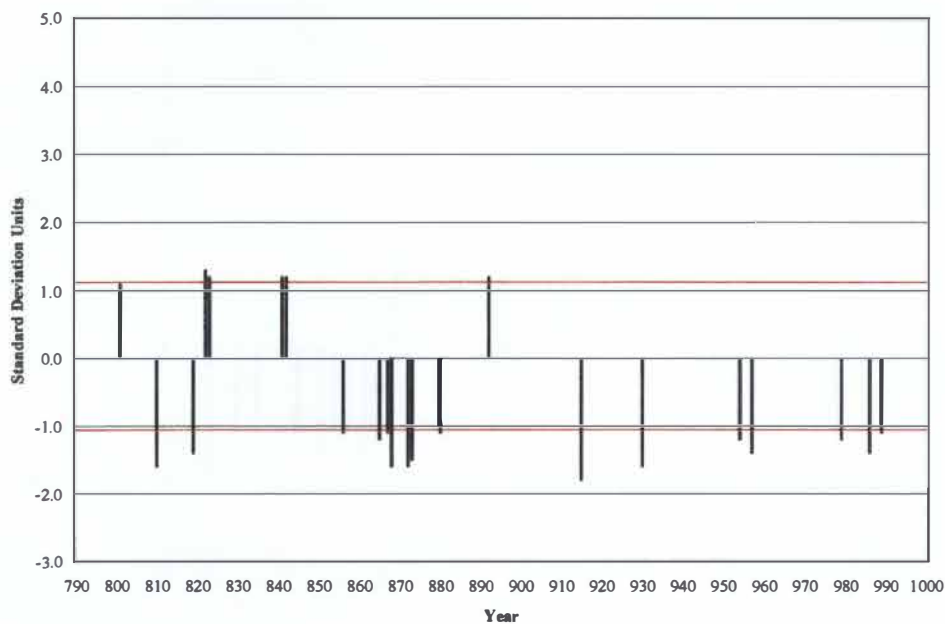


Figure 5.22 Marker year trends (A.D. 799–1000). Values \geq the upper threshold of 1.1 and values \leq the lower threshold of -1.1 are significantly anomalous.

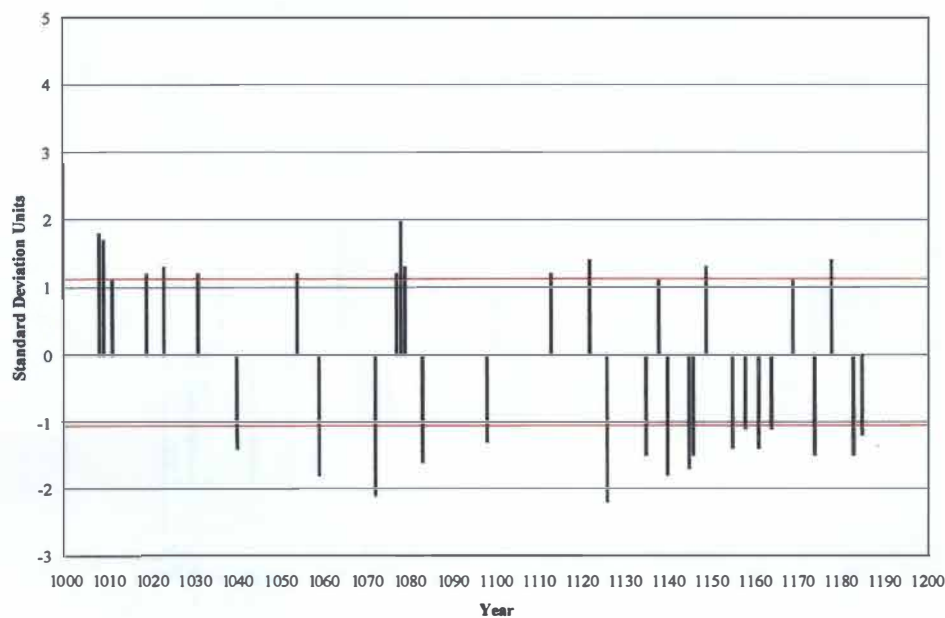


Figure 5.23 Marker year trends (A.D. 1001–1200). Values \geq the upper threshold of 1.1 and values \leq the lower threshold of -1.1 are significantly anomalous.

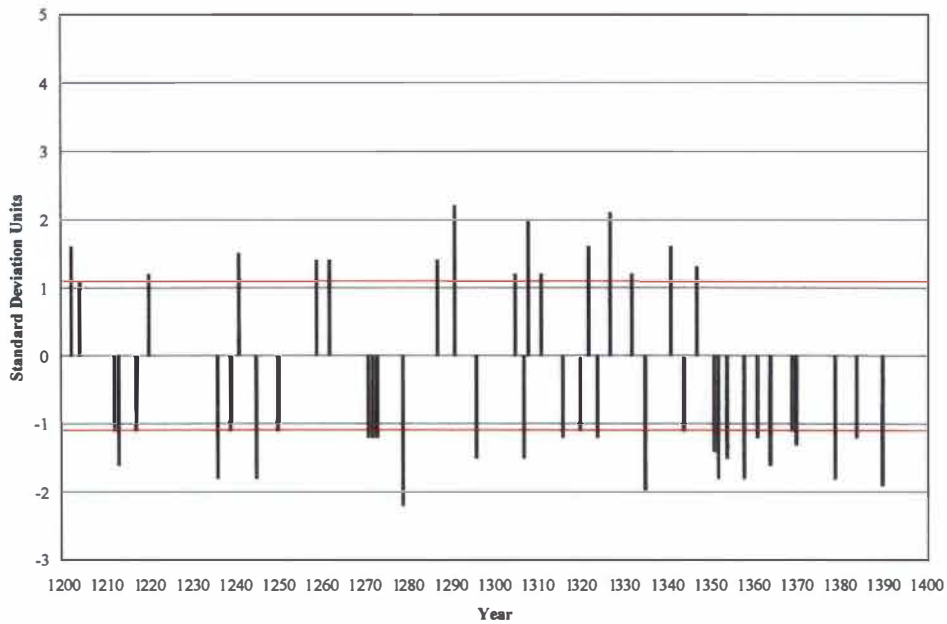


Figure 5.24 Marker year trends (A.D. 1201–1400). Values \geq the upper threshold of 1.1 and values \leq the lower threshold of -1.1 are significantly anomalous.

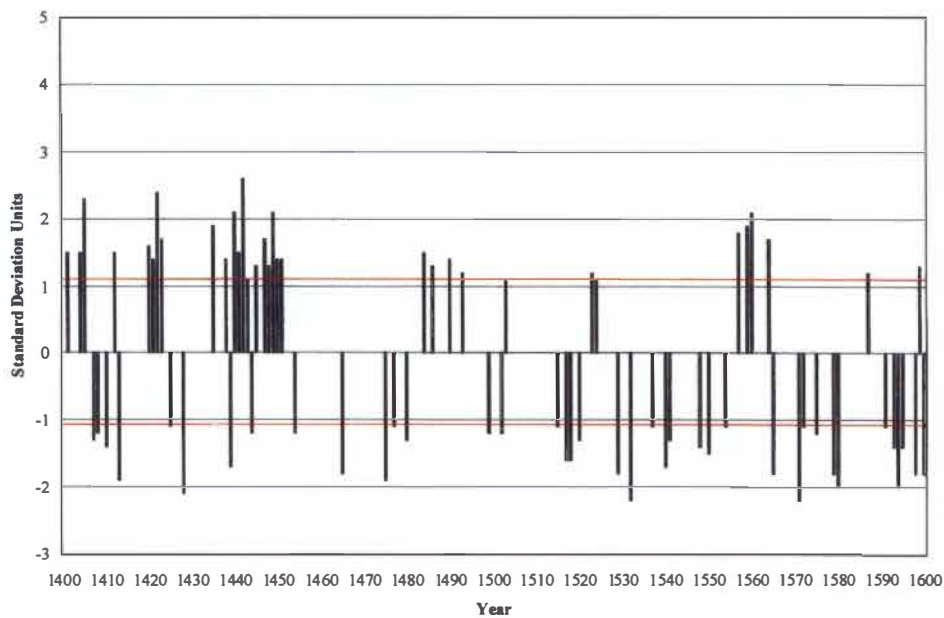


Figure 5.25 Marker year trends (A.D. 1401–1600). Values \geq the upper threshold of 1.1 and values \leq the lower threshold of -1.1 are significantly anomalous.

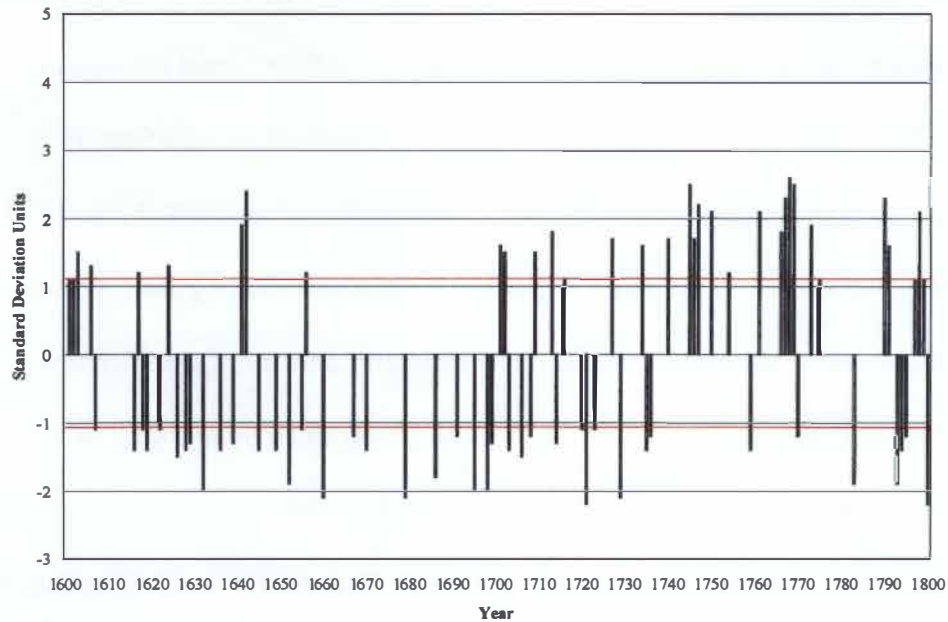


Figure 5.26 Marker year trends (A.D. 1601–1800). Values \geq the upper threshold of 1.1 and values \leq the lower threshold of -1.1 are significantly anomalous.

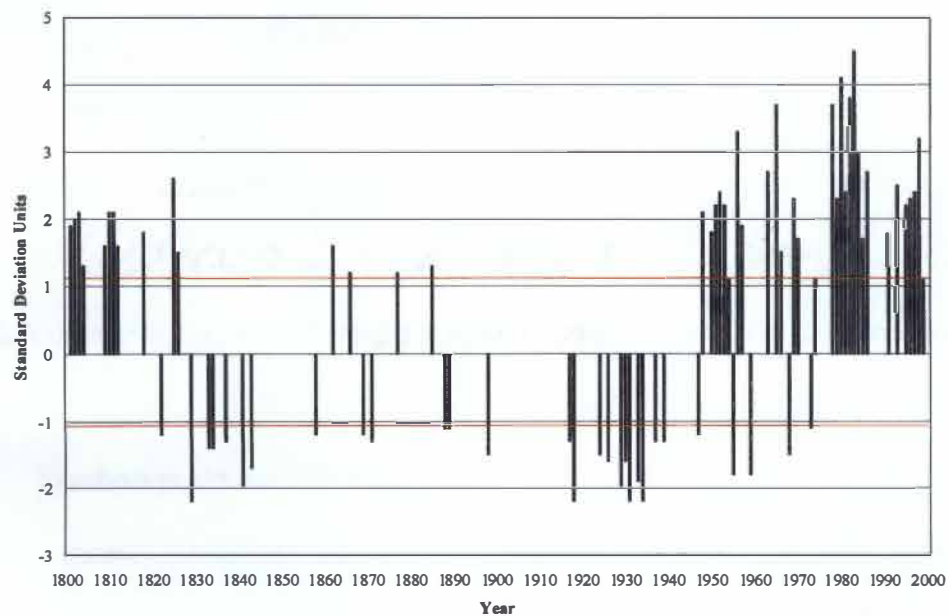


Figure 5.27 Marker year trends (A.D. 1801–2000). Values \geq the upper threshold of 1.1 and values \leq the lower threshold of -1.1 are significantly anomalous.

Anomalous years of growth increased in number from A.D. 1001–1200 (Figure 5.23). Short-term periods of significantly above-average growth occurred during A.D. 1054, 1077–1079, 1138, 1149, 1169, and 1178. Short-term periods of significantly below-average growth occurred during A.D. 1040, 1059, 1072, 1083, 1098, 1126, 1174, and 1183–1185. Two long-term periods of significantly above-average growth occurred from A.D. 1008–1031 and from 1113–1122. Two long-term periods of significantly below-average growth occurred from A.D. 1135–1146 (interrupted by one year of significantly above average growth in 1138) and from 1155–1164.

Multiple periods of anomalous growth occurred during the 13th and 14th centuries (Figure 5.24). Significantly above- and below-average years of growth alternated with little periodicity during most of this period. The short-term episodes of significantly above-average radial growth occurred during A.D. 1202–1204, 1220, 1241, 1259, 1262, 1287–1291, 1305, 1308–1311, 1322, 1327–1332, 1341, and 1347. The short-term episodes of significantly below-average radial growth occurred during A.D. 1212–1213, 1217, 1236–1239, 1245, 1250, 1271–1273, 1279, 1296, 1307, 1316, 1320, 1324, 1335, and 1344. A marked shift to significantly below-average growth, however, began in A.D. 1351 and continued through 1390.

The period A.D. 1401–1600 (Figure 5.25) also contained multiple episodes of anomalous annual radial growth. Short-term periods of significantly above-average growth occurred during A.D. 1401–1405, 1412, 1420–1423, 1435–1438, 1503, 1523–1524, 1557–1564, 1587, and 1599. Short-term periods of significantly below-average growth occurred during A.D. 1407–1410, 1413, 1425, 1428, 1439, 1444, 1454, 1465, 1475–1480, 1499–1502, 1515–1518, 1520, and 1600. Two long-term periods of

significantly above-average growth occurred from A.D. 1440–1451 (interrupted by one year of significantly below-average growth in 1444) and from 1484–1493. Three long-term periods of significantly below-average growth occurred from A.D. 1529–1554, 1565–1580, and from 1591–1600 (interrupted by one year of significantly above-average growth in 1599).

As with the previous 200 years, the period A.D. 1601–1800 contained multiple episodes of anomalous radial growth (Figure 5.26). Short-term periods of significantly above-average growth occurred during A.D. 1601–1606, 1617, 1624, 1641–1642, 1656, 1701–1702, 1709–1713, 1716, 1727, 1734, 1761–1769, 1773–1775, 1790–1791, and 1797–1799. Short-term periods of significantly below-average growth occurred during A.D. 1607, 1616, 1618–1622, 1626–1632, 1636, 1639, 1660, 1667, 1670, 1679, 1686, 1691, 1695, 1698–1699, 1703–1708, 1714, 1720–1723, 1729, 1735–1736, 1759, 1770, 1783, 1793–1795, and 1800. One long-term period of significantly below-average growth occurred from A.D. 1645–1655, while one long-term period of significantly above-average growth occurred from A.D. 1740–1754.

The final 200 years of the chronology are remarkable in regard to the intensity and duration of anomalous annual radial growth episodes (Figure 5.27). Two short-term periods of significantly above-average growth occurred from A.D. 1862–1866 and from 1877–1885. Short-term periods of significantly below-average growth occurred during A.D. 1822, 1858, 1869–1871, 1888–1889, 1898, 1955, 1959, 1968, and 1973. Two long-term periods of significantly above-average growth occurred from A.D. 1801–1826 (interrupted by one year of significantly below-average growth in 1822) and from 1948–1999 (interrupted by four years of significantly below-average growth in 1955, 1959,

1968, and 1973). Two long-term periods of significantly below-average growth occurred from A.D. 1829–1843 and from 1917–1947.

Chapter 6

Discussion

6.1 Chronology

The Frederick Butte chronology spans the period A.D. 797 to 2000 and complements and extends the previous chronologies for this area. Of the 78 samples collected in August 2001, 25 were used in this study. The time constraints of this study prohibited an analysis of the other 53 samples. Integration of the unprocessed samples may eventually push the Frederick Butte chronology back to the B.C. period. Western juniper from this area is an excellent species for dendrochronological research. Because this wood is such a valuable proxy source, the Bureau of Land Management should consider active conservation practices to preserve both the living and dead western juniper specimens in central Oregon. Because the dead wood is so well preserved in the dry climate, the potential for the existence of pre-B.C. western juniper specimens in central Oregon is high. Currently, much of the dead wood is sawn and burned as fuel by ranchers and in campfires.

6.2 Dynamics of Oregon Climate

Tree growth in south central Oregon more closely reflects changes in precipitation than any other climatic variable. The rate of cambial growth is clearly responsive to the amount of precipitation and its seasonal distribution. Precipitation from July of the previous year until June of the current year was one of the primary factors that controlled western juniper radial growth in this study. There are, however, many climatic factors

(e.g., the PDO, ENSO, and the location of air mass boundaries) that affect the amount of precipitation the region receives. Because of this, I was able to analyze the effects of the PDO and ENSO on the growth of western juniper trees. I found that all of these climatic variables were positively correlated with radial growth of western junipers in south central Oregon. In the following sections, I will address the dynamics of each of these climatic factors individually and discuss how each factor may have affected western juniper radial growth and, therefore, my inferences about precipitation in this study.

6.2.1 The PDO and ENSO

At least two previous studies found evidence of “paradoxical” ENSO and/or PDO signals in tree ring studies in central Oregon. Pohl *et al.* (2002) found that La Niña coincided with reduced radial tree growth in central Oregon. This is seemingly anomalous, since La Niña events typically bring cooler and wetter conditions to the Pacific Northwest. This led Pohl *et al.* to conclude that high elevation, rain shadow, lower regional temperatures, and the influence of continental air masses in central Oregon may effectively counteract any growth benefits associated with La Niña conditions east of the Cascade Range (Pohl *et al.* 2002). Knapp *et al.* (2004) also found evidence of a seemingly anomalous ENSO/PDO signal in the interior Pacific Northwest. They discovered a regionally widespread drought (1917 to 1919) that occurred in synchrony with an active La Niña and a neutral PDO.

Both El Niño and positive phase PDO typically bring warmer and drier conditions to much of the Pacific Northwest, while La Niña and negative phase PDO typically usher in cooler and wetter conditions. There are many explanations, however, for a seemingly

paradoxical behavior of the PDO and ENSO in the Pacific Northwest. In addition to the factors mentioned by Pohl *et al.* (2002), other climatic variables may interact with the PDO and ENSO to produce unexpected climatic oscillatory signals in tree-ring chronologies. For example, one climatic oscillation may override another if the oscillations occur out of phase. This is especially true with ENSO and the PDO. Other synoptic-scale climatic oscillations, such as the Atlantic Multidecadal Oscillation (AMO), may also affect climate in the Pacific Northwest and interact with, or even override, the PDO and ENSO.

Both ENSO and the PDO are positively correlated with tree growth at the Frederick Butte sites. The positive correlation does not correspond with the significant negative correlations typically found for these climatic oscillations in other areas of the Pacific Northwest. I suggest that the positive correlation may be related to air mass boundaries. Because Frederick Butte is located in the interior Pacific Northwest in an air mass transitional area, continental air masses play a major role in determining the climate at Frederick Butte. I suggest that the influence of these continental air masses is so great that it causes the climate at Frederick Butte to respond differently to the PDO and ENSO than climate at many other areas in the Pacific Northwest, especially in those areas along the coast. The following section will address the climatic effects of the air mass transitional zone that occurs over central Oregon.

6.2.2 Air Mass Boundaries

The influence of elevation change on climate is great in the western United States. This often makes it difficult to gain insight into the causes of climate in mountainous

areas (Mitchell 1976). It is difficult to discuss the climate of such areas in the usual terms of mean temperature and precipitation because these common meteorological parameters are significantly modified by orography. This is especially true in the Pacific Northwest, where the Coast Ranges, Cascade Range, and Rocky Mountains all help define climate. To better understand the climatology of the western United States, Mitchell (1976) used equivalent potential temperature (a function of water vapor and temperature) as a delimiting factor for climatic regions in the area (Figure 6.1). Equivalent potential temperature was used because of its relatively conservative behavior with altitude change. This climatic parameter indicates that the six climatic regions illustrated in Figure 6.1 are homogenous entities and that the climate of each is distinct from that of the other regions (Mitchell 1976). Based on Mitchell's results, two major air masses affect the Pacific Northwest. Region 1 is characterized by the frequent migration of air masses from the Pacific during winter and much of the summer. Region 2 is also affected by Pacific air masses during the winter, but is under the influence of interior air during the summer. Frederick Butte lies directly within the transitional zone between these two air masses.

Knapp *et al.* (2002) found that two of the three Pacific Northwest climatic regions they identified closely approximate those determined by Mitchell (1976). The East and Southwest subregions of Knapp *et al.* (2002) closely resemble climatic regions 2 and 5 of Mitchell (Figure 6.2). Much of the Northwest region of Knapp *et al.*, however, is dominated by the transitional boundary between regions 1 and 2 of Mitchell. This led

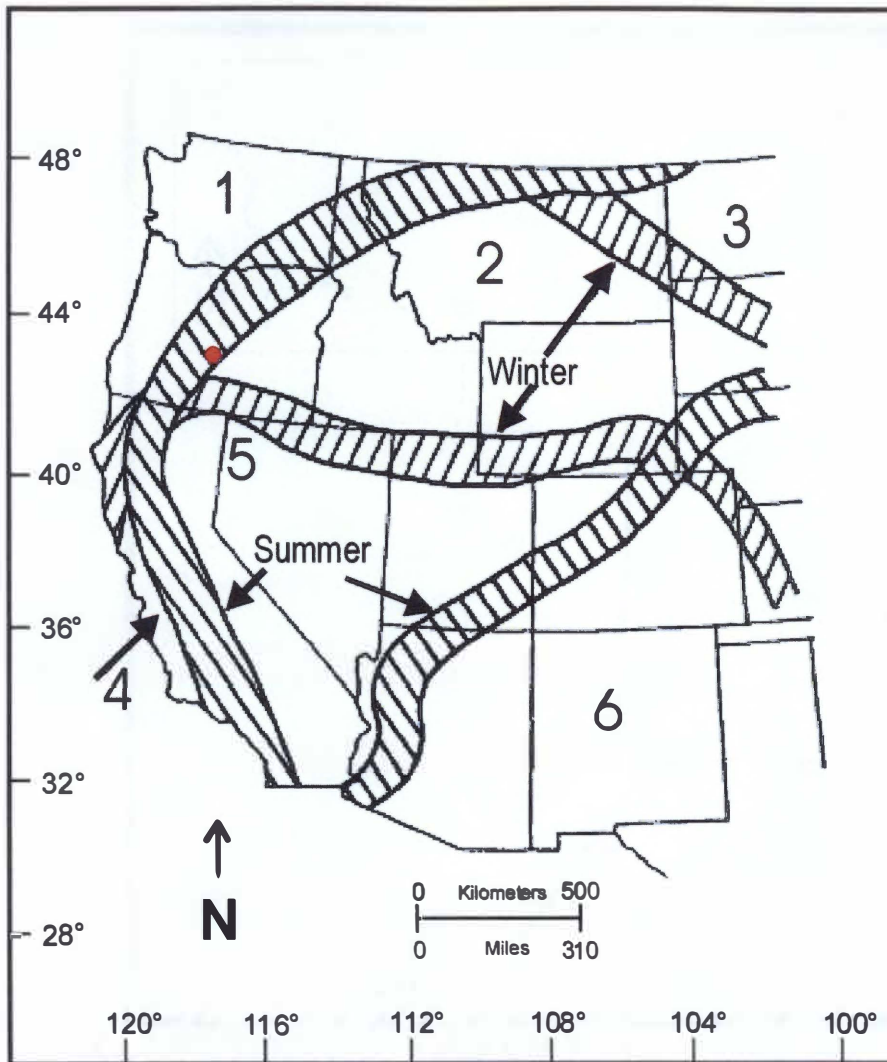


Figure 6.1 Western United States major equivalent air mass boundaries and climatic regions. Frederick Butte, the location of the study sites, is marked in red. The hatched areas are transitional zones between equivalent air mass boundaries (adapted from Mitchell 1976).

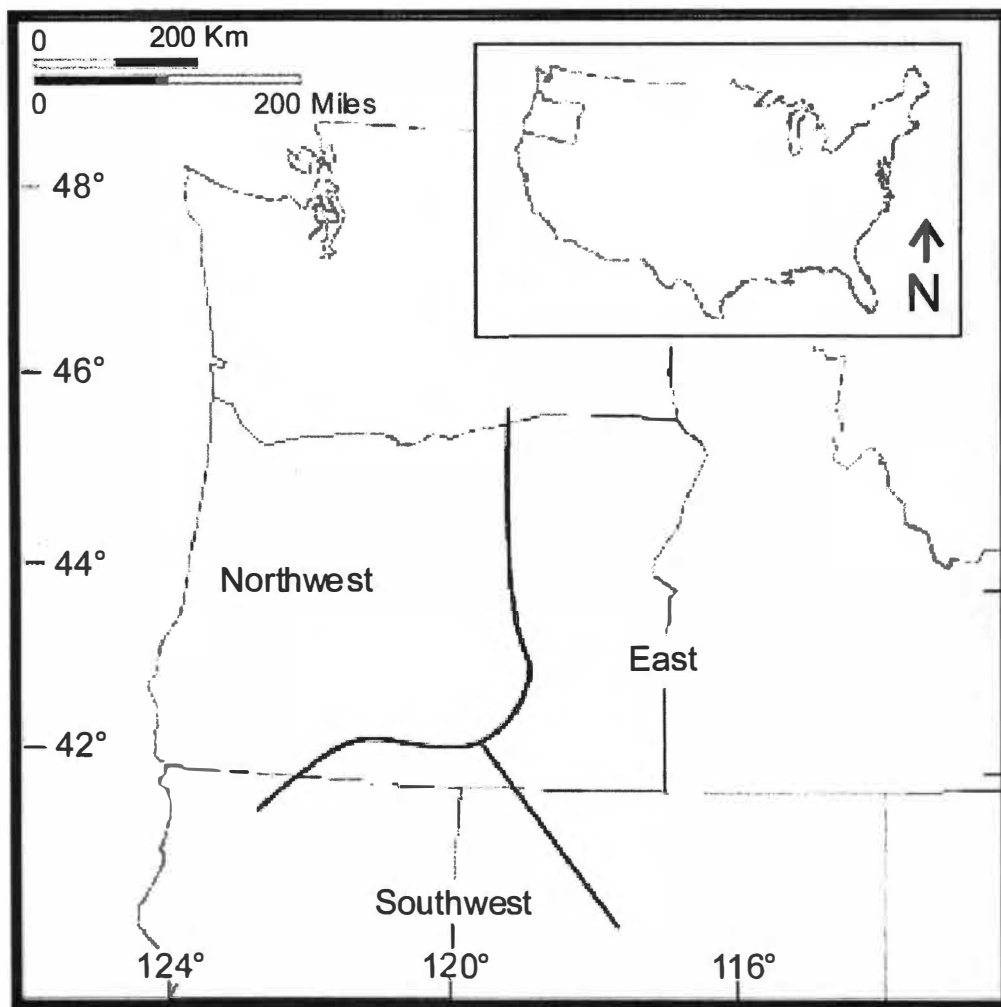


Figure 6.2 Pacific Northwest climatic subregions (adapted from Knapp *et al.* 2002).

Knapp *et al.* to conclude that the high climatic variability at their Northwest-region sites may be caused by their location on the seasonal marine/interior air mass boundary defined by Mitchell (Knapp *et al.* 2002).

The high climatic sensitivity of western juniper at Frederick Butte may be partially attributed to the location of the study sites within this transitional air mass boundary. The location of the air mass boundary may also cause the trees in this area to respond differently than other locations in the Pacific Northwest to various climatic variables such as the PDO and ENSO.

6.3 Trends in Central Oregon Climate

Decadal and multidecadal trends in radial tree growth and, therefore, climate are apparent throughout the chronology. These long-term periods may have been driven by the PDO. To aid in the visualization of these trends, the chronology was smoothed with 10-year, 20-year, and 50-year moving averages. Marker years were also used to illustrate periods of above- and below-average radial growth. Sections 6.3.1–6.3.6 focus on the climatic trends of the chronology within the successive 200-year increments previously established in Figures 5.2–5.7. Periods of major drought and wetness will be the focus of the following sections.

Multiple short-term (i.e., single-year, etc.) growth anomalies are also abundant throughout the chronology, and it is possible that these short-term anomalies were driven by ENSO, or by a combination of ENSO and the PDO. All single-year events are listed in Tables 5.4 and 5.5. The years of greatest negative departure of radial growth are, in ascending order, 1126, 1279, 1532, 1571, 1721, 1800, 1829, 1918, 1931, 1934, 1679,

1729, 1660, 1072, 1428, 1335, 1580, 1632, 1594, 1695, 1698, 1929, and 1841. There is supporting evidence of a La Niña that occurred during 1632 which may have led to drought conditions in the area (Lough 1992). Interestingly, however, an El Niño occurred during 1721, and El Niño conditions would not typically lead to below-average radial growth at Frederick Butte. The results found in this study closely correspond with the drought records reconstructed by Knapp *et al.* (2002, 2004). Their Northwest subregional extreme climatic pointer year index corresponds well with many of the single-year droughts I discovered in the Frederick Butte chronology (Knapp *et al.* 2002).

The years of greatest positive departure of radial growth are, in descending order, 1983, 1980, 1982, 1965, and 1978. The synergistic effects of El Niño and a positive-phase PDO likely led to the above-average growth in 1982 and 1983. The PDO was in a positive phase in 1978 and 1980, as well. Interestingly, however, the above average growth that occurred in 1965 occurred during a negative phase of the PDO.

6.3.1 A.D. 799–1000

The period A.D. 799–1000 contained relatively few anomalous years of radial tree growth. Short-term periods of significantly above-average growth occurred during A.D. 801, 822–823, 841–842, and 892, while short-term periods of significantly below-average growth occurred during A.D. 810, 819, 915, 930, 954, 957, 979, 986, and 989. The long-term period A.D. 856–880 contained seven years of significantly below-average radial growth.

6.3.2 A.D. 1001–1200

Anomalous years of growth increased in number from A.D. 1001–1200. Short-term periods of significantly above-average growth occurred during A.D. 1054, 1077–1079, 1138, 1149, 1169, and 1178, while short-term periods of significantly below-average growth occurred during A.D. 1040, 1059, 1072, 1083, 1098, 1126, 1174, and 1183–1185. The long-term period A.D. 1008–1031 contained six years of significantly above-average radial growth, while another long-term period, A.D. 1113–1122, contained only two years of significantly above-average radial growth. The long-term period A.D. 1135–1146 contained four years of significantly below-average radial growth (interrupted by one year of significantly above-average radial growth in 1138), while another long-term period, A.D. 1155–1164, also contained four years of significantly above-average radial growth.

6.3.3 A.D. 1201–1400

Significantly above- and below-average years of growth alternated with little periodicity during this period until a marked shift to significantly below-average growth began in A.D. 1351 and continued through 1390. Short-term episodes of significantly above-average radial growth occurred during A.D. 1202–1204, 1220, 1241, 1259, 1262, 1287–1291, 1305, 1308–1311, 1322, 1327–1332, 1341, and 1347, while short-term episodes of significantly below-average radial growth occurred during A.D. 1212–1213, 1217, 1236–1239, 1245, 1250, 1271–1273, 1279, 1296, 1307, 1316, 1320, 1324, 1335, and 1344. The 40-year period that occurred from A.D. 1351–1390 included 11 years of significantly below-average radial growth.

There is a slight possibility that this period of suppressed radial growth may have been associated with the Medieval Warm Period, a time of unusually warm climate in the North Atlantic region that lasted from approximately the 11th through the 14th century (IPCC 2007). The Medieval Warm Period partially coincided with the Medieval Maximum, a peak in solar activity that occurred from A.D. 1100–1250. The period of overall warmth and dryness was possibly related to changes in the strength of the North Atlantic thermohaline circulation and the North Atlantic Oscillation (USGS 2007). A radiocarbon-dated box core taken from the Sargasso Sea indicated that SST was approximately 1 °C warmer 1,000 years ago than it is today (Keigwin 1996). Prolonged droughts affected parts of western North America, especially eastern California and the western Great Basin, during the Medieval Warm Period (Bradley *et al.* 2003).

It was initially believed that the Medieval Warm Period may have affected a relatively broad spatial area in the Northern Hemisphere; however, this view was challenged by the 2001 Intergovernmental Panel on Climate Change report that states that the term “Medieval Warm Period” has limited utility in describing trends in hemispheric or global mean temperature changes in past centuries (IPCC 2007).

6.3.4 A.D. 1401–1600

The period A.D. 1401–1600 also contained multiple episodes of anomalous annual radial growth. Short-term episodes of significantly above-average radial growth occurred during A.D. 1401–1405, 1412, 1420–1423, 1435–1438, 1503, 1523–1524, 1557–1564, 1587, and 1599, while short-term episodes of significantly below-average

radial growth occurred during A.D. 1407–1410, 1413, 1425, 1428, 1439, 1444, 1454, 1465, 1475–1480, 1499–1502, 1515–1518, and 1520.

A relatively strong positive-phase PDO may have occurred during A.D. 1440–1451. Ten years of significantly above-average radial growth occurred during this 12-year period (interrupted by one year of significantly below-average growth in 1444). Another period, A.D. 1484–1493, included four years of significantly above-average radial growth. After 1493, no other long-term climatic trends were noticeable until A.D. 1529–1554, during which eight years of significantly below-average radial growth occurred.

The 16th century came to a close with two more periods of below-average radial growth. Six years of significantly below-average radial growth occurred during A.D. 1565–1580, and again during A.D. 1591–1600 (interrupted by one year of significantly above-average growth in 1599). These periods may have been associated with the 16th century megadrought, the most severe and prolonged North American drought in the last 500 years (Meko *et al.* 1995, Grissino-Mayer 1996, Stahle *et al.* 2000). The 16th century megadrought lasted approximately 40 years and is believed to have affected the lives of the early Spanish and English settlers, as well as Native Americans throughout North America. Tree-ring chronologies from the Great Lakes region, the northwestern United States, and the southeastern United States have previously established that drought conditions affected Mexico, the Rocky Mountains, and the Mississippi Valley during the last half of the 16th century.

The 16th century megadrought was likely associated with fluctuating ocean currents, and its appearance mimicked the signatures of a negative-phase PDO. In this

instance, however, a multidecadal warm phase of the AMO in the North Atlantic Ocean may have contributed to the severe drought conditions, as well (Gray *et al.* 2003).

Although it is believed that changes in equatorial Pacific Ocean currents may have also contributed to the 16th century megadrought, no one knows for certain the causative agents that came together to create such a devastating drought.

It is not likely that anthropogenic factors contributed to the conditions that facilitated the megadrought, and the natural factors that produced it could occur again. Recent analyses have shown that the AMO has a very strong influence on summer rainfall across much of North America and may affect the strength of the teleconnection between ENSO and winter precipitation (Enfield *et al.* 2001, McCabe *et al.* 2004). A positive phase of the AMO since 1995 and a possible cold phase of the PDO from 1998 to 2002 have raised concerns about the potential for another megadrought occurrence (Gray *et al.* 2003, McCabe *et al.* 2004). A scenario such as this may have been responsible for the 16th century megadrought.

6.3.5 A.D. 1601–1800

As with the previous 200 years, the period A.D. 1601–1800 contained multiple episodes of anomalous radial growth. This period is defined by episodes of very active climatic oscillations, both short- and long-term. Short-term periods of significantly above-average growth occurred during A.D. 1601–1606, 1617, 1624, 1641–1642, 1656, 1701–1702, 1709–1713, 1716, 1727, 1734, 1761–1769, 1773–1775, 1790–1791, and 1797–1799, while short-term periods of significantly below-average growth occurred during A.D. 1607, 1616, 1618–1622, 1626–1632, 1636, 1639, 1660, 1667, 1670, 1679,

1686, 1691, 1695, 1698–1699, 1703–1708, 1714, 1720–1723, 1729, 1735–1736, 1759, 1770, 1783, 1793–1795, and 1800. The long-term period A.D. 1645–1655 contained four years of significantly below-average radial growth, while another long-term period, A.D. 1740–1754, contained six years of significantly above-average radial growth.

The smoothed versions of the chronology indicate a noticeable trend in increased radial growth during the latter part of the 18th century and the early part of the 19th century. This trend in above-average radial growth might be related to a climatic phenomenon other than the PDO or ENSO. The Little Ice Age was a period of climatic cooling that occurred from approximately the middle 16th to the middle 19th century in Europe, North America, and Asia. Increased precipitation also occurred in many parts of the Northern Hemisphere during the Little Ice Age. It is widely accepted that three temperature minima occurred during the course of the Little Ice Age. The three minima began around 1650, 1770, and 1850. All three minima were separated by slightly warmer periods (NASA 2007a).

Severely cold temperatures affected many parts of the world during the Little Ice Age, but the brunt of the severe weather seems to have occurred in the North Atlantic region (O'Brien *et al.* 1995). Glaciers advanced, especially in the Alps, Norway, Ireland, and Alaska, and multiple rivers froze throughout the Northern Hemisphere. The New York harbor froze during the winter of 1780, and New Yorkers were able to walk from Manhattan to Staten Island. In response to food shortages, Native Americans were forced to form leagues to avoid starvation (NASA 2007b).

A decrease in solar activity and an increase in volcanic eruptions are the two most widely accepted causes of the Little Ice Age. The deepest trough in temperature during

the Little Ice Age occurred concomitantly with the Maunder Sunspot Minimum. During the coldest part of the Little Ice Age, from 1645 to 1715, total solar energy output decreased, as indicated by little or no sunspot activity (NASA 2007b). Astronomers of the time, including Galileo Galilei, noticed approximately 50 sunspots during a 30-year period – a major decline from the thousands that typically occur during a similar period (NASA 2007b). During this period, diminished jet stream winds (caused by a reduction in solar energy) and a reduction in the transport of warm Pacific air to North America and warm Gulf Stream air to Europe led to colder land temperatures. During this shift, winter temperatures cooled as much as 1 to 1.5 °C (NASA 2007b).

An increase in volcanic activity also occurred during the Little Ice Age.

Tambora, an Indonesian volcano, erupted in 1815 and introduced an abundance of ash into the atmosphere. The ash eventually spread around the world and blocked some of the incoming solar radiation. This compounded the already cooler conditions of the time and led to the “Year without a Summer” in 1816, when frost and snow occurred in June and July in New England and Northern Europe.

The effects of the Little Ice Age are not extensively documented in the Pacific Northwest. Campbell (1998), however, found a pattern of alternating multi-century wet and dry regimes by analyzing the grain sizes of sediment cores obtained from Pine Lake, Alberta, Canada. High precipitation and high streamflow corresponded with a higher occurrence of coarse sediment in the sediment cores, while low precipitation and low streamflow corresponded with a higher occurrence of fine sediment in the sediment cores. This study provided a high-resolution record of climatic variability for this part of North America over the past 4000 years. A peak in radial growth occurred at Frederick

Butte from the middle 18th through the middle 19th century. This peak might be related to increased precipitation and less evaporation that could have occurred around the last two minima of the Little Ice Age.

As with the Medieval Warm Period, the IPCC has recently cautioned wholesale acceptance of the Little Ice Age as a global phenomenon. The IPCC report states that the Little Ice Age occurred only as a modest cooling of < 1 °C in the Northern Hemisphere. The report also states that “current evidence does not support globally synchronous periods of anomalous cold over this timeframe” (IPCC 2007).

6.3.6 A.D. 1801–2000

The final 200 years of the chronology are extraordinary in regard to the intensity of the climatic oscillations that occurred during this period. Two short-term periods of significantly above-average growth occurred from A.D. 1862–1866 and from 1877–1885, while short-term periods of significantly below-average growth occurred during A.D. 1822, 1858, 1869–1871, 1888–1889, 1898, 1955, 1959, 1968, and 1973.

The long-term period A.D. 1801–1826 contained 11 years of significantly above-average radial growth (interrupted by one year of significantly below-average radial growth in 1822) and may have been associated with the Little Ice Age. Two episodes of significantly below-average radial growth occurred from A.D. 1829–1843 and from A.D. 1917–1947. The earlier 15-year period contained six years of significantly below-average growth, while the later 31-year period contained 12 years of significantly below-average growth. The Dust Bowl of the 1930s occurred during the same time as the 1917–1947 drought at Frederick Butte. The Dust Bowl drought was caused, at least in part, by

cooler than normal tropical Pacific Ocean SSTs. These changes in SSTs created shifts in broad-scale weather patterns and low-level winds that reduced the normal supply of atmospheric moisture to much of the United States (Schubert *et al.* 2004).

The PDO was in a state of weakened oscillation from 1844 to 1916. No decadal climatic oscillatory activity appeared in the Frederick Butte chronology during this period. Gedalof and Smith (2001) discovered a similar decrease in PDO activity during this time.

During the early 1940s, the trees at the Frederick Butte sites did not respond to the increased levels of precipitation that occurred in the area. Figure 5.19 clearly shows a peak in observed (i.e., instrumental) precipitation. The radial growth curve, however, does not follow this peak. A disturbance that affected tree growth (e.g., insect infestations, ice storms, etc.) may have occurred concurrently with this anomaly. This analysis did not consider disturbances.

The allocation of photosynthate in trees is complex and the addition of xylem is generally a low priority compared to maintenance respiration, production of fine roots and leaves, flower and seed production, branch growth, and root extension (Kozlowski 1971, Oliver and Larson 1990). Many other variables, such as phenotypic characteristics, tree age, or other climatic factors, could account for this anomaly.

Cambial growth is also influenced by needle and fruit development (Kozlowski 1971). Abundant fruit production in western juniper occurs nearly every year (Sowder and Mowat 1965, Dealy 1990), but it takes two years for fruit to mature. If, however, a period of higher than normal seed production occurs, growth and foliage production are often slowed (Kozlowski 1971). During years of heavy seed-crop production, more

carbohydrates may be allocated to fruit production, and the effects of reproduction could mask the climatic signal.

Another possible explanation may be the type of precipitation that occurred during the early 1940s. High intensity, short duration precipitation, while supplying frequent and abundant rainfall, tends to produce more runoff or throughflow and less effective moisture for tree growth (Henderson 2006). The radial growth response from precipitation events such as this may be less than expected because precipitation intensity is high.

Tree age and sample depth may also have affected the correlation between precipitation and radial growth during this period. Older trees are less vigorous than younger trees, and the climatic response between tree groups of different age is not the same (Douglass 1919). As tree biomass changes, the relationship between climate and tree growth may change as well (Grissino-Mayer and Butler 1993). As trees grow older, the relations between photosynthate, water, and hormones change as the proportion of crown to stem decreases and translocation becomes more complex (Kozlowski 1971). Furthermore, the ratio of younger, physiologically active tissue versus older, less active tissue decreases as trees mature (Kramer and Kozlowski 1979). Annual radial growth tends to slow in older trees, and the response to precipitation becomes weaker than in younger, more vigorous trees. Tree age, compounded with low sample depth, may have been an important factor in climatic response for the 1900–1949 segment of the Frederick Butte chronology. The three trees represented in this segment, FBS 010A, FBN 065, and FBN 069, were at least 863, 575, and 647 years old, respectively, when they died. The

average segment correlation for the years 1900–1949 was 0.74 – the third lowest of any segment in the chronology.

Approximately A.D. 1948, another unusual and unexpected observance occurred. The reconstructed precipitation curve again began to follow the observed precipitation curve when the PDO shifted to the negative phase in 1947. This negative-phase PDO lasted until 1976, and, based on previous occurrences of negative-phase PDO, it was expected that this, too, would have been a period of decreased radial growth at Frederick Butte. Instead, this was a period of significantly above-average growth, interspersed with only four years of significantly below-average growth (1955, 1959, 1968, and 1973). This suggests that the trees at Frederick Butte were able to compensate for any decrease in precipitation that might have been caused by the negative phase of the PDO. This may be explained by the drought-ameliorating effects of atmospheric CO₂ fertilization. Levels of atmospheric CO₂ have risen dramatically during the past century, and recent studies on western junipers suggest that this species was less sensitive to drought during the latter part of the 20th century because increased levels of atmospheric CO₂ increased the water-use efficiency in these trees (Knapp *et al.* 2001a, 2001b, Soulé *et al.* 2003).

The PDO shifted to a positive phase in A.D. 1977 that resulted in a strong period of significantly above-average radial growth that lasted through (at least) 1999. Radial growth during this period was greater than at any other time throughout the chronology. This may be a synergistic result of the positive phase PDO, increased atmospheric CO₂, and the El Niño events that occurred in 1982–1983 and 1997–1998. The positive phase PDO that occurred from A.D. 1925–1946 did not appear in this reconstruction. This, too,

may be associated with the potential contributors of non-climatic noise (e.g., phenotypic characteristics, tree age, and sample depth) previously mentioned.

Chapter 7

Conclusions

The overall purpose of this study was to interpret data obtained from western juniper trees to reconstruct climatic history in the Pacific Northwest over the past several centuries. This reconstruction complements the climatic historical record, extends the dendrochronological record for the Frederick Butte area, and helps us understand the frequency of occurrence and extent of past climatic variation in central Oregon. The statistical strength and temporal depth of this reconstruction further expands the growing network of dendrochronological reconstructions in the Pacific Northwest. This study suggests that the PDO and ENSO are two of the major climatic oscillations that affect the climate of central Oregon. This is a slightly different conclusion than that reached by Pohl *et al.* (2002), who found very weak relationships between tree growth and the PDO and ENSO in central Oregon. This chapter summarizes the major findings of my research.

7.1 Major Conclusions

1. The western juniper trees of Frederick Butte respond to multiple climatic factors.

Of all the climatic variables analyzed in this study, July_{t-1} to June_t Oregon Zone 7 precipitation had the strongest overall relationship with radial tree growth ($r = 0.68$, $p < 0.0001$). March_t to April_t PDO ($r = 0.37$, $p < 0.01$) and May_t to June_t ENSO ($r = 0.35$, $p < 0.05$) also showed significant relationships with radial tree growth.

2. *The PDO and ENSO indices were positively correlated with radial tree growth.*

ENSO and the PDO are typically negatively correlated with tree growth in the Pacific Northwest. Both ENSO and the PDO, however, are positively correlated with tree growth at the Frederick Butte sites. Previous studies also noted these “paradoxical” correlations (Pohl *et al.* 2002, Knapp *et al.* 2004). Topography and rain shadow, lower regional temperatures, simultaneously and antagonistically occurring phases of the PDO and ENSO, climatic oscillations that originate in other oceanic basins, and the influence of continental air masses in central Oregon may all produce unexpected climatic oscillatory signals in tree-ring chronologies. My results suggest that the main factor, however, is related to air mass boundaries. Because Frederick Butte is located in the interior Pacific Northwest in an air mass transitional area, continental air masses play a major role in determining the climate at Frederick Butte. It is possible that the influence of these continental air masses is so great that it causes the climate of Frederick Butte to respond differently to the PDO and ENSO than in many other areas in the Pacific Northwest.

The effects of atmospheric and oceanic teleconnections on western juniper growth in Oregon are complex. Understanding the effects of regional climate in the past certainly provides some insight into the present workings of the climatic system. Climate, however, seldom exhibits the same patterns through time (Burroughs 1996). This statement is particularly true for teleconnections, such as the PDO and ENSO, that interact with each other as well as with the prevailing “background” climate of a local region (Henderson 2006).

3. The tree-ring chronology for Frederick Butte exhibits many short-term climatic episodes.

The Frederick Butte western juniper chronology recorded several below-average radial-growth episodes (Figures 5.30–5.35). The periods of suppressed radial growth that occurred during the 11th through the 14th century may have been associated with the dry conditions of the Medieval Warm Period. Other short-term periods of suppressed radial growth may have been associated with La Niña events, except for one period (1720–1723) that was associated with an El Niño event. The years during which radial growth was lowest are, in ascending order, A.D. 1126, 1279, 1532, 1571, 1721, 1800, 1829, 1918, 1931, 1934, 1679, 1729, 1660, 1072, 1428, 1335, 1580, 1632, and 1594. The lowest average radial growth during a 2 to 9 year period occurred from A.D. 1698–1699.

The Frederick Butte western juniper chronology also recorded several above-average radial-growth episodes (Figures 5.30–5.35). The periods of increased radial growth that occurred during the middle 16th through the middle 19th century may have been associated with the wetter conditions of the Little Ice Age. Other short-term periods of increased radial growth may have been associated with El Niño events. The years during which radial growth was greatest are, in descending order, A.D. 1983, 1980, 1982, 1965, and 1978. The highest average radial growth during a 2 to 9 year period occurred from A.D. 1641–1642. It should be noted, however, that all of the short-term climatic episodes mentioned in this section may have been associated with, and affected by, other climatic oscillations such as the AMO.

4. *The final tree-ring chronology also exhibits many long-term (decadal) climatic episodes.*

The Frederick Butte western juniper chronology recorded several below-average radial-growth episodes that occurred from A.D. 856–880, 1135–1146, 1155–1164, 1351–1390, 1529–1554, 1565–1580, 1591–1600, 1645–1655, 1829–1843, and 1917–1947. The periods of below-average growth that occurred during the 11th through the 14th century may have been associated with the Medieval Warm Period. The periods of below-average growth that occurred during the 16th century may have been associated with the extremely dry conditions of the 16th century megadrought. The period of suppressed radial growth that occurred from 1917–1947 was partially concurrent with the Dust Bowl drought, as well as La Niña events (1920–1921 and 1924–1925), and the latter stages of a negative-phase PDO (1900–1924). Other long-term periods of decreased radial growth were possibly associated with negative PDO events. The lowest average radial growth during a long-term period (≥ 10 years) occurred from A.D. 1645–1655, while the longest sustained period of below-average radial growth occurred from A.D. 1351–1390.

Above-average radial-growth episodes occurred from A.D. 1008–1031, 1113–1122, 1440–1451, 1484–1493, 1740–1754, 1801–1826, and 1948–1999. The periods of increased radial growth that occurred during the 18th and 19th centuries may have been associated with the Little Ice Age. Increased radial growth during A.D. 1815–1816, 1982–1983, and 1997–1998 also coincided with El Niño episodes. The highest average radial growth during a long-term period (≥ 10 years) occurred from A.D. 1440–1451, while the longest sustained period of above-average radial growth occurred from A.D. 1948–1999.

The period of above-average radial growth that occurred from 1948–1999 was associated with the negative-phase PDO that occurred from 1947–1976 and a positive-phase PDO from 1977 through (at least) the middle 1990s. The negative-phase PDO should have coincided with a period of decreased radial growth at Frederick Butte. Instead, this was a period of significantly above-average growth. This indicates that the trees at Frederick Butte were able to compensate for any decrease in precipitation that might have been caused by the negative phase of the PDO. Increased levels of atmospheric CO₂ may have been responsible for this, as CO₂ fertilization can mask a drought signal by ameliorating the effects of drought on tree growth.

A very strong period of significantly above-average radial growth began when the PDO shifted in 1977. This pattern lasted through (at least) 1999. Radial growth during this period was greater than at any other time throughout the chronology. This may be a synergistic result of the positive phase PDO, increased atmospheric CO₂, and the El Niño events that occurred in 1982–1983 and 1997–1998. The positive phase PDO that occurred from A.D. 1925–1946 is not illustrated in this reconstruction. This may be associated with non-climatic noise that could have masked the PDO signal. Other long-term periods of increased radial growth were potentially associated with positive phases of the PDO. It should be noted, however, that all of these long-term climatic episodes may have been associated with, and affected by, other climatic oscillations such as the AMO.

5. *The western juniper trees of Frederick Butte are a highly valuable asset for dendroclimatological studies.*

Western junipers that grow in this area are remarkably long-lived (some are over 1,000 years old) and particularly sensitive to annual variations in precipitation. The rate of decomposition in the Frederick Butte area is relatively slow, and very old dead and downed remnant wood (often older than 1,000 years) is abundant and readily available for analysis. This combination of longevity and sensitivity makes it possible to derive ring-width indices from the trees at the Frederick Butte study sites that are highly reliable. Because this wood is such a valuable proxy source, active conservation practices to preserve both the living and dead western juniper specimens in central Oregon should be considered. Future reconstructions from this area may provide further broad-scale interpolations of climate, both spatially and temporally, that may help answer some very important climatic questions.

6. *Because of its unique location, Frederick Butte is a highly valuable dendroclimatological study site.*

The study area is situated on the edge of the *Juniperus occidentalis* Zone, an ecotone between ponderosa pine forest and sagebrush-steppe (Driscoll 1964). In this ecotone, the precipitation regime changes drastically from the wet Cascades to the dry High Desert along a west to east gradient. The area is also located along the seasonal marine/continental interior air mass boundary. Because of these factors, the area can act as a very sensitive climatic-change indicator region.

7. *The western juniper samples at Frederick Butte produced some of the longest continuous tree-ring chronologies obtained in Oregon.*

The final chronology dated from A.D. 797 to 2000. When compared to previously constructed western juniper chronologies in the western United States, the Frederick Butte chronology ranked among the most temporally robust. The span of 1,204 years makes the Frederick Butte chronology the third longest western juniper chronology in the United States. The Frederick Butte chronology ranked fourth overall in statistical quality when compared to the previously constructed western juniper chronologies, and has the highest interseries correlation ($r = 0.86$) of any western juniper chronology in the United States.

7.2 Improvements and Limitations to This Study

1. *Disturbances were not investigated by this research.*

Other factors, such as ice storms, fungal outbreaks, and insect infestations were not considered by this research. These are factors that could create noise in a dendroclimatological study. Every precaution was taken to remove non-climatic noise from the chronology, and I am confident that the chronology has a very strong climatic signal. Nevertheless, these are factors that should not be overlooked. Sufficient sample depth and a spatially broad sampling area should mitigate any problems these factors might introduce.

2. Sample depth should be stronger in some areas of the chronology.

The first two years of the chronology (A.D. 797 and 798) likely deviated from the mean because of low sample depth and therefore were not included in the climatic analyses. The early part of the chronology is also composed of rings formed when the trees were relatively young, and may be less reliable proxies of climate because of juvenile growth (Fritts 1976). Increased sample depth would help alleviate this problem. Any conclusions drawn from the data where sample depth is low are made with the recognition of these limitations.

7.3 Future Research

While this study illustrates the usefulness of western juniper for climatic research in the Pacific Northwest, much remains to be answered. Future studies would further increase our understanding of temporal and spatial changes of teleconnections and their effects on tree growth in Oregon. More information is necessary to define how these teleconnections affect climate in various regions of the Pacific Northwest. Research on the effects of long-term climatic oscillations (e.g., the AMO) on climate in the Pacific Northwest is also needed.

1. The additional samples collected at Frederick Butte should be processed.

Because the wood at Frederick Butte is such a strong recorder of regional climate, the remainder of the samples collected at Frederick Butte should be processed. This would strengthen the chronology created during this study. Further collections at Frederick Butte could potentially push the chronology back to the B.C. era.

2. *More investigation is needed to determine why observed and reconstructed precipitation do not follow the same trend in the 1940s.*

This is most likely related to a non-climatic disturbance or internal physiological response within the trees that affected radial growth and caused the trees to respond to something other than precipitation. Increased sample depth coupled with an investigation into regional environmental disturbances could shed light onto this anomaly. Increased levels of atmospheric CO₂ may have also affected tree growth during this period.

3. *The effects of interhemispheric and interoceanic teleconnections on the climate of the Pacific Northwest should be further studied.*

The AMO signal is strongest in the North Atlantic Ocean where the effects of the oscillation can be seen throughout the entire basin. The signal, however, is global in scope, with a positively correlated co-oscillation that appears in parts of the North Pacific Ocean (Enfield *et al.* 2001). The teleconnection between multidecadal variability in the North Atlantic Ocean and oscillations in the Pacific Ocean might be explained by way of the Arctic Oscillation (AO) and a possible atmospheric bridge via wind anomalies at very high latitudes (Gray *et al.* 2004).

AMO oscillations are also linked to fluctuations in the intensity of the thermohaline circulation (Gray *et al.* 2003). The thermohaline current transports warm ocean water from the Pacific Ocean, through the Indian Ocean and into the Atlantic Ocean. In the North Atlantic Ocean, the warm, salty water cools and sinks because of its greater density. This, in turn, creates a sub-surface countercurrent that transports the newly cooled water back to the Indian and Pacific Oceans (Figure 7.1). The

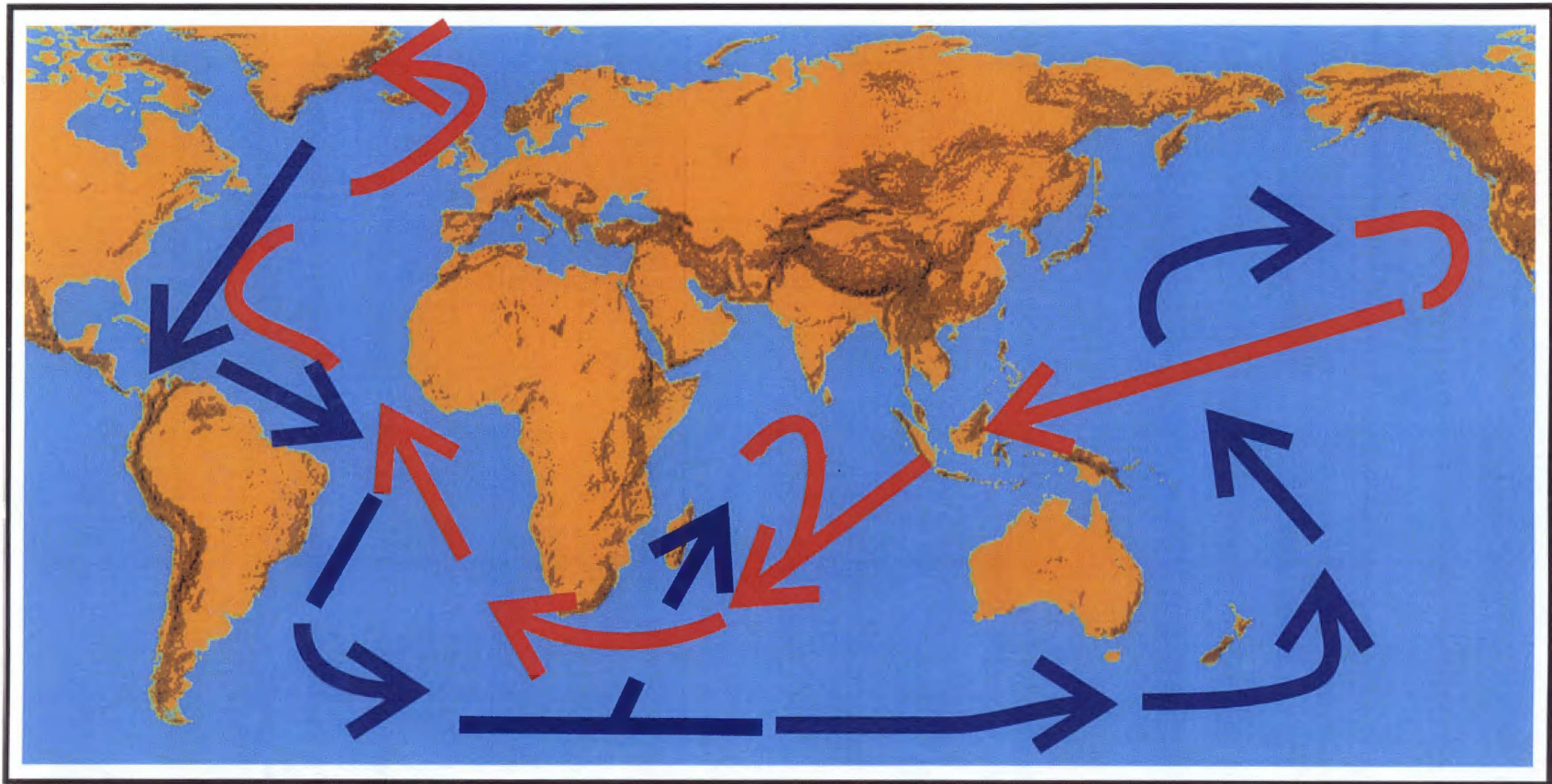


Figure 7.1 Global thermohaline circulation. The red arrows indicate a warm, shallow current, while the blue arrows indicate a cold, deep, and more saline current.

thermohaline current links every major oceanic basin in the world and is a possible link between North Atlantic Ocean SST and precipitation regimes in the Pacific Northwest.

Global air temperature also responds strongly to the thermohaline circulation. This is of no surprise because the tropical Pacific Ocean is the largest heat source of the atmosphere (i.e., when the Pacific Ocean warms or cools, so does the atmosphere above it). El Niño events tend to cluster around periods of thermohaline current inactivity, as the migration of tropical Pacific Ocean waters slows down and allows SSTs to rise.

During the 20th century, the thermohaline current shifted through four distinct phases. Two of these phases were active (1920s–1946 and 1977–1990s), while two were inactive (early 1900s–1920s and 1947–1976) (Gray and Landsea 1993). Interestingly, these periods closely correspond to PDO phase shifts. Several other atmospheric phenomena also correlate well with the thermohaline current. When thermohaline circulation is active, Atlantic basin hurricane activity increases, Sahel, Africa, precipitation increases, and Pacific Northwest precipitation (at least coastally) may increase (Gray and Landsea 1993, Taylor and Hannan 1999).

Further studies that focus on these teleconnections will help us better understand the interhemispheric and interoceanic factors that affect climate in the Pacific Northwest. A better understanding of the temporal and spatial extents of ENSO and the PDO, as well as their interactions with other climatic teleconnections (e.g., the AMO), will assist us in preparing for future climatic changes. Research of this type is especially necessary to fully examine the function of synoptic-scale climatic oscillations in the interior portion of the Pacific Northwest. The effects of these climatic fluctuations on ecosystems of the more arid interior locations of the Pacific Northwest deserve more attention, especially

since these climatic transitional zones appear to be sensitive recorders of the spatio-temporal variability of climatic regimes.

4. Stable isotopic studies may provide additional valuable data.

To obtain the most complete representation of the effects of climate on tree growth, all available information should be extracted from the tree rings. A study of the stable oxygen isotopes trapped within the tree rings at Frederick Butte could illustrate the dominant water sources for western juniper. These oxygen isotopic signatures could inform us whether the majority of precipitation is coming from continental or maritime air masses.

7.4 Concluding Remarks

Future studies could also reveal whether the PDO is currently experiencing a phase shift, or if the increase in radial growth that occurred during the latter part of the 20th century will continue. Research performed properly should create as many questions as it answers. I believe this study helps answer many climatic questions that concern the Pacific Northwest. Many questions, however, still remain, especially those concerning the exact cause and effect relationships between tree growth and climatic oscillations. More research is necessary to determine the extraordinarily complex interactions between the multiple climatic oscillations that undoubtedly affect the Pacific Northwest. Our knowledge of how these factors interact to produce our day-to-day weather and long-term climate is limited. Only through continued research can we begin to fully understand this complex puzzle.

References

References

- Agee, J.K. 1993. *Fire Ecology of Pacific Northwest Forests*. Island Press, Washington, D.C., 493 pp.
- Aguado, E., and Burt, J.E. 2007. *Understanding Weather and Climate, Fourth Edition*. Pearson Prentice Hall, Upper Saddle River, New Jersey, 562 pp.
- Arno, S.F., and Sneek, K.M. 1977. *A Method for Determining Fire History in Coniferous Forests of the Mountain West*. General Technical Report INT-42. United States Department of Agriculture, Forest Service, Intermountain Forest and Range Experiment Station, Ogden, Utah, 28 pp.
- Augustin, L., Barbante, C., Barnes, R.F., Barnola, J.M., Bigler, M., Castellano, E., Cattani, O., Chappallaz, J., Dahl-Jensen, D., Delmonte, B., Dreyfus, G., Durand, G., Falourd, S., Fischer, H., Flückiger, J., Hansson, M.E., Huybrechts, P., Jugie, G., Johnsen, S.J., Jouzel, J., Kaufmann, P., Kipfstuhl, J., Lambert, F., Lipenkov, V.Y., Littot, G.C., Longinelli, A., Lorrain, R., Maggi, V., Masson-Delmotte, V., Miller, H., Mulvaney, R., Oerlemans, J., Oerter, H., Orombelli, G., Parrenin, F., Peel, D.A., Petit, J.-R., Raynaud, D., Ritz, C., Ruth, U., Schwander, J., Siegenthaler, U., Souchez, R., Stauffer, B., Steffensen, J.P., Stenni, B., Stocker, T.F., Tabacco, I.E., Udisti, R., van de Wal, R.S.W., van den Broeke, M., Weiss, J., Wilhelms, F., Winther, J.-G., Wolff, E.W., and Zucchelli, M. 2004. Eight glacial cycles from an Antarctic ice core. *Nature* 429(6992), 623–628.
- Babkina, A.M. 2003. *El Niño: Overview and Bibliography*. Nova Science Publishers, Hauppauge, New York, 196 pp.
- Baisan, C.H., and Swetnam, T.W. 1990. Fire history on a desert mountain range: Rincon Mountain Wilderness, Arizona, U.S.A. *Canadian Journal of Forestry* 20(10), 1559–1569.
- Baldwin, E.M. 1964. *Geology of Oregon*. University of Oregon Cooperative Bookstore, Eugene, Oregon, 165 pp.
- Banks, J.C.G. 1991. A review of the use of tree rings for the quantification of forest disturbances. *Dendrochronologia* 9, 51–70.
- Benson, L., Linsley, B., Smoot, J., Mensing, S., Lund, S., Stine, S., and Sarna-Wojcicki, A. 2003. Influence of the Pacific Decadal Oscillation on the climate of the Sierra Nevada, California and Nevada. *Quaternary Research* 59(2), 151–159.
- Berry, J.B. 1924. *Western Forest Trees: A Guide to the Identification of Trees and Woods to Accompany Farm Woodlands*. World Book Company, Yonkers-on-Hudson, New York and Chicago, Illinois, 212 pp.

- Biondi, F., Gershunov, A., and Cayan, D.R. 2001. North Pacific decadal climate variability since 1661. *Journal of Climate* 14(1), 5–10.
- Bork, J.L. 1984. *Fire History in Three Vegetation Types on the Eastern Side of the Oregon Cascades*. Ph.D. dissertation, Oregon State University, Corvallis, Oregon, 112 pp.
- Bradley, R.S. 1976. *Precipitation History of the Rocky Mountain States*. Westview Press, Boulder, Colorado, 334 pp.
- Bradley, R.S., Hughes, M.K., and Diaz, H.F. 2003. Climate in Medieval time. *Science* 302(5644), 404–405.
- Briffa, K.R., Jones, P.D., Schweingruber, F.H., Karlen, W., and Shiyatov, S.G. 1996. Tree-ring variables as proxy indicators: problems with low-frequency signals. In Jones, P.D., Bradley, R.S., and Jouzel, J., eds., *Climatic Variations and Forcing Mechanisms of the Last 2000 years*. NATO ASI Series I, Volume 41, Springer, 62–74.
- Brubaker, L.B. 1980. Spatial patterns of tree-growth anomalies in the Pacific Northwest. *Ecology* 61(4), 798–807.
- Burkhardt, J.W., and Tisdale, E.W. 1976. Causes of juniper invasion in southwestern Idaho. *Ecology* 57(3), 472–484.
- Burroughs, W.J., Crowder, B., Robertson, T., Vallier-Talbot, E., and Whitaker, R. 1996. *The Nature Company Guides: Weather*. U.S. Weldon Owen, Inc., Sydney, Australia, 288 pp.
- Campbell, C. 1998. Late Holocene lake sedimentology and climate change in southern Alberta, Canada. *Quaternary Research* 49(1), 96–101.
- Catchings, R.D., and Mooney, W.D. 1988. Crustal structure of east central Oregon: relation between Newberry Volcano and regional crustal structure. *Journal of Geophysical Research* 93(B9), 10,081–10,094.
- Climate Diagnostics Center. 2006. Data archived at: <http://www.cdc.noaa.gov/>
- Climate Prediction Center. 2006. Data archived at: <http://www.cpc.ncep.noaa.gov/data/indices/>
- Cole, J. 2001. A slow dance for El Niño. *Science* 291(5508), 1496–1497.
- Cook, E.R. 1985. *A Time Series Analysis Approach to Tree Ring Standardization*. Ph.D. dissertation, The University of Arizona, Tucson, Arizona, 171 pp.

- D'Arrigo, R., Villalba, R., and Wiles, G. 2001. Tree ring estimates of Pacific decadal climate variability. *Climate Dynamics* 18(3), 219–224.
- Dieterich, J.H. 1983. Fire history of southwestern mixed conifer: a case study. *Forest Ecology and Management* 6, 13–31.
- Dealy, J.E. 1990. *Juniperus occidentalis* Hook. western juniper. In Burns, R.M., and Honkala, B.H., technical coordinators, *Silvics of North America. Volume 1, Conifers. Agriculture Handbook 654*. United States Department of Agriculture, Forest Service, 109–115.
- Dettinger, M.D., Battisti, D.S., Garreaud, R.D., McCabe, G.J., and Bitz, C.M. 2001. Interhemispheric effects of interannual and decadal ENSO-like climate variations on the Americas. In Markgraf, V., ed., *Interhemispheric Climate Linkages*. Academic Press, San Diego, California, 1–16.
- Dodge, R.E., and Helmle, K.P. 2003. Past stony coral growth (extension) rates on reefs of Broward County, Florida: possible relationships with Everglades drainage. Presentation, Joint Conference on the Science and Restoration of the Greater Everglades and Florida Bay Ecosystem. Palm Harbor, Florida. April 13–18.
- Dodge, R.E., and Vaisnys, J.R. 1975. Hermatypic coral growth banding as environmental recorder. *Nature* 258(5537), 706–708.
- Douglass, A.E. 1919. *Climatic Cycles and Tree Growth: Volume I: A Study of the Annual Rings of Trees in Relation to Climate and Solar Activity*. Publication 289. Carnegie Institute of Washington, 127 pp.
- Douglass, A.E. 1946. Precision of ring dating in tree-ring chronologies. *Tree-Ring Bulletin* 17(3), 5–21.
- Driscoll, R.S. 1964. Vegetation-soil units in the central Oregon juniper zone. Research Paper PNW-19. United States Department of Agriculture, Forest Service, Pacific Northwest Forest and Range Experiment Station, Portland, Oregon, 60 pp.
- Druffel, E.M. 1982. Banded corals: changes in oceanic carbon-14 during the Little Ice Age. *Science* 218(4567), 13–19.
- Eddleman, L.E. 1989. Oregon's High Desert – legacy for today. In: *Oregon's High Desert: the Last 100 Years*. Special Report 841. United States Department of Agriculture, Agricultural Research Service, Agricultural Experiment Station, Oregon State University, Corvallis, Oregon, 2–6.

- Enfield, D.B., and Mestas-Núñez, A.M. 2001. Interannual to multidecadal climate variability and its relationship to global sea surface temperatures. In Markgraf, V., ed., *Interhemispheric Climate Linkages*. Academic Press, San Diego, California, 17–29.
- Enfield, D.B., Mestas-Núñez, A.M., and Trimble, P.J. 2001. The Atlantic Multidecadal Oscillation and its relation to rainfall and river flows in the continental U.S. *Geophysical Research Letters* 28(10), 2077–2080.
- Erdtman, G. 1969. *Handbook of Palynology: An Introduction to the Study of Pollen Grains and Spores*. Hafner Publishing Company, New York, New York, 486 pp.
- Evans, M.N., Kaplan, A., Cane, M.A., and Villalba, R. 2001. Globality and optimality in climate field reconstructions from proxy data. In Markgraf, V., ed., *Interhemispheric Climate Linkages*. Academic Press, San Diego, California, 53–72.
- Everett, P., Hessburg, P., Lehmkuhl, J., Jensen, M., and Bourgeron, P. 1994. Old forests in dynamic landscapes: dry site forests of eastern Oregon and Washington. *Journal of Forestry* 92(1), 22–25.
- Fedorov, A.V., and Philander, S.G. 2000. Is El Niño changing? *Science* 288(5473), 1997–2002.
- Foster, J.H. 1917. The spread of timbered areas in central Texas. *Journal of Forestry* 15(4), 443–445.
- Francis, R.C., and Hare, S.R. 1997. Regime scale climate forcing of salmon populations in the Northeast Pacific – some new thoughts and findings. In Emmett, R.L., and Schiewe, M.H., eds., *Estuarine and Ocean Survival of Northeastern Pacific Salmon: Proceedings of the Workshop*. United States Department of Commerce, NOAA Tech. Memo. NMFS-NWFSC-29, 113–128.
- Francis, R.C., Hare, S.R., Hollowed, A.B., and Wooster, W.S. 1998. Effects of interdecadal climate variability on the oceanic ecosystems of the NE Pacific. *Fisheries Oceanography* 7(1), 1–21.
- Franklin, J.F., and Dyrness, C.T. 1988. *Natural Vegetation of Oregon and Washington*. Oregon State University Press, Corvallis, Oregon, 452 pp.
- Franklin, J.F., Moir, W.H., Douglas, G.W., and Wiberg, C. 1971. Invasion of subalpine meadows by trees in the Cascade Range, Washington and Oregon. *Arctic and Alpine Research* 3(3), 215–224.

- Fritts, H.C. 1976. *Tree Rings and Climate*. Academic Press, New York, New York, 567 pp.
- Gedalof, Z, and Smith, D.J. 2001. Interdecadal climate variability and regime-scale shifts in Pacific North America. *Geophysical Research Letters* 28(8), 1515–1518.
- Gershunov, A., Barnett, T., and Cayan, D. 1999. North Pacific interdecadal oscillation seen as factor in ENSO-related North American climate anomalies. *Eos* 80(3), 25–30.
- Graumlich, L.J., Pisaric, M.F.J., Waggoner, L.A., Littell, J.S., and King, J.C. 2003. Upper Yellowstone River flow and teleconnections with Pacific basin climate variability during the past three centuries. *Climatic Change* 59(2), 245–262.
- Gray, S.T., Betancourt, J.L., Fastie, C.L., and Jackson, S.T. 2003. Patterns and sources of multidecadal oscillations in drought-sensitive tree-ring records from the central and southern Rocky Mountains. *Geophysical Research Letters* 30(6), 1316–1319.
- Gray, S.T., Graumlich, L.J., Betancourt, J.L., and Pederson, G.T. 2004. A tree-ring based reconstruction of the Atlantic Multidecadal Oscillation since 1567 A.D. *Geophysical Research Letters* 31(12), L12205.
- Gray, W.M., and Landsea, C.W. 1993. West African rainfall and Atlantic basin hurricane activity as proxy signals for Atlantic conveyor belt circulation strength. Presentation, Conference on Hydrology, American Meteorological Society, Anaheim, California.
- Green, P.M., Legler, D.M., Miranda, C.J., and O'Brien, J.J. 1997. *The North American Climate Patterns Associated with the El Niño-Southern Oscillation*. COAPS Project Report Series 97-1. Center for Ocean-Atmospheric Prediction Studies, Florida State University, Tallahassee, Florida. Booklet archived at: <http://www.coaps.fsu.edu/lib/booklet/>
- Griffin, J.R., and Critchfield, W.B. 1972. *The Distribution of Forest Trees in California*. Research Paper PSW-82. United States Department of Agriculture, Forest Service, Pacific Southwest Forest and Range Experiment Station, Berkeley, California, 114 pp.
- Grissino-Mayer, H.D. 1995. *Tree-Ring Reconstructions of Climate and Fire History at El Malpais National Monument, New Mexico*. Ph.D. dissertation. The University of Arizona, Tucson, Arizona, 407 pp.

- Grissino-Mayer, H.D. 1996. A 2129-year reconstruction of precipitation for northwestern New Mexico, U.S.A. In Dean, J.S., Meko, D.M., and Swetnam, T.W., eds., *Tree Rings, Environment and Humanity: Proceedings of the International Conference, Tucson, Arizona, 17–21 May 1994*. Department of Geosciences, University of Arizona Press, Tucson, Arizona, 191–204.
- Grissino-Mayer, H.D. 2001. Evaluating crossdating accuracy: A manual and tutorial for the computer program COFECHA. *Tree-Ring Research* 57(2), 205–221.
- Grissino-Mayer, H.D., and Butler, D.R. 1993. Effects of climate on growth of shortleaf pine (*Pinus echinata* Mill.) in northern Georgia: a dendroclimatic study. *Southeastern Geographer* 33(1), 65–81.
- Grissino-Mayer, H.D., Romme, W.H., Floyd, M.L., and Hanna, D.D. 2004. Climatic and human influences on fire regimes of the southern San Juan Mountains, Colorado, U.S.A. *Ecology* 85(6), 1708–1724.
- Grissino-Mayer, H.D., and Swetnam, T.W. 2000. Century-scale climate forcing of fire regimes in the American Southwest. *The Holocene* 10(2), 213–220.
- Gutmanis, J.C. 1989. Wrench faults, pull-apart basins, and volcanism in central Oregon: a new tectonic model based on image interpretation. *Geological Journal* 24(3), 183–192.
- Hadley, K.S. 1999. Forest history and meadow invasion at the Rigdon Meadows Archaeological Site, western Cascades, Oregon. *Physical Geography* 20(2), 116–133.
- Hamlet, A.F., and Lettenmaier, D.P. 1999. Columbia River streamflow forecasting based on ENSO and PDO climate signals. *Journal of Water Resources Planning and Management* 125(6), 333–341.
- Henderson, J.P. 2006. *Dendroclimatological Analysis and Fire History of Longleaf Pine (Pinus palustris Mill.) in the Atlantic and Gulf Coastal Plain*. Ph.D. dissertation. The University of Tennessee, Knoxville, Tennessee, 463 pp.
- Henry, A.J. 1906. *The Climatology of the United States*. United States Department of Agriculture, United States Weather Bureau, Washington, D.C., 1012 pp.
- Heyerdahl, E.K., Brubaker, L.B., and Agee, J.K. 2001. Spatial controls of historical fire regimes: a multiscale example from the interior West, U.S.A. *Ecology* 82(3), 660–678.

- Heyerdahl, E.K., Brubaker, L.B., and Agee, J.K. 2002. Annual and decadal climate forcing of historical fire regimes in the interior Pacific Northwest, USA. *The Holocene* 12(5), 597–604.
- Hollowed, A.B., Hare, S.R., and Wooster, W.S. 1998. Pacific basin climate variability and patterns of Northeast Pacific marine fish production. In Holloway G., *et al.*, eds., *Proceedings of the 10th 'Aha Huliko' a Hawaiian Winter Workshop on Biotic Impacts of Extratropical Climate Variability in the Pacific*. NOAA Award # NA67RJ0154, SOEST Special Publication, 89–104.
- Holmes, R. 1983. Computer-assisted quality control in tree-ring dating and measurement. *Tree-Ring Bulletin* 43, 69–78.
- Holmes, R.L., Adams, R.K., and Fritts, H.C. 1986. *Tree-Ring Chronologies of Western North America: California, Eastern Oregon, and Northern Great Basin. Chronology Series VI*. Laboratory of Tree-Ring Research, University of Arizona Press, Tucson, Arizona, 182 pp.
- Ingraham, W.J., Jr., Ebbesmeyer, C.C., Hinrichsen, R.A. 1998. Imminent climate and circulation shift in northeast Pacific Ocean could have major impact on marine resources. *Eos* 79(16), 197–201.
- Intergovernmental Panel on Climate Change. 2007. *IPCC Third Assessment Report: Climate Change 2001*. Report archived at: <http://www.ipcc.ch>
- International Tree-Ring Data Bank. 2006. Data archived at: http://hurricane.ncdc.noaa.gov/pls/paleo/fm_createpages.treering
- Jackman, E.R., and Long, R.A. 1964. *The Oregon Desert*. The Caxton Printers, Ltd., Caldwell, Idaho, 407 pp.
- Jessup, L.T. 1935. Precipitation and tree growth in the Harney Basin, Oregon. *Geographical Review* 25(2), 310–312.
- Kadonaga, L.K., Podlaha, O., and Whiticar, M.J. 1999. Time series analyses of tree-ring chronologies from Pacific North America: evidence for sub-century climate oscillations. *Chemical Geology* 161(3), 339–363.
- Kaplan, A., Kushnir, Y., and Cane, M.A. 2000. Reduced space optimal interpolation of historical marine sea level pressure: 1854–1992. *Journal of Climate* 13(16), 2987–3002.

- Kauffman, J.B., and Sapsis, D.B. 1989. The natural role of fire in Oregon's High Desert. In: *Oregon's High Desert: the Last 100 Years*. Special Report 841. United States Department of Agriculture, Agricultural Research Service, Agricultural Experiment Station, Oregon State University, Corvallis, Oregon, 15–19.
- Keen, F.P. 1937. Climatic cycles in eastern Oregon as indicated by tree rings. *Monthly Weather Review* 65(5), 175–188.
- Keigwin, L.D. 1996. The Little Ice Age and Medieval Warm Period in the Sargasso Sea. *Science* 274(5292), 1503–1508.
- Kitzberger, T., Swetnam, T.W., and Veblen, T.T. 2001. Inter-hemispheric synchrony of forest fires and the El Niño-Southern Oscillation. *Global Ecology and Biogeography* 10, 315–326.
- Knapp, P.A., Grissino-Mayer, H.D., and Soulé, P.T. 2002. Climatic regionalization and the spatio-temporal occurrence of single-year drought events (1500–1998) in the interior Pacific Northwest. *Quaternary Research* 58(3), 226–233.
- Knapp, P.A., and Soulé, P.T. 1998. Recent *Juniperus occidentalis* (western juniper) expansion on a protected site in central Oregon. *Global Change Biology* 4(3), 347–357.
- Knapp, P.A., and Soulé, P.T. 1999. Geographical distribution of an 18th-century heart rot outbreak in western juniper (*Juniperus occidentalis* ssp. *occidentalis* Hook.). *Journal of Arid Environments* 41(3), 247–256.
- Knapp, P.A., Soulé, P.T., and Grissino-Mayer, H.D. 2001a. Detecting potential regional effects of increased atmospheric CO₂ on growth rates of western juniper. *Global Change Biology* 7(8), 903–917.
- Knapp, P.A., Soulé, P.T., and Grissino-Mayer, H.D. 2001b. Post-drought growth response of western juniper (*Juniperus occidentalis* var. *occidentalis*) in central Oregon. *Geophysical Research Letters* 28(13), 2657–2660.
- Knapp, P.A., Soulé, P.T., and Grissino-Mayer, H.D. 2004. Occurrence of sustained droughts in the interior Pacific Northwest (A.D. 1733–1980) inferred from tree-ring data. *Journal of Climate* 17(1), 140–150.
- Köppen, W. 1931. *Grundriss der Klimakunde*. Walter de Gruyter and Company, Berlin, 388 pp.
- Kozlowski, T.T. 1971. *Growth and Development of Trees, Volumes I and II*. Academic Press, New York, New York, 443 and 560 pp.

- Kramer, P.J., and Kozlowski, T.T. 1979. *Physiology of Woody Plants*. Academic Press, New York, New York, 811 pp.
- Leopold, A. 1924. Grass, brush, timber and fire in southern Arizona. *Journal of Forestry* 22(6), 1–10.
- Linsley, B.K., Dunbar, R.B., Wellington, G.M., and Mucciarone, D.A. 1994. A coral-based reconstruction of intertropical convergence zone variability over Central America since 1707. *Journal of Geophysical Research* 99(C5), 9977–9994.
- Linsley, B.K., Ren, L., Dunbar, R.B., and Howe, S.H. 2000a. ENSO and decadal-scale climate variability at 10°N in the eastern Pacific from 1893 to 1994: a coral-based reconstruction from Clipperton Atoll. *Paleoceanography* 15(3), 322–335.
- Linsley, B.K., Wellington, G.M., and Schrag, D.P. 2000b. Decadal sea surface temperature variability in the subtropical South Pacific from 1726 to 1997 A.D. *Science* 290(5494), 1145–1148.
- Little, E.L., Jr. 1971. *Atlas of United States Trees, Volume 1. Conifers and Important Hardwoods*. Miscellaneous Publication 1146. United States Department of Agriculture, Washington, D.C., 9 pp., 313 maps.
- Liu, K., Reese, C.A., and Thompson, L.G. 2005. Ice-core pollen record of climate changes in the central Andes during the last 400 yr. *Quaternary Research* 64(2), 272–278.
- Liu, K., Yao, Z., and Thompson, L.G. 1998. A pollen record of Holocene climatic changes from the Dunde Ice Cap, Qinghai-Tibetan Plateau. *Geology* 26(2), 135–138.
- Lough, J.M. 1992. An index of the Southern Oscillation reconstructed from western North American tree-ring chronologies. In: Diaz, H.F., and V. Markgraf, eds., *El Niño: Historical and Paleoclimatic Aspects of the Southern Oscillation*. Cambridge University Press, Cambridge, United Kingdom, 215–226.
- Mantua, N.J., and Hare, S.R. 2002. The Pacific Decadal Oscillation. *Journal of Oceanography* 58(1), 35–44.
- Mantua, N.J., Hare, S.R., Zhang, Y., Wallace, J.M., and Francis, R.C. 1997. A Pacific interdecadal climate oscillation with impacts on salmon production. *Bulletin of the American Meteorological Society* 78(6), 1069–1079.
- Mayewski, P.A. 1988. Ice cores and global change. *Eos* 69(46), 1579.

- McCabe, G.J., and Dettinger, M.D. 1999. Decadal variations in the strength of ENSO teleconnections with precipitation in the western United States. *International Journal of Climatology* 19(13), 1399–1410.
- McCabe, G.J., Palecki, M.A., and Betancourt, J.L. 2004. Pacific and Atlantic Ocean influences on multidecadal drought frequency in the United States. *Proceedings of the National Academy of Sciences of the United States of America* 101(12), 4136–4141.
- Meko, D.M., Baisan, C.H., Adams, R.K., Holmes, R.L., Rose, M.R., and Wu, X. 1996. Frederick Butte Recollection Western Juniper Chronology. IGBP PAGES/World Data Center for Paleoclimatology Data Contribution Series # +4335-12027. NOAA/NCDC Paleoclimatology Program, Boulder, Colorado, USA.
- Meko, D.M., Stockton, C.W., and Boggess, W.R. 1995. The tree-ring record of severe sustained drought. *Water Resources Bulletin* 31(5), 789–801.
- Miksicek, C.H. 1987. Formation processes of the archaeobotanical record. In: Schiffer, M.B., ed., *Advances in Archaeological Method and Theory, Volume 10*. Harcourt Publishers, Ltd., Orlando, Florida, 211–247.
- Miller, R.F. 1989. Plant competition in Oregon's High Desert. In: *Oregon's High Desert: the Last 100 Years*. Special Report 841. United States Department of Agriculture, Agricultural Research Service, Agricultural Experiment Station, Oregon State University, Corvallis, Oregon, 7–14.
- Miller, R.F., and Rose, J.A. 1995. Historic expansion of *Juniperus occidentalis* (western juniper) in southeastern Oregon. *Great Basin Naturalist* 55(1), 37–45.
- Miller, R.F., and Rose, J.A. 1999. Fire history and western juniper encroachment in sagebrush steppe. *Journal of Range Management* 52(6), 550–559.
- Minobe, S. 1997. A 50–70 year climatic oscillation over the North Pacific and North America. *Geophysical Research Letters* 24(6), 683–686.
- Mitchell, V.L. 1976. The regionalization of climate in the western United States. *Journal of Applied Meteorology* 15(9), 920–927.
- Morris, W.G. 1934. Lightning storms and fires on the national forests of Oregon and Washington. *Monthly Weather Review* 62, 370–375.
- Morrison, P.H., and Swanson, F.J. 1990. *Fire History and Pattern in a Cascade Range Landscape*. General Technical Report PNW-GTR-254. United States Department of Agriculture, Forest Service, Pacific Northwest Research Station, Portland, Oregon, 77 pp.

- Myhrum, R., and Ferry, W. 2002. *Soil Survey of Upper Deschutes River Area, Oregon, Including Parts of Deschutes, Jefferson, and Klamath Counties*. United States Department of Agriculture, Natural Resources Conservation Service, Washington, D.C., 515 pp.
- Nash, J.M. 2002. *El Niño: Unlocking the Secrets of the Master Weather-Maker*. Warner Books, Inc., New York, New York, 340 pp.
- Nash, S.E. 1999. *Time, Trees, and Prehistory: Tree-Ring Dating and the Development of North American Archaeology, 1914–1950*. The University of Utah Press, Salt Lake City, Utah, 294 pp.
- National Aeronautics and Space Administration. 2007a. Little Ice Age. Information archived at: <http://eobglossary.gsfc.nasa.gov/Library/>
- National Aeronautics and Space Administration. 2007b. The sun's chilly impact on Earth. Information archived at: http://svs.gsfc.nasa.gov/stories/iceage_20011207/
- National Climatic Data Center. 2006. Data archived at: <http://www1.ncdc.noaa.gov/pub/data/cirs/>
- National Oceanic and Atmospheric Administration. 2002a. The economic implications of an El Niño. *NOAA Magazine*. Article archived at: <http://www.magazine.noaa.gov/stories/mag24.htm>
- National Oceanic and Atmospheric Administration. 2002b. *Climatography of the United States, No. 81: Monthly Station Normals of Temperature, Precipitation, and Heating and Cooling Days 1971–2000, Oregon*. United States Department of Commerce, National Oceanic and Atmospheric Administration, Asheville, North Carolina, 44 pp.
- Norman, S.P., and Taylor, A.H. 2003. Tropical and north Pacific teleconnections influence fire regimes in pine-dominated forests of north-eastern California, USA. *Journal of Biogeography* 30(7), 1081–1092.
- O'Brien, S., Mayewski, P.A., Meeker, L.D., Meese, D.A., Twickler, M.S., and Whitlow, S.I. 1995. Complexity of Holocene climate as reconstructed from a Greenland ice core. *Science* 270(5244), 1962–1964.
- Oliver, C.D., and Larson, B.C. 1990. *Forest Stand Dynamics*. McGraw-Hill, Inc., New York, New York, 520 pp.
- Oregon Climate Service. 2006. Data archived at: <http://www.ocs.oregonstate.edu>

- Orr, E.L., Orr, W.N., and Baldwin, E.M. 1992. *The Geology of Oregon*. Kendall/Hunt Publishing Company, Dubuque, Iowa, 254 pp.
- Orvis, K.H., and Grissino-Mayer, H.D. 2002. Standardizing the reporting of abrasive papers used to surface tree-ring samples. *Tree-Ring Research*. 58(1–2), 47–50.
- Percival D.B., Walden A.T. 1993. *Spectral Analysis for Physical Applications*. Cambridge University Press, Cambridge, United Kingdom, 583 pp.
- Peterson, D.W., and Peterson, D.L. 2001. Mountain hemlock growth responds to climatic variability at annual and decadal time scales. *Ecology* 82(12), 3330–3345.
- Petit, J.R., Jouzel, J., Raynaud, D., Barkov, N.I., Barnola, J.-M., Basile, I., Bender, M., Chappellaz, J., Davis, M., Delaygue, G., Delmotte, M., Kotlyakov, V.M., Legrand, M., Lipenkov, V.Y., Lorius, C., Pepin, L., Ritz, C., Saltzman, E., and Stievenard, M. 1999. Climate and atmospheric history of the past 420,000 years from the Vostok ice core, Antarctica. *Nature* 399(6735), 429–436.
- Pisias, N.G., Mix, A.G., and Heusser, L. 2001. Millennial scale climate variability of the northeast Pacific Ocean and northwest North America based on radiolarian and pollen. *Quaternary Science Reviews* 20(14), 1561–1576.
- Pohl, K.A., Hadley, K.S., and Arabas, K.B. 2002. A 545-year drought reconstruction for central Oregon. *Physical Geography* 23(4), 302–320.
- Rasmusson, E.M., and Wallace, J.M. 1983. Meteorological aspects of the El Niño/Southern Oscillation. *Science* 222(4629), 1195–1202.
- Rogers, J.E. 1917. *Trees Worth Knowing*. Doubleday, Page and Company, Garden City, New York, 291 pp.
- Rorig, M.L., and Ferguson, S.A. 1999. Characteristics of lightning and wildland fire ignition in the Pacific Northwest. *Journal of Applied Meteorology* 38(11), 1565–1575.
- Schlotzhauer, S.D., and Littell, R.C. 1987. *SAS System for Elementary Statistical Analysis*. SAS Institute, Inc. Cary, North Carolina, 416 pp.
- Schubert, S.D., Suarez, M.J., Pegion, P.J., Koster, R.D., and Bacmeister, J.T. 2004. On the cause of the 1930s Dust Bowl. *Science* 303(5665), 1855–1859.
- Schulman, E. 1954. Longevity under adversity in conifers. *Science* 119(3091), 396–399.

- Silenzi, S., Bard, E., Montagna, P., and Antonioli, F. 2005. Isotopic and elemental records in a non-tropical coral (*Cladocora caespitosa*): discovery of a new high-resolution climate archive for the Mediterranean Sea. *Global and Planetary Change* 49(2), 94–120.
- Soulé, P.T., and Knapp, P.A. 2000. *Juniperus occidentalis* (western juniper) establishment history on two minimally disturbed research natural areas in central Oregon. *Western North American Naturalist* 60(1), 43–55.
- Soulé, P.T., Knapp, P.A., and Grissino-Mayer, H.D. 2003. Comparative rates of western juniper afforestation in south-central Oregon and the role of anthropogenic disturbance. *The Professional Geographer* 55(1), 26–33.
- Soulé, P.T., Knapp, P.A., and Grissino-Mayer, H.D. 2004. Human agency, environmental drivers, and western juniper establishment during the late Holocene. *Ecological Applications* 14(1), 96–112.
- Sowder, J.E., and Mowat, E.L. 1965. Western juniper (*Juniperus occidentalis* Hook.). In Fowells, H.A., ed., *Silvics of Forest Trees of the United States. Agriculture Handbook 271*. United States Department of Agriculture, Forest Service, 223–225.
- Speth, J.G. 2004. *Red Sky at Morning: America and the Crisis of the Global Environment*. Yale University Press, New Haven, Connecticut, 299 pp.
- SSA-MTM Group, Department of Atmospheric Sciences, University of California, Los Angeles. 2006. SSA-MTM Toolkit for Spectral Analysis. Article archived at: <http://www.atmos.ucla.edu/tcd/ssa/guide/guide4.html>
- Stahle, D.W., Cook, E.R., Cleaveland, M.K., Therrell, M.D., Meko, D.M., Grissino-Mayer, H.D., Watson, E., and Luckman, B.H. 2000. Tree-ring data document 16th century megadrought over North America. *Eos* 81(12), 121–132.
- Stokes, M.A., and Smiley, T.L. 1996. *An Introduction to Tree-Ring Dating*. The University of Arizona Press, Tucson, 73 pp.
- Swetnam, T.W. 1993. Fire history and climate change in giant sequoia groves. *Science* 262(5135), 885–889.
- Swetnam, T.W., Betancourt, J.L. 1990. Fire-Southern Oscillation relations in the southwestern United States. *Science* 249(4972), 1017–1020.
- Taylor, G.H., and Hannan, C. 1999. *The Climate of Oregon: From Rain Forest to Desert*. Oregon State University Press, Corvallis, Oregon, 211 pp.

- Thompson, L.G., Mosley-Thompson, E., Bolzan, J.F., and Koci, B.R. 1985. A 1,500 year record of tropical precipitation recorded in ice cores from the Quelccaya Ice Cap, Peru. *Science* 229(4717), 971–973.
- Thompson, L.G., Mosley-Thompson, E., Dansgaard, W., and Grootes, P.M. 1986. The “Little Ice Age” as recorded in the stratigraphy of the tropical Quelccaya ice cap. *Science* 234(4774), 361–364.
- United States Environmental Protection Agency. 2006. Ecoregions of Oregon. Data archived at: http://www.epa.gov/wed/pages/ecoregions/or_eco.htm
- United States Geological Survey. 2007. Medieval Warm Period, Little Ice Age and 20th century temperature variability from Chesapeake Bay. Article archived at: <http://geology.er.usgs.gov/eespteam/Atlantic/GPCabs.htm>
- Urban, F.E., Cole, J.E., and Overpeck, J.T. 2000. Influence of mean climate change on climate variability from a 155-year tropical Pacific coral record. *Nature* 407(6807), 989–993.
- Vale, T.R. 1981. Tree invasion of montane meadows in Oregon. *The American Midland Naturalist* 105(1), 61–69.
- Vale, T.R. 1982. *Plants and People: Vegetation Change in North America*. Association of American Geographers, Washington, D.C., 56–63.
- Vandenbosch, R. 2000. Effects of ENSO and PDO events on seabird populations as revealed by Christmas bird count data. *Waterbirds* 23(3), 416–422.
- Vasek, F. C. 1966. The distribution and taxonomy of three western junipers. *Brittonia* 18(4), 350–372.
- Veblen, T.T., Kitzberger, T., and Donnegan, J. 2000. Climatic and human influences on fire regimes in ponderosa pine forests in the Colorado Front Range. *Ecological Applications* 10(4), 1178–1195.
- Walker, G.W., and Nolf, B. 1981. High Lava Plains, Brothers fault zone to Harney Basin, Oregon. In Johnston, D.A., and Donnelly-Nolan, J., eds., *Guides to Some Volcanic Terranes in Wasington, Idaho, Oregon, and Northern California: U.S. Geological Survey Circular 838*. United States Geological Survey, Menlo Park, California, 105–114.
- Wall, T.G., Miller, R.F., and Svejcar, T.J. 2001. Juniper encroachment into aspen in the Northwest Great Basin. *Journal of Range Management* 54, 691–698.

- Wallin, D.O., Swanson, F.J., Marks, B., Cissel, J.H., and Kertis, J. 1996. Comparison of managed and pre-settlement landscape dynamics in forests of the Pacific Northwest, U.S.A. *Forest Ecology and Management* 85(3), 291–309.
- Weaver, H. 1959. Ecological changes in the ponderosa pine forest of the Warm Springs Indian Reservation in Oregon. *Journal of Forestry* 57, 15–20.
- Weisberg, P.J., and Swanson, F.J. 2003. Regional synchronicity in fire regimes of western Oregon and Washington, U.S.A. *Forest Ecology and Management* 172(1), 17–28.
- West, N.E., and Young, J.A. 2000. Intermountain valleys and lower mountain slopes. In Barbour, M.B., and Billings, W.D., eds., *North American Terrestrial Vegetation*. Cambridge University Press, Cambridge, United Kingdom, 255–284.
- Westerling, A.L., Hidalgo, H.G., Cayan, D.R., and Swetnam, T.W. 2006. Warming and earlier spring increases western U.S. forest wildfire activity. *Scienceexpress* 6 July 2006/page 1/10.1126/science.1128834. Article archived at: <http://www.sciencemag.org/cgi/rapidpdf/1128834v1.pdf>
- Western Regional Climate Center. 2006. Data archived at: <http://www.wrcc.dri.edu>
- Wright, H.A., Neuenschwander, L.F., and Britton, C.M. 1979. *The Role and Use of Fire in Sagebrush-Grass and Pinyon-Juniper Plant Communities: a State-of-the-Art Review*. General Technical Report INT-58. United States Department of Agriculture, Forest Service, Intermountain Forest and Range Experiment Station, Ogden, Utah, 48 pp.
- Young, K.R., Blumler, M.A., Daniels, L.D., Veblen, T.T., and Ziegler, S.S. 2003. Biogeography. In Gaile, G.L., and Willmott, C.J., eds., *Geography in America at the Dawn of the 21st Century*. Oxford University Press, New York, New York, 17–30.
- Young, J.A., and Evans, R.A. 1981. Demography and fire history of a western juniper stand. *Journal of Range Management* 34(6), 501–505.

Appendix

A-1. Frederick Butte COFECHA Output

Correlations of 50-year dated segments, lagged 25 years

Flags: A = correlation under .3281 but highest as dated; B = correlation higher at other than dated position

Seq Series	Time_span	800 849	825 874	850 899	875 924	900 949	925 974	950 999	975 1024	1000 1049	1025 1074	1050 1099	1075 1124	1100 1149	1125 1174	1150 1199	1175 1224	1200 1249	1225 1274	1250 1299	1275 1324
1 FBS001	1016 1300									.89	.89	.92	.92	.92	.93	.92	.93	.89	.88	.84	.83
2 FBS003	894 1152				.86	.88	.86	.87	.86	.86	.88	.83	.73	.72	.73						
3 FBS004	797 1576	.66	.74	.74	.84	.86	.85	.90	.82	.81	.90	.86	.79	.88	.91	.93	.95	.93	.87	.89	.89
4 FBS005-2	941 1644						.86	.85	.83	.85	.92	.94	.93	.92	.94	.93	.91	.92	.90	.89	.91
5 FBS009	1269 1623																			.93	.93
6 FBS010A	1138 2000														.95	.95	.91	.88	.90	.91	.88
7 FBS010B	1133 1782														.94	.94	.92	.84	.81	.89	.89
8 FBS014	1152 1606															.93	.93	.91	.92	.94	.96
9 FBS016	963 1569							.76	.80	.88	.88	.89	.83	.85	.91	.90	.90	.89	.88	.94	.94
10 FBS019A	1237 1627																		.87	.87	.90
11 FBS020A	1148 1922														.86	.86	.81	.78	.87	.90	.87
12 FBS027	1014 1418									.87	.92	.88	.81	.92	.95	.90	.90	.91	.89	.89	.87
13 FBN028	906 1274					.64	.75	.90	.88	.88	.96	.93	.89	.92	.96	.91	.92	.91	.88		
14 FBN032	1229 1658																		.86	.93	.91
15 FBN037	815 1276	.67	.70	.83	.91	.92	.91	.88	.86	.86	.82	.81	.78	.73	.81	.85	.86	.89	.88	.88	
16 FBN039	1002 1461									.83	.88	.94	.90	.90	.92	.90	.90	.74	.70	.93	.95
17 FBN040B	1089 1542												.81	.82	.91	.94	.93	.91	.91	.93	.93
18 FBN046	851 1318			.79	.86	.87	.87	.81	.79	.87	.89	.87	.88	.91	.94	.94	.94	.90	.88	.88	.87
19 FBN047	900 1624					.73	.85	.90	.93	.95	.94	.94	.93	.91	.94	.94	.93	.95	.88	.84	.89
20 FBN050	835 1896		.69	.77	.78	.78	.76	.79	.84	.90	.93	.92	.90	.94	.95	.95	.90	.88	.93	.92	.89
21 FBN053	861 1197			.82	.89	.93	.87	.86	.84	.84	.93	.94	.85	.80	.86	.80					
22 FBN054	965 1588						.84	.88	.85	.87	.91	.84	.87	.93	.89	.86	.82	.84	.87	.83	
23 FBN061	1241 1657																	.90	.90	.90	
Av segment correlation		.66	.71	.79	.86	.83	.84	.85	.85	.87	.90	.90	.85	.87	.91	.91	.91	.88	.87	.90	.90

Correlations of 50-year dated segments, lagged 25 years

Flags: A = correlation under .3281 but highest as dated; B = correlation higher at other than dated position

Seq	Series	Time_span	1300 1349	1325 1374	1350 1399	1375 1424	1400 1449	1425 1474	1450 1499	1475 1524	1500 1549	1525 1574	1550 1599	1575 1624	1600 1649	1625 1674	1650 1699	1675 1724	1700 1749	1725 1774	1750 1799	1775 1824
3	FBS004	797 1576	.87	.90	.82	.80	.88	.89	.75	.69	.76	.84	.85									
4	FBS005-2	941 1644	.89	.88	.81	.84	.91	.79	.78	.87	.84	.93	.84	.79	.76							
5	FBS009	1269 1623	.94	.95	.88	.88	.95	.92	.89	.92	.92	.92	.93	.92								
6	FBS010A	1138 2000	.91	.92	.91	.89	.88	.92	.80	.76	.84	.89	.90	.89	.92	.84	.82	.90	.86	.88	.90	.86
7	FBS010B	1133 1782	.92	.94	.86	.86	.93	.93	.87	.84	.86	.90	.89	.89	.92	.86	.85	.89	.88	.86	.87	
8	FBS014	1152 1606	.96	.94	.93	.94	.97	.90	.87	.87	.86	.88	.88	.88								
9	FBS016	963 1569	.91	.92	.88	.86	.88	.87	.82	.81	.82	.87										
10	FBS019A	1237 1627	.89	.85	.84	.85	.91	.82	.76	.85	.87	.87	.88	.84	.83							
11	FBS020A	1148 1922	.89	.80	.70	.78	.89	.87	.82	.80	.81	.70	.76	.92	.92	.83	.80	.85	.81	.82	.87	.83
12	FBS027	1014 1418	.89	.86	.76	.79																
14	FBN032	1229 1658	.87	.83	.78	.84	.96	.94	.90	.90	.92	.95	.93	.93	.91	.90						
16	FBN039	1002 1461	.95	.90	.88	.89	.89	.88														
17	FBN040B	1089 1542	.90	.91	.91	.90	.95	.92	.86	.85	.81											
19	FBN047	900 1624	.91	.90	.78	.83	.93	.87	.81	.89	.92	.93	.90	.87								
20	FBN050	835 1896	.91	.94	.92	.91	.92	.92	.91	.86	.85	.88	.89	.91	.92	.80	.78	.87	.79	.81	.84	.71
22	FBN054	965 1588	.89	.93	.78	.78	.91	.91	.84	.82	.86	.88	.88									
23	FBN061	1241 1657	.88	.90	.90	.87	.89	.86	.85	.89	.81	.69	.80	.90	.83	.82						
24	FBN065	1423 1997					.85	.85	.85	.87	.79	.73	.82	.92	.88	.84	.88	.91	.73	.73	.85	.83
25	FBN069	1300 1946	.87	.84	.77	.79	.88	.86	.82	.85	.85	.82	.78	.75	.79	.85	.79	.74	.76	.78	.80	.64
Av segment correlation			.90	.90	.84	.85	.91	.88	.84	.84	.85	.86	.86	.88	.87	.84	.82	.86	.81	.81	.85	.77

Correlations of 50-year dated segments, lagged 25 years

Flags: A = correlation under .3281 but highest as dated; B = correlation higher at other than dated position

Seq	Series	Time_span	1800	1825	1850	1875	1900	1925	1950
			1849	1874	1899	1924	1949	1974	1999
6	FBS010A	1138 2000	.75	.77	.85	.82	.76	.74	.74
11	FBS020A	1148 1922	.86	.86	.80	.78			
20	FBN050	835 1896	.72	.83	.68				
24	FBN065	1423 1997	.91	.86	.82	.84	.79	.79	.76
25	FBN069	1300 1946	.68	.78	.70	.69	.68		
Av segment correlation			.78	.82	.77	.78	.74	.76	.75

For each series with potential problems the following diagnostics may appear:

- [A] Correlations with master dating series of flagged 50-year segments of series filtered with 32-year spline, at every point from ten years earlier (-10) to ten years later (+10) than dated
- [B] Effect of those data values which most lower or raise correlation with master series
Symbol following year indicates value in series is greater (>) or lesser (<) than master series value
- [C] Year-to-year changes very different from the mean change in other series
- [D] Absent rings (zero values)
- [E] Values which are statistical outliers from mean for the year

=====

FBS001 1016 to 1300 285 years Series 1

- [B] Entire series, effect on correlation (.895) is:
- | | | | | | | | | | |
|-------|-------------|-------------|-------------|-------------|-------------|-------------|--------|------|------|
| Lower | 1101< -.002 | 1286< -.002 | 1043> -.002 | 1022< -.002 | 1233< -.002 | 1234< -.001 | Higher | 1040 | .003 |
| | | | | | | | | 1098 | .003 |
- [D] 2 Absent rings: Year Master N series Absent
- | | | | | |
|--|------|--------|----|----|
| | 1072 | -2.747 | 14 | 7 |
| | 1279 | -4.367 | 19 | 10 |
- [E] Outliers 2 3.0 SD above or -4.5 SD below mean for year
- | | | | | |
|--|------|----------|------|---------|
| | 1098 | -4.7 SD; | 1126 | +3.6 SD |
|--|------|----------|------|---------|

FBS005-2 941 to 1644 704 years

Series 4

[B] Entire series, effect on correlation (.870) is:

Lower	1012< -.007	1463< -.004	1637< -.003	1383< -.002	1532< -.002	1465> -.002	Higher	1279	.002
								1098	.002

[D] 13 Absent rings: Year Master N series Absent

1012	-2.592	12	1
1059	-3.118	14	1
1072	-2.747	14	7
1126	-4.896	15	8
1183	-2.457	18	2
1279	-4.367	19	10
1364	-1.317	18	1
1379	-2.683	18	4
1428	-3.101	18	7
1532	-.003	17	17
1571	-2.053	15	9
1580	-2.146	14	6
1594	-1.855	13	4

>> WARNING: Ring is not usually narrow

[E] Outliers 5 3.0 SD above or -4.5 SD below mean for year

1012	-9.5 SD;	1126	+3.5 SD;	1413	-4.5 SD;	1463	-5.2 SD;	1465	+3.3 SD
------	----------	------	----------	------	----------	------	----------	------	---------

=====

FBS009 1269 to 1623 355 years Series 5

[B] Entire series, effect on correlation (.918) is:

Lower	1532< -.007	1473< -.002	1390> -.002	1278< -.001	1377< -.001	1427> -.001	Higher	1279	.004
								1335	.004

[D] 7 Absent rings: Year Master N series Absent

1379	-2.683	18	4	
1465	-2.702	17	6	
1532	-.003	17	17	>> WARNING: Ring is not usually narrow
1565	-1.850	16	3	
1571	-2.053	15	9	
1598	-1.447	13	2	
1600	-1.420	13	4	

[E] Outliers 3 3.0 SD above or -4.5 SD below mean for year

1379	-4.9 SD;	1390	+3.3 SD;	1532	-5.3 SD
------	----------	------	----------	------	---------

=====

FBS010A 1138 to 2000 863 years Series 6

[*] Later part of series cannot be checked from 1998 to 2000 -- not matched by another series

[B] Entire series, effect on correlation (.866) is:

Lower 1849< -.003 1417< -.003 1489> -.003 1847< -.002 1583< -.002 1532< -.002 Higher 1279 .003
1335 .002

[D] 14 Absent rings: Year Master N series Absent

1529	-1.423	17	3
1532	-.003	17	17
1571	-2.053	15	9
1660	-2.049	6	3
1679	-3.200	6	3
1686	-2.056	6	2
1698	-1.740	6	1
1721	-2.547	6	4
1800	-3.195	5	4

>> WARNING: Ring is not usually narrow

Absent in series	11	FBS020A	time span	1148 to	1922
Absent in series	20	FBN050	time span	835 to	1896
Absent in series	24	FBN065	time span	1423 to	1997
Present in series	25	FBN069	time span	1300 to	1946

1829	-3.430	5	3
------	--------	---	---

Absent in series	11	FBS020A	time span	1148 to	1922
Absent in series	20	FBN050	time span	835 to	1896
Present in series	24	FBN065	time span	1423 to	1997
Present in series	25	FBN069	time span	1300 to	1946

1918	-2.582	4	3
------	--------	---	---

Present in series	11	FBS020A	time span	1148 to	1922
Absent in series	24	FBN065	time span	1423 to	1997
Absent in series	25	FBN069	time span	1300 to	1946

1931	-2.442	3	2
------	--------	---	---

Present in series	24	FBN065	time span	1423 to	1997
Absent in series	25	FBN069	time span	1300 to	1946

1934	-2.984	3	2
------	--------	---	---

Present in series	24	FBN065	time span	1423 to	1997
Absent in series	25	FBN069	time span	1300 to	1946

1959	-1.851	2	1
------	--------	---	---

Present in series	24	FBN065	time span	1423 to	1997
-------------------	----	--------	-----------	---------	------

[E] Outliers 7 3.0 SD above or -4.5 SD below mean for year

1217 +3.0 SD; 1390 -7.5 SD; 1417 -5.7 SD; 1489 +4.4 SD; 1741 +3.1 SD; 1849 -4.6 SD; 1934 +3.1 SD

FBS010B 1133 to 1782 650 years Series 7

[B] Entire series, effect on correlation (.889) is:

Lower	1379< -.004	1227< -.002	1663< -.002	1583< -.002	1217> -.001	1532< -.001	Higher	1390 .003
								1335 .002

[D] 9 Absent rings: Year Master N series Absent

1413	-2.000	18	1	
1529	-1.423	17	3	
1532	-.003	17	17	>> WARNING: Ring is not usually narrow
1632	-1.710	9	3	
1660	-2.049	6	3	
1679	-3.200	6	3	
1686	-2.056	6	2	
1721	-2.547	6	4	
1729	-2.204	6	3	

[E] Outliers 2 3.0 SD above or -4.5 SD below mean for year

1279 -6.0 SD; 1379 -6.3 SD

FBS014 1152 to 1606 455 years Series 8

[B] Entire series, effect on correlation (.924) is:

Lower	1532< -.003	1462> -.002	1522< -.002	1384< -.001	1200> -.001	1455< -.001	Higher	1335 .003
								1390 .003

[D] 10 Absent rings: Year Master N series Absent

1279	-4.367	19	10	
1335	-4.140	18	7	
1428	-3.101	18	7	
1532	-.003	17	17	>> WARNING: Ring is not usually narrow
1571	-2.053	15	9	
1579	-1.602	14	2	
1580	-2.146	14	6	
1594	-1.855	13	4	
1598	-1.447	13	2	
1600	-1.420	13	4	

[E] Outliers 1 3.0 SD above or -4.5 SD below mean for year

1379 -5.7 SD

FBS020A 1148 to 1922 775 years

Series 11

[B] Entire series, effect on correlation (.829) is:

Lower 1532< -.007 1658< -.004 1351> -.002 1238> -.002 1670> -.002 1386< -.001 Higher 1428 .002
1236 .002

[D] 26 Absent rings: Year Master N series Absent

1245	-2.449	20	1
1279	-4.367	19	10
1335	-4.140	18	7
1344	-1.259	18	1
1379	-2.683	18	4
1390	-4.220	18	4
1410	-1.468	18	2
1428	-3.101	18	7
1439	-2.481	18	3
1465	-2.702	17	6
1532	-.003	17	17
1565	-1.850	16	3
1571	-2.053	15	9
1580	-2.146	14	6
1600	-1.420	13	4
1632	-1.710	9	3
1636	-.817	9	2
1652	-1.818	8	1
1658	.589	7	1
1659	-.553	6	1
1660	-2.049	6	3
1695	-1.910	6	3
1729	-2.204	6	3
1793	-1.269	5	2

>> WARNING: Ring is not usually narrow

>> WARNING: Ring is not usually narrow

Present in series	6	FBS010A	time span	1138 to	2000
Present in series	20	FBN050	time span	835 to	1896
Absent in series	24	FBN065	time span	1423 to	1997
Present in series	25	FBN069	time span	1300 to	1946

1800	-3.195	5	4
------	--------	---	---

Absent in series	6	FBS010A	time span	1138 to	2000
Absent in series	20	FBN050	time span	835 to	1896
Absent in series	24	FBN065	time span	1423 to	1997
Present in series	25	FBN069	time span	1300 to	1946

1829 -3.430 5 3

Absent in series 6 FBS010A time span 1138 to 2000
 Absent in series 20 FBN050 time span 835 to 1896
 Present in series 24 FBN065 time span 1423 to 1997
 Present in series 25 FBN069 time span 1300 to 1946

[E] Outliers 10 3.0 SD above or -4.5 SD below mean for year
 1238 +3.6 SD; 1245 -5.5 SD; 1351 +3.5 SD; 1390 +4.7 SD; 1532 -6.2 SD; 1569 +3.4 SD; 1670 +3.3 SD;
 1739 +3.4 SD; 1817 +3.8 SD; 1920 +3.4 SD

FBS027 1014 to 1418 405 years Series 12

[B] Entire series, effect on correlation (.872) is:
 Lower 1392< -.003 1103< -.002 1359< -.002 1014> -.002 1379> -.002 1386< -.002 Higher 1126 .008
 1335 .005

[E] Outliers 3 3.0 SD above or -4.5 SD below mean for year
 1014 +3.0 SD; 1098 +4.6 SD; 1379 +3.8 SD

FBN028 906 to 1274 369 years Series 13

[B] Entire series, effect on correlation (.883) is:
 Lower 915> -.014 1087< -.006 935< -.005 1239> -.003 1016< -.003 936< -.002 Higher 1126 .009
 1098 .004

[D] 2 Absent rings: Year Master N series Absent
 930 -2.865 8 1
 1126 -4.896 15 8

[E] Outliers 5 3.0 SD above or -4.5 SD below mean for year
 915 +7.6 SD; 935 -4.7 SD; 1012 +3.2 SD; 1087 -5.2 SD; 1239 +3.1 SD

[B] Entire series, effect on correlation (.891) is:

[illegible]

```
[D] 9 Absent rings: Year Master N series Absent
```

```

1279    -4.367    19    10
1335    -4.140    18     7
1352    -1.830    18     2
1358    -1.685    18     2
1465    -2.702    17     6
1532     -0.003    17    17 >> WARNING: Ring is not usually narrow
1632    -1.710     9     3
1636     -0.817     9     2
1644     -0.097     9     1 >> WARNING: Ring is not usually narrow

```

[E] Outliers	5	3.0 SD above or -4.5 SD below mean for year
--------------	---	---

1384 +3.9 SD; 1390 +3.1 SD; 1465 -7.4 SD; 1499 -4.5 SD; 1532 -5.2 SD

[B] Entire series, effect on correlation (.837) is:

[illegible]

```
[D]      4 Absent rings:  Year  Master  N series Absent
```

1072	-2.747	14	7
1083	-2.177	14	1
1126	-4.896	15	8
1213	-2.439	17	1

[E] Outliers	9	3.0 SD above or -4.5 SD below mean for year
--------------	---	---

819 -6.4 SD; 822 +3.7 SD; 843 +3.4 SD; 877 +3.2 SD; 1012 +4.8 SD; 1067 +3.3 SD; 1084 -5.1 SD;
1100 -4.6 SD; 1127 -5.3 SD

[illegible]

[D]	1 Absent rings:	Year	Master	N series	Absent
		1335	-4.140	18	7

[E] Outliers 3 3.0 SD above or -4.5 SD below mean for year
1126 -6.8 SD; 1231 +3.4 SD; 1232 -5.7 SD

FBN040B 1089 to 1542 454 years Series 17

Lower	1115< -.006	1126> -.004	1532< -.003	1246< -.002	1286< -.002	1337< -.001	Higher	1390 .003	1335 .003
-------	-------------	-------------	-------------	-------------	-------------	-------------	--------	-----------	-----------

[D]	6 Absent rings:	Year	Master	N series	Absent
		1335	-4.140	18	7
		1390	-4.220	18	4
		1475	-2.346	17	2
		1529	-1.423	17	3
		1532	-.003	17	17
		1540	-1.408	17	2

[E] Outliers 2 3.0 SD above or -4.5 SD below mean for year
 1115 -6.9 SD; 1126 +4.8 SD

FBN046 851 to 1318 468 years Series 18

[illegible]

[D]	1 Absent rings:	Year	Master	N series	Absent
		1126	-4.896	15	8

[E] Outliers 7 3.0 SD above or -4.5 SD below mean for year
896 +3.9 SD; 900 +3.0 SD; 915 -4.8 SD; 979 +4.6 SD; 1084 +3.3 SD; 1094 +3.1 SD; 1279 +4.6 SD

FBN047 900 to 1624 725 years

Series 19

[B] Entire series, effect on correlation (.889) is:

Lower	900 < -.007	1126 > -.003	915 > -.002	1473 < -.002	1256 < -.001	1532 < -.001	Higher	1390 .003
								1098 .002

[D] 20 Absent rings: Year Master N series Absent

1072	-2.747	14	7
1126	-4.896	15	8
1217	-1.576	17	1
1279	-4.367	19	10
1352	-1.830	18	2
1354	-1.101	18	1
1358	-1.685	18	2
1379	-2.683	18	4
1390	-4.220	18	4
1428	-3.101	18	7
1465	-2.702	17	6
1532	-.003	17	17
1540	-1.408	17	2
1565	-1.850	16	3
1571	-2.053	15	9
1579	-1.602	14	2
1580	-2.146	14	6
1593	-.847	13	1
1607	-1.061	12	1
1619	-.986	12	1

>> WARNING: Ring is not usually narrow

[E] Outliers 3 3.0 SD above or -4.5 SD below mean for year
 900 -8.5 SD; 915 +4.7 SD; 1126 +4.7 SD

[B] Entire series, effect on correlation (.860) is:

[illegible]

[D] 17 Absent rings: Year Master N series Absent

1072	-2.747	14	7
1126	-4.896	15	8
1279	-4.367	19	10
1532	-.003	17	17
1571	-2.053	15	9
1580	-2.146	14	6
1594	-1.855	13	4
1600	-1.420	13	4
1679	-3.200	6	3
1695	-1.910	6	3
1721	-2.547	6	4
1729	-2.204	6	3
1741	-.026	6	1
1800	-3.195	5	4

```
>> WARNING: Ring is not usually narrow
```

```
>> WARNING: Ring is not usually narrow
```

Absent	in series	6	FBS010A	time span	1138 to	2000
Absent	in series	11	FBS020A	time span	1148 to	1922
Absent	in series	24	FBN065	time span	1423 to	1997
Present	in series	25	FBN069	time span	1300 to	1946

1829	-3.430	5	3
------	--------	---	---

Absent	in series	6	FBS010A	time span	1138 to	2000
Absent	in series	11	FBS020A	time span	1148 to	1922
Present	in series	24	FBN065	time span	1423 to	1997
Present	in series	25	FBN069	time span	1300 to	1946

1888	-1.030	5	1
------	--------	---	---

Present in series	6	FBS010A	time span	1138 to	2000
Present in series	11	FBS020A	time span	1148 to	1922
Present in series	24	FBN065	time span	1423 to	1997
Present in series	25	FBN069	time span	1300 to	1946

1896	-.575	5	1
------	-------	---	---

Present in series	6	FBS010A	time span	1138 to	2000
Present in series	11	FBS020A	time span	1148 to	1922
Present in series	24	FBN065	time span	1423 to	1997
Present in series	25	FBN069	time span	1300 to	1946

```
>> WARNING: Last ring in series is ABSENT
```

[E] Outliers	13	3.0 SD above or -4.5 SD below mean for year
--------------	----	---

835 +4.0 SD; 896 +5.1 SD; 902 +3.1 SD; 979 -4.5 SD; 983 +3.5 SD; 1012 -5.7 SD; 1660 +3.1 SD;
1741 -5.1 SD; 1816 +3.6 SD; 1817 +4.8 SD; 1849 +3.7 SD; 1889 +4.5 SD; 1892 +3.2 SD

[B] Entire series, effect on correlation (.874) is:

Lower	967< -.005	1012> -.005	1115> -.004	1111< -.003	1188< -.003	1002< -.002	Higher	1126 .008
								915 .007

[D] 4 Absent rings: Year Master N series Absent

1072	-2.747	14	7
1126	-4.896	15	8
1183	-2.457	18	2
1194	-.392	18	1

```
>> WARNING: Ring is not usually narrow
```

[E] Outliers	3	3.0 SD above or -4.5 SD below mean for year
--------------	---	---

967 -4.7 SD; 1012 +3.8 SD; 1115 +4.4 SD

FBN054 965 to 1588 624 years Series 22

[B] Entire series, effect on correlation (.863) is:

[illegible]

```
[D] 3 Absent rings: Year Master N series Absent
```

1279	-4.367	19	10
1390	-4.220	18	4
1532	-.003	17	17

```
>> WARNING: Ring is not usually narrow
```

[E] Outliers	4	3.0 SD above or -4.5 SD below mean for year
--------------	---	---

1012 +3.5 SD; 1383 +3.6 SD; 1489 +4.1 SD; 1532 -4.9 SD

FBN061 1241 to 1657 417 years Series 23

[B] Entire series, effect on correlation (.851) is:

Lower	1571> -.009	1451< -.007	1532< -.006	1566< -.005	1321< -.003	1411< -.002	Higher	1390 .005	1279 .005
-------	-------------	-------------	-------------	-------------	-------------	-------------	--------	-----------	-----------

```
[D]      1 Absent rings:  Year   Master  N series Absent
```

1532	-.003	17	17
------	-------	----	----

```
>> WARNING: Ring is not usually narrow
```

[E] Outliers	7	3.0 SD above or -4.5 SD below mean for year
--------------	---	---

1321 -4.6 SD; 1390 -5.0 SD; 1451 -5.0 SD; 1465 -5.4 SD; 1532 -5.9 SD; 1566 -5.5 SD; 1571 +5.8 SD

[B] Entire series, effect on correlation (.815) is:

Lower	1532< -.010	1565> -.003	1992> -.003	1742< -.003	1465> -.003	1933> -.002	Higher	1679 .004 1829 .003
-------	-------------	-------------	-------------	-------------	-------------	-------------	--------	------------------------

[D] 6 Absent rings: Year Master N series Absent

1532	-.003	17	17
1695	-1.910	6	3
1721	-2.547	6	4
1793	-1.269	5	2

```
>> WARNING: Ring is not usually narrow
```

Present in series	6	FBS010A	time span	1138 to 2000
Absent in series	11	FBS020A	time span	1148 to 1922
Present in series	20	FBN050	time span	835 to 1896
Present in series	25	FBN069	time span	1300 to 1946

1800	-3.195	5	4
------	--------	---	---

Absent	in series	6	FBS010A	time span	1138 to 2000
Absent	in series	11	FBS020A	time span	1148 to 1922
Absent	in series	20	FBN050	time span	835 to 1896
Present	in series	25	FBN069	time span	1300 to 1946

1918	-2.582	4	3
------	--------	---	---

Absent	in series	6	FBS010A	time span	1138	to	2000
Present	in series	11	FBS020A	time span	1148	to	1922
Absent	in series	25	FBN069	time span	1300	to	1946

[E] Outliers	9	3.0 SD above or -4.5 SD below mean for year
--------------	---	---

1465 +4.1 SD; 1532 -8.4 SD; 1552 +3.5 SD; 1565 +4.0 SD; 1663 +3.2 SD; 1721 -5.9 SD; 1734 +3.3 SD;
1742 -4.6 SD; 1899 +3.6 SD

FBN069 1300 to 1946 647 years

Series 25

[B] Entire series, effect on correlation (.783) is:

Lower 1817< -.009 1383< -.006 1679> -.005 1532< -.003 1583< -.003 1885< -.003 Higher 1335 .006
1390 .006

[D] 5 Absent rings: Year Master N series Absent

1335 -4.140 18 7
1532 -.003 17 17
1918 -2.582 4 3

>> WARNING: Ring is not usually narrow

Absent in series 6 FBS010A time span 1138 to 2000
Present in series 11 FBS020A time span 1148 to 1922
Absent in series 24 FBN065 time span 1423 to 1997

1931 -2.442 3 2

Absent in series 6 FBS010A time span 1138 to 2000
Present in series 24 FBN065 time span 1423 to 1997

1934 -2.984 3 2

Absent in series 6 FBS010A time span 1138 to 2000
Present in series 24 FBN065 time span 1423 to 1997

[E] Outliers 14 3.0 SD above or -4.5 SD below mean for year

1383 -6.3 SD; 1413 -5.2 SD; 1495 -5.4 SD; 1532 -6.5 SD; 1550 +3.5 SD; 1583 -5.2 SD; 1679 +5.7 SD;
1708 +3.4 SD; 1776 +3.2 SD; 1813 +3.6 SD; 1814 +3.8 SD; 1817 -9.8 SD; 1822 +3.3 SD; 1851 +3.1 SD

[*] All segments correlate highest as dated with correlation with master series over .3281

Seq	Series	Interval	No. Years	No. Segmt	No. Flags	Corr	//----- Unfiltered -----\\				//---- Filtered ----\\				AR ()
						with Master	Mean msmt	Max msmt	Std dev	Auto corr	Mean sens	Max value	Std dev	Auto corr	
1	FBS001	1016 1300	285	12	0	.895	.80	1.95	.396	.441	.463	2.50	.341	-.011	2
2	FBS003	894 1152	259	11	0	.824	.60	1.33	.336	.684	.430	2.47	.341	-.007	2
3	FBS004	797 1576	780	31	0	.837	.41	1.77	.208	.536	.432	2.61	.340	-.032	6
4	FBS005-2	941 1644	704	28	0	.870	.52	1.90	.309	.469	.557	2.62	.299	-.008	1
5	FBS009	1269 1623	355	14	0	.918	.57	2.79	.361	.406	.618	2.70	.398	-.011	1
6	FBS010A	1138 2000	863	34	0	.866	.42	2.09	.274	.575	.582	2.61	.312	-.028	6
7	FBS010B	1133 1782	650	26	0	.889	.45	2.24	.345	.672	.567	2.50	.322	-.022	2
8	FBS014	1152 1606	455	18	0	.924	.66	2.38	.399	.411	.581	2.55	.407	-.025	1
9	FBS016	963 1569	607	24	0	.877	.52	1.96	.357	.654	.546	2.73	.400	-.027	1
10	FBS019A	1237 1627	391	16	0	.865	.64	2.40	.392	.318	.688	2.63	.484	-.051	1
11	FBS020A	1148 1922	775	31	0	.829	.35	1.68	.248	.486	.665	2.67	.410	-.024	6
12	FBS027	1014 1418	405	16	0	.872	.70	2.53	.499	.755	.431	2.61	.372	-.048	5
13	FBN028	906 1274	369	14	0	.883	.80	3.68	.532	.725	.442	2.55	.351	-.024	1
14	FBN032	1229 1658	430	17	0	.891	.52	2.12	.353	.570	.592	2.51	.336	-.020	1
15	FBN037	815 1276	462	19	0	.837	.64	2.35	.449	.777	.434	2.64	.381	-.010	1
16	FBN039	1002 1461	460	18	0	.882	.80	3.07	.588	.836	.380	2.44	.269	-.037	2
17	FBN040B	1089 1542	454	18	0	.898	.69	3.08	.505	.599	.607	2.64	.389	-.045	1
18	FBN046	851 1318	468	18	0	.870	.68	1.87	.380	.585	.466	2.54	.316	-.028	2
19	FBN047	900 1624	725	28	0	.889	.49	2.58	.411	.673	.669	2.58	.360	-.030	1
20	FBN050	835 1896	1062	42	0	.860	.49	1.68	.259	.466	.542	2.59	.340	-.025	6
21	FBN053	861 1197	337	13	0	.874	1.02	3.03	.615	.723	.449	2.45	.309	-.033	2
22	FBN054	965 1588	624	25	0	.863	.63	2.62	.415	.722	.429	2.52	.274	-.018	2
23	FBN061	1241 1657	417	17	0	.851	.47	1.66	.285	.555	.509	2.50	.327	-.018	1
24	FBN065	1423 1997	575	23	0	.815	.81	3.31	.576	.521	.576	2.83	.398	-.015	1
25	FBN069	1300 1946	647	25	0	.783	.58	1.98	.308	.551	.443	2.61	.359	-.020	2
Total or mean:			13559	538	0	.864	.58	3.68	.371	.582	.532	2.83	.351	-.025	

A-2. Frederick Butte Standard ARSTAN Output

Year	Value
797	2.099
798	2.342
799	1.398
800	1.282
801	1.499
802	1.346
803	0.931
804	0.951
805	0.722
806	0.638
807	0.771
808	0.697
809	0.735
810	0.284
811	1.086
812	1.299
813	0.899
814	1.388
815	1.459
816	1.227
817	1.138
818	1.329
819	0.385
820	1.395
821	1.422
822	1.593
823	1.532
824	1.304
825	1.434
826	0.758
827	0.818
828	0.973
829	1.077
830	1.093
831	0.987
832	0.871
833	0.603
834	0.861
835	0.765
836	0.907
837	0.943
838	1.001
839	1.002
840	1.063
841	1.54
842	1.557
843	0.94
844	0.853

Year	Value
845	0.857
846	1.242
847	0.903
848	1.087
849	0.694
850	0.988
851	1.186
852	0.736
853	1.299
854	0.788
855	0.835
856	0.504
857	0.767
858	0.783
859	0.858
860	0.62
861	0.703
862	1.195
863	0.667
864	0.721
865	0.477
866	0.98
867	0.487
868	0.288
869	0.954
870	1.154
871	0.635
872	0.258
873	0.323
874	0.955
875	1.058
876	0.989
877	0.732
878	1.05
879	1.426
880	0.482
881	1.09
882	0.805
883	1.097
884	1.22
885	1.32
886	1.322
887	0.782
888	0.917
889	1.131
890	0.817
891	1.172
892	1.536

Year	Value
893	0.627
894	0.948
895	0.897
896	0.765
897	1.058
898	0.866
899	1.072
900	0.922
901	1.104
902	1.114
903	1.244
904	0.971
905	1.087
906	1.092
907	0.814
908	0.807
909	0.785
910	0.82
911	1.063
912	1.209
913	0.748
914	0.879
915	0.206
916	0.989
917	1.206
918	0.675
919	0.929
920	1.074
921	0.964
922	0.65
923	0.852
924	0.951
925	1.331
926	1.457
927	1.249
928	0.758
929	0.758
930	0.269
931	0.774
932	1.14
933	1.183
934	1.155
935	1.448
936	1.183
937	0.769
938	0.849
939	0.622
940	1.058

Year	Value	Year	Value	Year	Value
941	1.191	989	0.488	1037	0.902
942	0.862	990	0.583	1038	0.793
943	0.726	991	0.894	1039	0.872
944	1.094	992	0.992	1040	0.385
945	0.536	993	1.232	1041	0.924
946	0.987	994	1.137	1042	1.332
947	0.614	995	0.781	1043	1.083
948	1.018	996	0.632	1044	0.852
949	0.827	997	0.938	1045	1.292
950	0.713	998	1.347	1046	1.361
951	1.216	999	0.825	1047	0.763
952	0.833	1000	1.284	1048	1.024
953	0.748	1001	1.399	1049	1.263
954	0.478	1002	1.297	1050	1.371
955	0.975	1003	1.056	1051	1.019
956	1.323	1004	1.331	1052	0.526
957	0.386	1005	1.134	1053	1.111
958	0.973	1006	1.121	1054	1.536
959	0.885	1007	0.926	1055	0.907
960	1.254	1008	1.787	1056	0.776
961	1.015	1009	1.772	1057	1.367
962	0.836	1010	1.364	1058	1.192
963	0.814	1011	1.505	1059	0.192
964	0.647	1012	0.554	1060	0.794
965	1.262	1013	1.259	1061	0.878
966	1.199	1014	0.845	1062	0.532
967	1.137	1015	0.864	1063	1.01
968	1.434	1016	1.046	1064	1.426
969	1.007	1017	0.856	1065	0.898
970	1.347	1018	1.054	1066	0.846
971	0.972	1019	1.544	1067	0.669
972	1.337	1020	0.972	1068	1.261
973	0.936	1021	0.706	1069	0.695
974	1.311	1022	0.964	1070	0.54
975	1.249	1023	1.595	1071	0.556
976	1.037	1024	0.871	1072	0.069
977	1.027	1025	0.912	1073	0.982
978	0.774	1026	1.262	1074	0.808
979	0.463	1027	1.262	1075	0.604
980	0.888	1028	0.715	1076	1.284
981	0.817	1029	0.77	1077	1.541
982	1.156	1030	1.211	1078	1.902
983	0.597	1031	1.533	1079	1.573
984	0.751	1032	0.659	1080	1.215
985	1.042	1033	1.122	1081	0.687
986	0.364	1034	1.055	1082	0.902
987	0.767	1035	1.033	1083	0.3
988	1.23	1036	1.453	1084	1.389

Year	Value	Year	Value	Year	Value
1085	0.99	1133	0.98	1181	1.027
1086	1.176	1134	1.038	1182	1.312
1087	0.822	1135	0.34	1183	0.319
1088	0.977	1136	0.649	1184	0.769
1089	1.133	1137	1.19	1185	0.468
1090	0.74	1138	1.485	1186	0.93
1091	1.217	1139	1.234	1187	0.685
1092	0.766	1140	0.204	1188	1.293
1093	0.758	1141	0.558	1189	0.782
1094	0.937	1142	1.077	1190	0.844
1095	1.033	1143	1.01	1191	0.585
1096	1.131	1144	0.689	1192	1.076
1097	0.998	1145	0.241	1193	0.992
1098	0.412	1146	0.331	1194	0.787
1099	1.063	1147	0.89	1195	1.357
1100	1.252	1148	0.616	1196	1.313
1101	1.171	1149	1.574	1197	1.149
1102	0.935	1150	1.003	1198	0.66
1103	0.792	1151	1.144	1199	0.547
1104	1.159	1152	1.178	1200	0.85
1105	1.181	1153	1.23	1201	1.005
1106	1.345	1154	0.747	1202	1.714
1107	1.394	1155	0.372	1203	1.069
1108	1.044	1156	0.716	1204	1.474
1109	0.866	1157	0.734	1205	1.448
1110	1.275	1158	0.496	1206	0.61
1111	1.148	1159	0.723	1207	1.113
1112	1.071	1160	1.118	1208	1.069
1113	1.536	1161	0.35	1209	1.271
1114	0.962	1162	1.035	1210	0.584
1115	0.645	1163	0.633	1211	0.699
1116	1.159	1164	0.482	1212	0.521
1117	1.263	1165	0.848	1213	0.261
1118	1.286	1166	1.114	1214	1.263
1119	1.393	1167	1.132	1215	1.168
1120	1.287	1168	0.612	1216	1.381
1121	1.17	1169	1.506	1217	0.497
1122	1.633	1170	0.608	1218	1.155
1123	0.868	1171	0.744	1219	1.423
1124	1.098	1172	1.028	1220	1.554
1125	1.231	1173	1.246	1221	1.262
1126	0	1174	0.315	1222	1.024
1127	1.342	1175	1.356	1223	0.611
1128	1.315	1176	0.907	1224	1.468
1129	1.375	1177	1	1225	1.3
1130	0.736	1178	1.625	1226	0.957
1131	0.715	1179	1.076	1227	1.446
1132	0.608	1180	1.114	1228	1.38

Year	Value
1229	1.188
1230	0.98
1231	0.704
1232	1.154
1233	1.097
1234	0.936
1235	0.973
1236	0.194
1237	0.638
1238	0.738
1239	0.515
1240	1.243
1241	1.671
1242	1.025
1243	1.364
1244	0.962
1245	0.174
1246	1.426
1247	1.454
1248	1.468
1249	1.111
1250	0.514
1251	0.694
1252	1.314
1253	1.075
1254	0.734
1255	1.321
1256	1.319
1257	1.128
1258	0.577
1259	1.628
1260	0.699
1261	0.65
1262	1.642
1263	1.205
1264	0.579
1265	1.181
1266	1.163
1267	0.681
1268	0.882
1269	0.716
1270	1.397
1271	0.456
1272	0.447
1273	0.441
1274	0.999
1275	1.077
1276	1.277

Year	Value
1277	1.414
1278	0.845
1279	0
1280	0.965
1281	1.224
1282	1.301
1283	1.064
1284	1.353
1285	0.667
1286	0.889
1287	1.626
1288	1.43
1289	1.22
1290	1.345
1291	1.985
1292	1.086
1293	0.927
1294	0.785
1295	1.165
1296	0.325
1297	0.751
1298	0.949
1299	0.564
1300	0.723
1301	0.889
1302	1.114
1303	1.361
1304	0.87
1305	1.522
1306	1.12
1307	0.312
1308	1.91
1309	0.809
1310	1.271
1311	1.539
1312	0.711
1313	0.724
1314	1.365
1315	0.649
1316	0.465
1317	0.75
1318	1.194
1319	1.036
1320	0.489
1321	1.191
1322	1.737
1323	1.356
1324	0.457

Year	Value
1325	1.165
1326	1.359
1327	1.95
1328	0.969
1329	0.987
1330	1.393
1331	1.206
1332	1.516
1333	1.058
1334	0.987
1335	0.076
1336	1.076
1337	1.321
1338	1.447
1339	1.457
1340	0.553
1341	1.697
1342	0.822
1343	1.026
1344	0.481
1345	0.936
1346	1.35
1347	1.589
1348	1.062
1349	1.428
1350	1.021
1351	0.356
1352	0.166
1353	0.701
1354	0.321
1355	0.56
1356	0.981
1357	1.043
1358	0.177
1359	1.042
1360	0.937
1361	0.453
1362	0.586
1363	0.709
1364	0.267
1365	0.799
1366	1.4
1367	1.114
1368	1.232
1369	0.516
1370	0.434
1371	0.633
1372	0.622

Year	Value
1373	0.82
1374	0.618
1375	0.626
1376	0.974
1377	0.662
1378	1.101
1379	0.175
1380	0.962
1381	0.699
1382	0.78
1383	0.703
1384	0.448
1385	1.029
1386	0.884
1387	1.358
1388	0.981
1389	0.899
1390	0.145
1391	1.183
1392	0.872
1393	0.882
1394	1.221
1395	1.093
1396	1.254
1397	1.308
1398	0.985
1399	0.729
1400	1.095
1401	1.656
1402	1.23
1403	1.332
1404	1.652
1405	2.035
1406	0.897
1407	0.434
1408	0.46
1409	0.695
1410	0.349
1411	1.437
1412	1.659
1413	0.146
1414	1.055
1415	0.887
1416	1.397
1417	1.278
1418	0.868
1419	0.995
1420	1.722

Year	Value
1421	1.622
1422	2.061
1423	1.785
1424	1.358
1425	0.501
1426	1.341
1427	1.1
1428	0.072
1429	1.212
1430	1.417
1431	1.389
1432	0.558
1433	1.402
1434	1.032
1435	1.86
1436	1.24
1437	0.746
1438	1.646
1439	0.244
1440	1.921
1441	1.675
1442	2.165
1443	1.471
1444	0.443
1445	1.598
1446	1.111
1447	1.755
1448	1.582
1449	1.941
1450	1.634
1451	1.634
1452	0.933
1453	1.057
1454	0.472
1455	0.827
1456	0.978
1457	0.762
1458	0.771
1459	0.756
1460	0.567
1461	0.903
1462	0.807
1463	0.99
1464	0.93
1465	0.176
1466	0.974
1467	1.021
1468	0.652

Year	Value
1469	1.173
1470	1.455
1471	0.632
1472	1.184
1473	0.843
1474	0.99
1475	0.164
1476	0.573
1477	0.502
1478	0.834
1479	0.539
1480	0.427
1481	0.958
1482	0.684
1483	0.927
1484	1.651
1485	1.086
1486	1.574
1487	1.139
1488	1.374
1489	0.628
1490	1.609
1491	1.171
1492	1.115
1493	1.525
1494	0.851
1495	1.066
1496	1.38
1497	0.802
1498	1.163
1499	0.463
1500	0.767
1501	0.694
1502	0.466
1503	1.509
1504	1.155
1505	0.617
1506	1.156
1507	0.961
1508	0.75
1509	0.583
1510	0.646
1511	1.379
1512	1.342
1513	0.866
1514	1.27
1515	0.513
1516	0.574

Year	Value	Year	Value	Year	Value
1517	0.288	1565	0.2	1613	0.753
1518	0.286	1566	0.886	1614	0.636
1519	1.279	1567	1.075	1615	0.619
1520	0.404	1568	1.012	1616	0.36
1521	0.841	1569	0.722	1617	1.546
1522	1.253	1570	0.869	1618	0.49
1523	1.539	1571	0	1619	0.371
1524	1.471	1572	0.492	1620	0.531
1525	1.265	1573	1.403	1621	1.111
1526	1.355	1574	1.18	1622	0.525
1527	0.858	1575	0.468	1623	1.259
1528	0.805	1576	0.6	1624	1.563
1529	0.196	1577	1.338	1625	1.135
1530	1.32	1578	0.802	1626	0.32
1531	0.541	1579	0.178	1627	1.045
1532	0	1580	0.09	1628	0.385
1533	0.719	1581	0.642	1629	0.4
1534	0.605	1582	1.012	1630	0.57
1535	0.807	1583	0.995	1631	0.648
1536	1.158	1584	0.814	1632	0.092
1537	0.484	1585	1.067	1633	1.276
1538	1.176	1586	0.902	1634	1.45
1539	1.255	1587	1.542	1635	1.032
1540	0.237	1588	0.983	1636	0.361
1541	0.396	1589	1.029	1637	0.993
1542	1.203	1590	0.575	1638	1.253
1543	0.922	1591	0.496	1639	0.43
1544	1.411	1592	0.619	1640	0.61
1545	0.84	1593	0.367	1641	1.862
1546	0.827	1594	0.097	1642	2.058
1547	0.641	1595	0.388	1643	0.879
1548	0.348	1596	1.429	1644	0.69
1549	0.97	1597	1.41	1645	0.379
1550	0.308	1598	0.167	1646	0.538
1551	1.171	1599	1.594	1647	0.825
1552	1.102	1600	0.195	1648	1.2
1553	1.468	1601	1.497	1649	0.383
1554	0.523	1602	1.486	1650	0.967
1555	0.621	1603	1.689	1651	0.571
1556	1.132	1604	1.313	1652	0.142
1557	1.798	1605	0.975	1653	0.596
1558	1.136	1606	1.589	1654	0.638
1559	1.837	1607	0.491	1655	0.488
1560	1.921	1608	1.442	1656	1.519
1561	0.693	1609	1.168	1657	0.647
1562	0.857	1610	0.783	1658	0.909
1563	1.03	1611	1.465	1659	0.528
1564	1.747	1612	1.084	1660	0.059

Year	Value
1661	1.196
1662	1.07
1663	0.805
1664	1.201
1665	1.129
1666	1.226
1667	0.437
1668	1.345
1669	1.178
1670	0.378
1671	0.981
1672	1.185
1673	0.86
1674	1.007
1675	1.201
1676	0.932
1677	1.432
1678	1.253
1679	0.037
1680	0.905
1681	0.923
1682	1.257
1683	1.4
1684	1.461
1685	1.399
1686	0.2
1687	1.402
1688	0.659
1689	1.314
1690	1.056
1691	0.48
1692	1.042
1693	1.189
1694	0.802
1695	0.101
1696	1.12
1697	0.924
1698	0.101
1699	0.4
1700	1.333
1701	1.717
1702	1.673
1703	0.348
1704	1.256
1705	0.705
1706	0.329
1707	1.096
1708	0.464

Year	Value
1709	1.692
1710	0.989
1711	1.095
1712	0.962
1713	1.819
1714	0.42
1715	0.963
1716	1.507
1717	0.556
1718	0.905
1719	0.725
1720	0.493
1721	0
1722	0.71
1723	0.508
1724	0.768
1725	1.072
1726	0.754
1727	1.766
1728	0.803
1729	0.044
1730	1.271
1731	0.734
1732	1.269
1733	0.683
1734	1.698
1735	0.377
1736	0.465
1737	0.577
1738	1.091
1739	0.843
1740	1.773
1741	0.963
1742	1.261
1743	1.376
1744	1.312
1745	2.123
1746	1.774
1747	2.004
1748	1.423
1749	1.288
1750	1.932
1751	0.635
1752	1.246
1753	1.356
1754	1.546
1755	0.929
1756	0.633

Year	Value
1757	0.579
1758	1.169
1759	0.358
1760	0.902
1761	1.924
1762	1.031
1763	1.424
1764	0.657
1765	0.697
1766	1.786
1767	2.045
1768	2.156
1769	2.104
1770	0.461
1771	1.453
1772	1.288
1773	1.867
1774	1.346
1775	1.473
1776	0.593
1777	1.055
1778	0.601
1779	1.171
1780	0.789
1781	1.403
1782	1.126
1783	0.161
1784	1.072
1785	0.624
1786	0.829
1787	0.614
1788	0.608
1789	1.084
1790	2.055
1791	1.717
1792	1.164
1793	0.156
1794	0.362
1795	0.445
1796	1.321
1797	1.488
1798	1.964
1799	1.511
1800	0
1801	1.847
1802	1.911
1803	1.95
1804	1.57

Year	Value
1805	1.136
1806	1.469
1807	1.369
1808	1.287
1809	1.71
1810	1.943
1811	1.955
1812	1.699
1813	0.954
1814	0.78
1815	0.975
1816	1.208
1817	0.948
1818	1.808
1819	1.325
1820	1.265
1821	1.207
1822	0.441
1823	1.19
1824	1.453
1825	2.19
1826	1.662
1827	1.161
1828	0.766
1829	0
1830	1.258
1831	0.588
1832	0.949
1833	0.367
1834	0.351
1835	1.297
1836	1.37
1837	0.42
1838	1.288
1839	0.553
1840	1.179
1841	0.114
1842	0.8
1843	0.223
1844	0.6
1845	0.649
1846	0.945
1847	1.072
1848	0.967
1849	0.834
1850	1.254
1851	1.037
1852	0.896

Year	Value
1853	1.448
1854	1.034
1855	0.803
1856	0.808
1857	1.371
1858	0.464
1859	1.048
1860	0.8
1861	1.207
1862	1.698
1863	0.937
1864	0.622
1865	0.942
1866	1.542
1867	1.289
1868	1.341
1869	0.45
1870	0.625
1871	0.431
1872	0.838
1873	0.904
1874	1.161
1875	0.611
1876	1.061
1877	1.522
1878	1.037
1879	0.916
1880	0.575
1881	1.352
1882	0.672
1883	0.821
1884	0.856
1885	1.596
1886	0.731
1887	0.69
1888	0.49
1889	0.481
1890	0.777
1891	1.308
1892	0.704
1893	0.955
1894	1.273
1895	0.63
1896	0.587
1897	0.906
1898	0.323
1899	0.698
1900	0.731

Year	Value
1901	0.843
1902	0.896
1903	0.658
1904	1.257
1905	0.84
1906	1.217
1907	1.312
1908	0.741
1909	0.766
1910	0.654
1911	0.625
1912	0.53
1913	1.036
1914	1.407
1915	0.808
1916	1.27
1917	0.423
1918	0
1919	0.536
1920	0.635
1921	1.107
1922	0.686
1923	0.616
1924	0.313
1925	0.911
1926	0.257
1927	1.064
1928	0.63
1929	0.102
1930	0.264
1931	0
1932	0.739
1933	0.127
1934	0
1935	0.706
1936	0.743
1937	0.419
1938	1.243
1939	0.432
1940	0.976
1941	0.634
1942	0.976
1943	0.888
1944	0.968
1945	1.224
1946	0.935
1947	0.458
1948	1.927

Year	Value	Year	Value
1949	1.336	1997	2.081
1950	1.806	1998	2.416
1951	2	1999	1.51
1952	2.07	2000	1.187
1953	1.995		
1954	1.492		
1955	0.169		
1956	2.464		
1957	1.869		
1958	1.019		
1959	0.187		
1960	1.059		
1961	0.68		
1962	1.035		
1963	2.194		
1964	0.536		
1965	2.67		
1966	1.661		
1967	0.989		
1968	0.325		
1969	2.047		
1970	1.75		
1971	1.201		
1972	0.849		
1973	0.511		
1974	1.507		
1975	0.768		
1976	0.894		
1977	1.046		
1978	2.658		
1979	2.013		
1980	2.86		
1981	2.082		
1982	2.714		
1983	3.014		
1984	2.365		
1985	1.756		
1986	2.212		
1987	0.905		
1988	1.066		
1989	1.277		
1990	0.808		
1991	1.821		
1992	0.579		
1993	2.123		
1994	1.105		
1995	2.003		
1996	2.016		

Vita

Chris Underwood was born in Oak Ridge, Tennessee, on April 17, 1974, to Charles and Mary Underwood. He graduated from Sunbright High School (Morgan County) in 1992. He attended Roane State Community College in Harriman, Tennessee, graduating with an Associate of Applied Science degree in Industrial Hygiene in 1995. From there, he moved on to East Tennessee State University in Johnson City, Tennessee, where he graduated with a Bachelor of Science degree in Environmental Health in 1997. He has also attended Texas Christian University in Fort Worth, Texas. After working and traveling for a few years, he returned to academia in 2003 and began working toward his Master of Science degree at the University of Tennessee. During the spring semester of 2004, he discovered physical geography and dendrochronology.

Chris has participated in research projects in Oregon, Tennessee, Kentucky, Virginia, and Louisiana. He is a member of the Association of American Geographers and the Southeastern Division of the Association of American Geographers. Chris received his Master of Science degree in Geography from the University of Tennessee in May 2007. He will remain at the University of Tennessee and begin working toward his Ph.D. degree in Geography.

